UNIVERSIDADE FEDERAL DE SANTA CATARINA
CENTRO DE CIÊNCIAS DA SAÚDE
PROGRAMA DE PÓS-GRADUAÇÃO EM ODONTOLOGIA

Fernanda Haverroth Schünemann

DEVELOPMENT OF BIOACTIVE-ZIRCONIA SURFACES FOR BIOMEDICAL APPLICATIONS

Florianopolis
2023

Fernanda Haverroth Schünemann

Development of bioactive-zirconia surfaces for biomedical applications

Thesis presented to the Post-Graduate Program in Dentistry of the Federal University of Santa Catarina, as a requirement for obtaining the Ph.D. title in Implantology.

Advisor: Prof. Bruno Henriques, Dr.

Florianopolis

2023

Ficha de identificação da obra elaborada pelo autor, através do Programa de Geração Automática da Biblioteca Universitária da UFSC.

Haverroth Schunemann, Fernanda
DEVELOPMENT OF BIOACTIVE- ZIRCONIA SURFACE FOR BIOMEDICAL APPLICATIONS / Fernanda Haverroth Schunemann ; orientador, Bruno Henriques, 2023.
85 p.

Tese (doutorado) - Universidade Federal de Santa Catarina, Centro de Ciências da Saúde, Programa de Pós-Graduação em Odontologia, Florianópolis, 2023.

Inclui referências.

1. Odontologia. 2. zirconia. 3. bioactive glass. 4. surface modification. 5. osseointegration . I. Henriques, Bruno. II. Universidade Federal de Santa Catarina. Programa de Pós-Graduação em Odontologia. III. Título.

Fernanda Haverroth Schünemann

Development of bioactive-zirconia surfaces for biomedical applications

O presente trabalho em nível de doutorado foi avaliado e aprovado por banca examinadora composta pelos seguintes membros:

Prof. Márcio Celso Fredel, Dr.

Member/ UFSC, Florianópolis, Brazil

Prof. Óscar Samuel Novais Carvalho, Dr.

Board Member/University of Minho, Braga, Portugal

Prof. Jorge Pereira, Dr. Board

Member/Fernando Pessoa University, Porto, Portugal

Certificamos que esta é a **versão original e fina**l do trabalho de conclusão que foi julgado adequado para obtenção do título de doutor em Odontologia.

Documento assinado digitalmente
Mariane Cardoso Carvalho
Data: 08/06/2023 10:08:52-0300
CPF: ***.647.159-**
Verifique as assinaturas em https://v.ufsc.br

_____

Coordenação do Programa de Pós-Graduação

Documento assinado digitalmente
Bruno Alexandre Pacheco de...Henriques
Data: 07/06/2023 14:59:47-0300
CPF: ***.584.754-**
Verifique as assinaturas em https://v.ufsc.br

_____

Prof. Bruno Alexandre Pacheco de Castro Henriques, Dr.

Orientador

Florianópolis, 2023

For of him, and through him, and to him, are all things.
Romanos 11:36

ACKNOWLEDGEMENT

First, I would thank ***Jesus Christ***. There are no reason for such great dedication if I thought that everything end here. He was, he is and will always be my best friend. He is the reason of everything in my life. My eternal thankfulness to my Lord.

To my love ***Wagner Von Helden Schünemann*** for making me immensely happy every single day. You are the most special person that Lord could give me. The love I have for you is immeasurable. Thanks forever.

To my child ***Isaac Haverroth Schünemann***. Son, you were not even in my unimaginable dreams when I started this doctorate, but you were in God's dreams for me, and as always, God surprised me. Son, thank you for loving me and making me feel like the most powerful woman in the world. You are the most precious gift I have been given. I love you my son, I give my whole life for you.

To my father ***AIdo*** and my mother ***Marlene*** for everything you did to see success in my profession and everything I do. This PhD title is for you. I hope you always been proud of me.

To everyone in my ***family*** who believed in my potential and for all support that only the family can provide.

To all the ***professors*** at Federal University of Santa Catarina (UFSC), especially my advisor ***Bruno Henriques*** for accepting to advise me, even though I came from another area (dentistry) and started a doctorate with almost no knowledge in implant dentistry, materials engineering, writing in English and many other aspects. Your patience and advice were extremely important for me. Thank you teacher and forgive me for probably not exceeding your expectations. The pandemic time made everything different from my original plans and made everything so much harder, still you did not give up on me. Thanks.

To all friends and professors that ***CEPID*** gave me, particularly to my PhD colleagues who became lifelong friends, especially ***Mariane Sordi*** and ***Carolina Morsh*** and ***Ariadne Cruz*** for all the support in this work.

To thank everyone who contributed to the realization of this thesis. Due to the pandemic I needed distance support and everyone was always very kind to me. Especially thanks to ***Douglas Fabris***, ***Jéssica Vavassori, Elvira Lopes, Rafael***

Oliveira, Thamyres Hellen da Silva, Francesca Tatiana Albino, Maria Elisa Galarraga and ***Mariane Sordi***. Everyone cooperated a lot and in different ways.

To ***Jania Caetano*** for taking care of my son, without you I would not have finished this work. To ***Cristiane Souza*** and ***Síntia Caetano*** for helping me every day in a lot of activities.

Thanks to the hundreds of ***"metalovers"*** who always encouraged.

To ***CNPq*** and ***CAPES*** for the funding during this period, speciality for development the bioglass extracts for bone defects (Ref.: CNPq/INOVSAUDE2018/441457/2018-5).

This work was also supported by ***FCT-Portugal*** (UID/EEA/04436/2013, NORTE-01-0145-FEDER-000018 – HAMaBICo, FCT/02/SAICT/2017/ 3103-LaserMULTICER), ***CNPq-Brazil*** (PVE/CAPES/CNPq/407035/ 2013-3; CNPq/421229/2018-7) and by the United States National Institutes of Health, National Institute of Dental and Craniofacial Research (grant numbers R01DE017925, R01DE026772, and R01DE026279).

Thank to ***Curityba Biotech***® for providing mesenchymal stem cells from human exfoliated deciduous teeth. Authors appreciate the support from the Laboratório Multiusuário de Estudos em Biologia (***LAMEB***), ***Vitrocer***, ***Biomechanical laboratory*** (UFSC) and Laboratório Central de Microscopia Eletrônica (***LCME***) at the UFSC for providing their equipment and infrastructures to perform some experimental analyses. The authors also thank the ***Sterilization Service*** *at* ***University Hospital*** (UFSC) for sample sterilization.

"I am very grateful for the adversities that have appeared in my life, they have taught me tolerance, sympathy, self-control, perseverance and other qualities that, without these adversities, I would never have known".

Napoleon Hill

AGRADECIMENTOS

*À **Jesus Cristo,*** não haveria motivo para tão grande dedicação se eu pensasse que tudo terminaria aqui, mas, graças ao que Cristo fez na cruz por amor a mim, eu entendi que há muito além desde mundo, o que eu preciso aqui é fazer meu melhor, sempre dedicando tudo a Ele. Ele foi, ele é e sempre será meu amigo fiel em todos os momentos, é a razão principal pela qual eu dedico todas as coisas na minha vida, com certeza este trabalho não teria acontecido se não fosse pelas oportunidades que Ele me deu, pelas pessoas que Ele colocou na minha vida. Minha eterna gratidão ao meu Senhor, especialmente por me perdoar diante te tantos erros que cometo e ainda assim continuar a me amando.

*Ao meu amor **Wagner Von Helden Schünemann***, por me fazer imensamente feliz todos os dias. Amor, você é insubstituível, incomparável, o homem mais especial que o Senhor poderia me dar. Eu não mereço você, sei que inúmeras vezes falhei e ainda falharei, mas você sempre esteve ao meu lado me amando e se eu tivesse direito de pedir apenas uma coisa a Deus, eu pediria para vivermos juntinhos por muitos anos. O amor que eu tenho por você é imensurável. Obrigada.

*Ao meu filho **Isaac Haverroth Schünemann***, você não estava nem nos meus maiores sonhos quando eu iniciei esse doutorado, porém você estava nos sonhos de Deus pra mim, e como sempre, Deus me surpreendeu. Filho, você jamais terá ideia do presente que você é pra mãe. Quando eu estou com você eu só desejo que o mundo pare, que eu fique naquele *segundo* pro resto da minha vida. Mas aquele *segundo* não para, as vezes eu fico brava por ele não ter parado, mas aí você vem de novo, de um jeito diferente, em um novo *segundo*, fazendo eu desejar novamente que ele pare. E assim eu vivo todos os dias desde que você nasceu, querendo que o tempo pare, mas também querendo que chegue o amanhã para viver com você de uma forma ainda mais intensa. Obrigada por me amar e fazer eu me sentir a mulher mais poderosa do mundo. Você é o presente mais precioso que eu ganhei. Eu te amo meu filho, eu dou a minha vida todinha por você.

Ao meu pai ***Aldo*** e minha mãe ***Marlene*** que com toda humildade e simplicidade sempre dedicaram o que podiam (e o que não podiam) para que eu tivesse sucesso na minha profissão e na vida. Esse título de doutora é para vocês. Espero que se orgulhem para sempre de mim.

À *todos* da minha ***família*** que acreditaram no meu potencial, sem dúvidas o apoio de cada um fez com que eu tivesse forças e coragem para não desistir.

Aos ***professores*** da UFSC, especialmente ao meu orientador ***Bruno Henriques*** por aceitar me orientar, mesmo eu vindo de outra área (dentistica) e chegar com conhecimento praticamente zero na implantodontia, na engenharia de materiais, na escrita em inglês e em muitos outros quesitos. Toda sua paciência e orientação foram fundamentais. Muitas vezes eu agendava uma reunião desanimada, querendo desistir, achando que não conseguiria e nada mais fazia sentido, mas após a reunião eu sempre voltava pra casa com eu ânimo renovado e acreditando que a minha pesquisa era, sem dúvidas, a mais incrível já realizada. Obrigada professor e me perdoe por provavelmente não ter superado suas expectativas. A pandemia tornou tudo muito mais difícil e mudou completamente meus planos, ainda assim você não desistiu de mim e conseguimos juntos realizar este trabalho a distância. Obrigada e me perdoe. Eu gostaria e sei que poderia ter sido uma aluna melhor.

À todos os amigos e professores que o ***CEPID*** me presenteou, especialmente aos meus colegas do doutorado que se tornaram amigos para toda a vida. Sei que 99% do que aprendi sobre implantodontia foi com a experiência e convivência que tive com cada um dos meus colegas, especialmente ***Mariane Sordi*** e ***Carolina Morsh***. Muito obrigada.

Aos que colaboraram para que esta tese fosse realizada. Devido a pandemia precisei de apoio a distância e todos foram muito gentis sempre. Agradeço especialmente ao ***Douglas Fabris, Jéssica Vavassori, Elvira Lopes, Rafael Oliveira, Thamyres Hellen da Silva, Francesca Tatiana Albino, Maria Elisa Galarraga*** *e a professora* ***Ariadne Cruz.*** Todos cooperaram muito e de formas distintas, sempre com muita prontidão e dispostos a darem o melhor.

À ***Jania Caetano*** por cuidar tão bem do meu filho para que eu pudesse finalizar este trabalho. Jania é como uma mãe para mim. Eternamente grata a Deus por sua vida. À ***Cristiane Souza*** e ***Síntia Caetano***, por estarem todos os dias comigo me ajudando em todas as atividades e ainda aturarem minha frase diária: “hoje não posso, preciso escrever meu doutorado”.

Às centenas de ***metalovers*** que aguardavam ansiosamente e diariamente minha postagem de batom vermelho escrevendo minha tese, que sempre me incentivavam com mensagens incríveis dizendo para eu não desistir da minha meta.

Vocês fizeram toda diferença, se eu cumpri esta meta foi também por cada uma de vocês.

À UFSC, em especial ao ***CEPID*** e ao ***CERMAT*** por toda infraestrutura oferecida aos alunos para que possamos desenvolver nossa pesquisa. Também ao **CNPq e CAPES,** por financiar esta tese, especialmente pelo desenvolvimento de excertos de biovidro para defeitos ósseos (Ref.: CNPq/INOVSAUDE2018/441457/2018-5).

Agradeço especialmente aos financiadores deste trabalho, ***FCT-Portugal*** (UID/EEA/04436/2013, NORTE-01-0145-FEDER-000018 – HAMaBICo, FCT/02/SAICT/2017/ 3103-LaserMULTICER), ***CNPq-Brasil*** (PVE/CAPES /CNPq/407035/ 2013-3; CNPq/421229/2018-7), Instituto Nacional de Saúde dos Estados Unidos, Instituto Nacional de Pesquisa Dentária e Craniofacial (números de concessão R01DE017925, R01DE026772 e R01DE026279). À ***Curityba Biotech***® por fornecer células-tronco mesenquimais de dentes decíduos esfoliados humanos. Para a realização deste trabalho também foi essencial o apoio do Laboratório Multiusuário de Estudos em Biologia (***LAMEB***), do Laboratório Central de Microscopia Eletrônica (***LCME***), ***VITROCER*** e da equipe da ***Biomecânica*** da UFSC, todos cooperaram de alguma forma para a confecção das amostras e realização das análises experimentais. Agradeço também ao ***Serviço de Esterilização do Hospital Universitário da UFSC*** pela esterilização das amostras.

“Sou muito grata às adversidades que apareceram na minha vida, pois elas me ensinaram a tolerância, a simpatia, o autocontrole, a perseverança e outras qualidades que, sem essas adversidades, eu jamais conheceria”

Napoleon Hill

ABSTRACT

Osseointegration is crucial for the long-term success of dental implants and depends on the tissue reaction at the implant interface. Mechanical properties and biocompatibility make zirconia a suitable material for dental implants, although surface processing are still problematic. The purpose of this study was to perform a literature review on current surface modification techniques to enhance the biological and osseointegration behaviour of zirconia-based implants in dentistry and to develop bioactive zirconia surfaces using two different bioactive glasses (BG) and dopamine (DOP) to improve hard and soft tissues integration around zirconia dental implants. A literature review was performed on PUBMED database to identify relevant studies regarding zirconia surface treatment to enhance osseointegration. For laboratorial studies, Y-TZP disks were made in two different protocols for biological and mechanical analysis. For biological tests, Y-TZP disks was infiltrated with 45S5 and 58S bioactive glass and/or dip-coated with dopamine and 58S bioactive glass. Biocompatibility of disks was evaluated by MTS colourimetric test, cell proliferation was assessed by PicoGreen dsDNA reagent, and cell adhesion and morphology were analyzed by scanning electron microscopy (SEM). MC3T3-E1 preosteoblasts and human mesenchymal stem cells (MSCs) were used for 3 or 7 days. For mechanical tests, disks were infiltrated with 45S5 BG and 58S BG and dip-coated with 58S BG. Mechanical properties was evaluated by roughness, contact angle, SEM images in surface and cross section samples w, X-ray diffractmeter (XRD) before and after biaxial flexural strength. The results on literature review reported a large number of physicochemical methods that have been used to change the implant surfaces and therefore to improve the early and late bone-to-implant integration. A BG-infiltration zirconia for implants has shown encouraging mechanical and biological behavior. The Y-TZP modified with BG and DOP were biocompatible to MC3T3-E1 and MSCs and reduced cell proliferation from day 3 to day 7 of MC3T3-E1 and MSCs, indicating cell commitment to differentiation pathways. On the mechanical tests, biaxial bending results was 579 $\pm$ 144 MPa on Y-TZP group and decreased on BG infiltration groups (496$\pm$50MPa for Y-TZP + 45S5 BG and 101 $\pm$ 244MPa for Y-TZP + 58 BG). XRD revealed the presence of tetragonal and monoclinic zirconia. The roughness of Y-TZP was lower (Sa=0.92$\pm$0.67) when compared to zirconia infiltrated with bioactive glasses [Y-TZP + 45S5 BG (Sa=4.31$\pm$2.16) and Y-TZP + 58S BG (Sa=4.08$\pm$0.69)]. BG-infiltrated zirconia evaluated in laboratorial studies presented favourable mechanical and biological properties, and should be evaluated in clinical studies to provide realistic point view.

Keywords: Zirconia 1; Surface modification 2; Bioactive glass 3; Dopamine 4; Osseointegration 5; BG - infiltrated zirconia 6.

RESUMO EXPANDIDO

DESENVOLVIMENTO DE SUPERFÍCIE BIOATIVAS DE ZIRCONIA PARA APLICAÇÃO BIOMEDICINAL

Introdução

A zircônia tetragonal estabilizada com ítria (Y-TZP) surgiu na odontologia como um material promissor para diversas aplicações devido ao seu bom resultado estético, imitando a aparência natural dos dentes (STADLINGER et al., 2010). Além da excelência estética, estudos afirmam que os implantes de zircônia apresentam resultados semelhantes aos implantes a base de titânio com relação a osseointegração, também apresentam características mecânicas únicas como tenacidade à fratura, resistência à fadiga, alta resistência à flexão, alta resistência à corrosão e radiopacidade (BONA; PECHO; ALESSANDRETTI, 2015; ZHANG, 2012). No entanto, apesar dos achados favoráveis, resultados clínicos de longo prazo ainda estão faltando e ainda há algumas controvérsias em relação a osseointegração da zircônia, pois alguns estudos relataram altas taxas de falha e perda óssea cristal peri-implantar nos implantes de zircônia (KOHAL et al., 2016). Outros autores consideram a zircônia um material bioinerte (ROEHLING *et al.*, 2017; SCARANO *et al.*, 2003). Portanto, pesquisadores vêm dedicado esforços para modificar a superfície da zircônia com a intenção de proporcionar aspectos morfológicos e bioativos apropriados para uma excelente adesão, proliferação e diferenciação celular durante a osseointegração, além de um bom desempenho mecânico.

Objetivos

O objetivo deste trabalho é desenvolver uma superfície bioativa de zircônia utilizando dois diferentes vidros bioativos (45S5 BG e 58S BG) e dopamina. O intuito é melhorar o comportamento biológico e mecânico de implantes à base de zircônia em odontologia e, consequentemente, melhorar a integração dos tecidos duros e moles em torno dos implantes dentários de zircônia.

Metodologia

A presente tese foi dividida em cinco capítulos. O primeiro capítulo contém a introdução de tópicos relevantes relacionados ao trabalho. O segundo capítulo é intitulado “Zirconia surface modifications for implant dentistry” publicado em 2019 na Materials Science and Engineering C. Este capítulo apresenta uma revisão da literatura relatando os diferentes tipos de tratamentos de superfície existentes para a zircônia (ZrO_2), com a intenção de melhorar a superfície, o comportamento biológico e a osseointegração. A pesquisa foi realizada em 2018 através de uma busca eletrônica na base de dados PubMed utilizando as seguintes combinações de palavras-chave: “tratamento de superfície de zircônia”, “modificação da superfície de zircônia”, “revestimento de zircônia”, “osseointegração”, “propriedades biológicas”, “bioatividade” e “propriedades funcionalmente graduadas”.

O capítulo 3 é intitulado “Dopamine - and graded bioactive glass-zirconia modified surfaces for implant dentistry: an in vitro study” submetido em 2023 para a Acta Biomaterialia. Neste capítulo foram desenvolvidas superfícies de zircônia bioativa utilizando dois diferentes vidros bioativos (45S5 e 58S) e a dopamina. A biocompatibilidade dos discos foi avaliada pelo teste colorimétrico MTS, a proliferação celular foi avaliada pelo reagente PicoGreen dsDNA e a adesão e morfologia celular foram analisadas por microscopia eletrônica de varredura (MEV). Osteoblastos MC3T3-E1 e células-tronco mesenquimais humanas (MSCs) foram usados por 3 e 7 dias.

No quarto capítulo, intitulado “Static and dynamic mechanical behaviour of Y-TZP structures with bioactive surfaces obtained by the infiltration of 45S5 and 58S bioactive glasses”, foram avaliadas as propriedades mecânicas estáticas e dinâmicas de estruturas de zircônia com superfícies bioativas. Discos de Y-TZP foram infiltrados com os vidros bioativos 45S5 e 58S e a densidade foi medida de acordo com a técnica de Arquimedes. As superfícies foram analisadas por meio da rugosidade e a Espectroscopia de Energia Dispersiva (EDS) foi realizada juntamente com a MEV (antes e depois dos testes de fadiga). As fases cristalinas foram identificadas por difração de raios-X. Ainda, metade das mostras por grupo foram submetidas a carregamento cíclico biaxial e, posteriormente, todas as amostras foram submetidas a flexão biaxial para determinação da resistência mecânica. A confiabilidade da resistência foi analisada através da distribuição de Weibull.

Por fim, no quinto e último capítulo foram apresentadas as conclusões gerais e perspectivas para trabalhos futuros.

Resultados e discussão

Quando um novo material é proposto para aplicações clínicas, importantes ensaios biológicos são necessários para responder a algumas questões. Primeiro, o material deve ser biocompatível, ou seja, não deve levar a danos às células e tecidos circundantes devido a reações inflamatórias. Em seguida, o material deve fornecer informações biológicas para permitir que as células venham aderir e se espalhem pela superfície, permitindo que as células exerçam suas funções. Finalmente, um material bioativo deve melhorar a proliferação celular até um número suficiente para suportar a cicatrização dos tecidos circundantes e o processo de diferenciação para permitir a osseointegração. Aqui, as superfícies modificadas com zircônia por infiltração de vidro bioativo e/ou revestimento com dopamina provaram ser biocompatíveis com células-tronco mesenquimais humanas e osteoblastos murinos. Os resultados da revisão de literatura exposta no segundo capítulo desta tese mostraram que a zircônia funcionalmente bioativa apresenta melhor desempenho mecânico e biológico quando comparado a zircônia pura ou ao titânio. Apesar disso, nenhum tratamento de superfície foi reivindicado como primeira escolha para aumentar o potencial de osseointegração da zircônia, embora as modificações da superfície aumentam a rugosidade, molhabilidade e energia de superfície, qinfluenciando no aumento da adesão, proliferação e diferenciação de osteoblastos.

Os estudos descritos no terceiro capítulo no presente trabalho mostram que a superfície da zircônia obteve sucesso no recobrimento com dopamina e na infiltração dos biovidros 45S5 e 58S. Nos testes biológicos realizados todas as amostras se mostraram biocompatíveis, reduziram a proliferação dos osteoblastos e das células mesenquimais, apresentando resultados mais promissores quando comparados ao Y-TZP. No entanto, outras análises osteogênicas devem ser realizadas para mostrar a diferenciação osteoblástica das células, como atividade da fosfatase alcalina, detecção de proteínas ósseas e avaliação da mineralização da matriz extracelular.

No quarto capítulo as imagens SEM mostraram que a infiltração de BG modificou a superfície da zircônia, criando uma microestrutura caracterizada por partículas de zircônia imersas em uma matriz de vidro. As imagens apresentam

também uma significante porosidade na região infiltrada. O teste mecânico de flexão biaxial mostrou valores de resistência à flexão mais baixos para zircônia pura (579 ± 144 MPa) quando comparado a estudos anteriores (aproximadamente 900 a 1400 MPa), possivelmente devido ao jateamento realizado na superfície. Os resultados de resistência à flexão diminuem ainda mais com a infiltração de BG (496± 50MPa para Y-TZP + 45S5 BG e 101 + 244MPa para Y-TZP + 58BG). Uma possível explicação para tal comportamento pode ser o tempo excessivo de sinterização descritos. Os resultados de DRX em todos os grupos revelaram presença de zircônia tetragonal e monoclínica. A rugosidade de Y-TZP foi menor (Sa=0.92±0.67) quando comparada a zircônia infiltrada com os vidros bioativos Y-TZP + 45S5 BG (Sa=4.31±2.16) e Y-TZP 58S (Sa=4.08±0.69). Nas imagens realizadas no microscópio eletrônico de varredura foi possível identificar o biovidro infiltrado com sucesso na zircônia, no entanto, a superfície exibe um grande número de poros em todos os grupos.

Considerações finais

Os avanços na tecnologia melhoraram a superfície da zircônia e aceleraram a resposta de cicatrização óssea, estimulando a osteogênese, a adesão celular e ainda promovendo um efeito antibacteriano. Desta forma, a superfície da zircônia quando modificada é transformada de “bioinerte” para “bioativa”, proporcionando respostas biológicas e mecânicas mais favoráveis ao tecido peri-implantar quando comp
às superfícies não tratadas.

Nesta tese a zircônia foi recoberta com sucesso por dopamina e obteve êxito na infiltração em ambos os biovidros (45S5 e 58S). Os estudos biológicos apresentaram descobertas favoráveis que foram alcançadas com metodologias simples e acessíveis que podem ser aplicadas em larga escala. Os estudo mecânicos apresentaram desempenho inferior da zircônia infiltrada em relação aos discos monolíticos de zircônia, tanto em condições estáticas quanto em condições de fadiga. Tais achados sugerem que os implantes de zircônia infiltrada com biovidros precisam de mais estudos para uso como solução alternativa aos implantes de zircônia monolítica na implantodontia.

Palavras-chave: zircônia 1; superfície do implante 2; biovidro 3; dopamina 4; osseointegração 5.

LIST OF FIGURES

Figure 1 - Schematics and SEM images on different zirconia surface modifications: machined (LIU *et al.*, 2015), acid etched (QUENTINFLAMANTA *et al.*, 2016), grit blasted (LIU *et al.*, 2015), ZLA (ROEHLING *et al.*, 2017), and multi-layered coatings (KAROLINE PARDUN *et al.*, 2015; LARANJEIRA *et al.*, 2014; LIU *et al.*, 2015)……....10

Figure 2 - Zirconia coatings showing biological advantages in terms of bioactivity, osseointegration, and antibacterial effects ……..…….…….26

Figure 3 - Optical micrographs of graded CPG/Y-TZP (a) rod (2 mm in radius) and (b) plate (1.2 mm thick) sections consisting of (c) CPG infiltrated Y-TZP (SEM image); (d) Energy dispersive X-ray line mapping from surface to interior, revealing a gradual transition in Ca and Zr contents. Higher magnification SEM images, insets of (c), showing: gradual transition from the surface residual CPG layer (left) to the graded CPG/Y-TZP structure (center) and to dense Y-TZP interior (right), modified from Zhang et al. (2014)……...…27

Figure 4 - Micrographs of graded CPG/Y-TZP (A) rod (2 mm radius) and (B) plate (1.2 mm thick) sections consisting of (C) CPG infiltrated Y-TZP (SEM images). Higher magnification SEM images, insets of (C) showing the gradual transition from the surface residual CPG layer (1, left) to the graded CPG/Y-TZP structure (2, centre) and to the dense Y-TZP interior (3, right). Adapted from Zhang et al. 2014. CPG: gradated compositional and mechanical transition from the surface. Y-TZP: bulk of the component.……32

Figure 5 - Clinical application of bioactive glass (BG) coating on zirconia surface of dental implant and prosthetic abutment. DOP: dopamine……..……35

Figure 6 - Scheme of zirconia (Y-TZP) specimens according to the surface treatment. BG: bioactive glass. DOP: dopamine……..37

Figure 7 - Representative image of cross-sectional views of water droplet in specimens……...43

Figure 8 - Cell viability assays. Viabilities percentages were calculated in relation to cellular control (100%). A-B) Mesenchymal stem cells (MSCs) from human exfoliated deciduous teeth (SHED) or C-D) Osteoblasts (MC3T3-E1) on A-C) day 3 and B-D) day 7 of cell culture. Equal letters mean no significant differences among groups (ANOVA/Tukey's post-hoc, p <0.005). ……..……..44

Figure 9 - Cell proliferation assays. Proliferation rates were calculated in relation to the standard curve to quantify the dsDNA of the cells. A-B) Mesenchymal stem cells (MSCs) from human exfoliated deciduous teeth (SHED) or C-D) Osteoblasts (MC3T3-E1) on A-C) day 3 and B-D) day 7 of cell culture. Equal letters mean no significant differences among groups (ANOVA/Tukey's post-test, p < 0.005). ……..…….45

Figure 10 - Cell micrographs on day 7 of cell culture of experimental groups (G1 to G7). The first image (cc) shows zirconia surface with no cells for comparison. Images with red borders represent greater magnified fields (x2.5k) for detailed analyses. A) Mesenchymal stem cells (MSCs) from human exfoliated deciduous teeth (SHED) and B) Osteoblasts (MC3T3-E1). ……...46

Figure 11 - Schematic representation of the press, sintering and BG infiltration technique used for the production of substrates. 1º Step: pouring the Y-TZP powder inside the stainless-steel die cavity; applying pressure; green compact extraction, and sintering. 2º Step: disk covered with 1g of BG powder + 0.06 ml of distillate water and sintering ..……54

Figure 12 - SEM images of different surfaces: A) monolithic zirconia B) zirconia infiltrated with bioglass 45S5 and C) zirconia infiltrated with bioglass 58S. Images B and C are characterized by the presence of BG at the grain boundaries of the zirconia particles..……58

Figure 13 - SEM cross section images of BG-infiltrated groups before fatigue tests and the EDX analysis performed on infiltrated zone…….59

Figure 14 - Micrograph of the porous found on Y-TZP + 45S5 BG…….60

Figure 15 - Weibull plots of surface porous zirconia specimens fractured in biaxial flexural strength tests.……...61

Figure 16 – Typical fracture patterns observed for the specimens after biaxial flexural test. The red circle indicate the central location of the loading piston……..62

Figure 17 - SEM micrographs of cross section on different groups: A) Y-TZP + 45S5 and B) Y-TZP + 58S, after mechanical tests. The presence of typical brittle marks such as compression curl (CC) can be observed……64

Figure 18 - Cross section analyses on all groups after de mechanical tests……..…65

LIST OF TABLES

Table 1 - BIC percentage and roughness values among machined surface, grit blasted surface, acid etched surface, laser, and UV light modified zirconia surface after different time points……..…….……10

Table 2 - Water contact angle and wettability measured in several studies for different types of zirconia surface treatments……..……..17

Table 3 - Previous studies on zirconia-modified surfaces by bioactive glasses or dopamine derivatives……..……...……..…..33

Table 4 - Mean of roughness (Ra/mm) and contact angle (CA/degrees) values of each group…….……..……..42

Table 5 - Roughness and density results of different surface treatments……...60

Table 6 - Biaxial flexural strength results of BG-infiltrated zirconia and pure zirconia groups, for non-fatigued and fatigued conditions…….....62

Table 7 – Data on mechanical cycling tests for zirconia and BG-infiltrated zirconia: number of failed specimens and number of cycles at fracture…….63

TABLE OS CONTENTS

Chapter 1 – Introduction and objectives 1
1.1. Introduction 1
1.2. Research objectives 5
1.3. Thesis structure 5
Chapter 2 – Literature review – Zirconia surface modifications for implant dentistry ...7
2.1. Introduction 7
2.2. Search strategy 9
2.3. Results and discussion 9
2.3.1. Machined zirconia implants 11
2.3.2. Grit blasted and acid etched zirconia surface treatment 12
2.3.3. Ultraviolet light treated zirconia 16
2.3.4. Zirconia laser modification 18
2.3.5. Coatings on zirconia 20
2.3.6. Magnesium, nitrogen, and carbon coatings 21
2.3.7. Hydroxyapatite and calcium phosphate based coatings 21
2.3.8. Dopamine 22
2.3.9. Graphene coatings 24
2.3.10. Bioactive graded zirconia-based structures 24
2.4. Conclusions 28
Chapter 3 - Dopamine- and graded bioactive glass-zirconia modified surfaces for implant dentistry: an in vitro study 30
3.1. Introduction 30
3.2. Material and methods 36
3.2.1. Zirconia disks preparation 36
3.2.2. Sol-gel production of bioactive glass 36
3.2.3. Melting route of bioactive glass 45S5 36
3.2.4. Zirconia surface modifications 37
3.2.4.1. Sandblasted and acid-etched zirconia specimens 38
3.2.4.2. Graded BG-zirconia specimens 38
3.2.4.3. Dopamine (DOP) coated specimens 38
3.2.4.4. BG-coated graded BG-zirconia specimens 38
3.2.5. Surface characterization 39
3.2.5.1. Surface roughness measurements 39

3.2.5.2. Contact angle measurements 39
3.2.5.3. X-ray Diffraction (XRD) for phase transformation analysis 39
3.2.6. Cell cultures 40
3.2.7. Cell viability assays 40
3.2.8. Cell proliferation assays 41
3.2.9. Cell morphology and adhesion analyses 41
3.2.10. Statistical analyses 41
3.3. Results 42
3.3.1. Surface analysis 42
3.3.2. Cell viability assays 43
3.3.3. Cell proliferation assays 44
3.3.4. Cell morphology and adhesion analyses 45
3.4. Discussion 47
3.5. Conclusion 49
Chapter 4 - Static and dynamic mechanical behaviour of Y-TZP structures with bioactive surfaces obtained by the infiltration of 45S5 and 58S bioactive glasses 51
4.1 Introduction 51
4.2. Materials and methods 53
4.2.1. Bioglass 45s5 Synthesis 53
4.2.2. Bioglass 58s synthesis 53
4.2.3. Zirconia surface modification 54
4.2.4. Microstructure analysis 55
4.2.5. Bulk density and roughness analysis 55
4.2.6. Mechanical characterization 56
4.2.7. Statistical analysis 57
4.3 Results 57
4.3.1. Surface microstructure 57
4.3.2. Density and roughness analysis 60
4.3.3. Mechanical results 61
4.3.4. XRD analysis 64
4.4 Discussion 65
4.5 Conclusion 69
Chapter 5 - Final remarks 70
References 70

Chapter 1 – Introduction and objectives

1.1. Introduction

Yttria-stabilized tetragonal zirconia polycrystal (Y-TZP) is a popular bioceramic and is increasingly being used for dental applications due to its capacity to stimulate osteogenic cells during osseointegration. Additionally, Y-TZP has unique mechanical characteristics such as high fracture toughness, fatigue resistance, high bending strength, high corrosion resistance, low temperature degradation and radiopacity (ZHANG *et al.,* 2012a). Despite the favorable findings, long-term clinical results are still lacking and some controversies regarding the zirconia osseointegration have been debated due some studies report high rates of failure and bone loss peri-implant zirconia crystal (KOHAL *et al.,* 2016) and some authors consider zirconia a bioinert material (ROEHLING *et al.,* 2017; SCARANO *et al.,* 2004). Therefore, implant technology has devoted substantial efforts to modify the zirconia "bioinert" surface to a bioactive one, allowing appropriate cell attachment, proliferation, and differentiation to promote bone-implant integration (PARDUN *et al.*, 2015; YIN *et al.*, 2017).

Previous investigations have considered methods to enhance biocompatibility and induce hydroxyapatite formation in a biological environment, essential for subsequent bone proliferation. These modifications accelerate osteoblasts and fibroblasts adhesion, proliferation, and differentiation, thus affecting peri-implant tissue attachment and integration on implant surfaces, in addition, the purposes of such modifications include antibacterial effect and osseointegration acceleration (SANON *et al.*, 2015). Some of this methods include sandblasting and acid-etching (BACCHELLI *et al.*, 2009), coatings with silica (MOEZZIZADEH; NOJEDEHIAN; HAGHI, 2017), nitrogen (SCHIENLE *et al.*, 2016), carbon (SCHIENLE *et al.*, 2016), calcium phosphate (YANG *et al.*, 2013), hydroxyapatite (CHO *et al.*, 2015), dopamine (LIU; LEE; LUI, 2013), graphene (LI *et al.*, 2014) and bioactive glass (MOEZZIZADEH; NOJEDEHIAN; HAGHI, 2017).

The sandblasting process using 50-110 μm Al_2O_3 particles is an alternative solution to increase the surface area in zirconia implant structure, providing a more attractive surface for osteoblasts attachment and accelerating the osseointegration process. (BACCHELLI *et al.*, 2009; GAHLERT *et al.*, 2007; KOHAL *et al.*, 2004).

Sandblasted zirconia implant surfaces presents significant advances on peri-implant osteogenesis compared to machined titanium surfaces surfaces (BACCHELLI *et al.*, 2009; GAHLERT *et al.,* 2007; KOHAL *et al.,* 2004). Moreover, using the sandblasting method with additional chemical treatments, and hydrofluoric acid (HF) etching, appears to be best technique to enhance bone apposition (FLAMANT *et al.*, 2016; GAHLERT *et al.*, 2010) . Flamant et al. (2016) reported that HF 40% etching leads to the fastest and most uniform etching method and seems to be the most appropriate substance for treating zirconia dental implants. Hempel *et al.* (2010) cultured SAOS-2 osteoblasts over sandblasted/etched zirconia surface and compared them with sandblasted/etched titanium surface. Sandblasted/etched zirconia promoted faster cell spread, and a higher number of adherent cells on zirconia than titanium surface. Therefore, this study indicated that topographical differences of sandblasted/etched zirconia mediate a pronounced effect on osteoblast adhesion, proliferation and differentiation compared to titanium surfaces (HEMPEL *et al.*, 2010).

Implant dentistry innovations face the primordial challenge of enhancing biological and mechanical properties of implants by approaches like bioactive bioglass (BG). The use of BG on zirconia surfaces combine the mechanical properties of the high-strength zirconia with the bioglass bioactivity. BG were discovered in 1969 by Larry Hench as a material capable of forming a hydroxyapatite surface layer after contact with biological fluids, promoting a stable bond to the bone (osteoconduction) and stimulating cells to differentiate (osteoinduction). Thus, the essential condition for glasses to form an interfacial bond with the bone is establishing a hydroxyapatite layer on their surface (HENCH *et al.*, 1977). BG stimulate bone cells towards a path of regeneration and self-repair, thus significantly accelerating tissue healing kinetics. This regeneration is due to the release of calcium and phosphate ions that are present in the BG composition and play an essential role in bone metabolism (angiogenesis and tissue mineralization). The first commercial BG was 45S5 and it is still widely studied due to its outstanding bone-bonding properties. In the 90s, a new BG was developed through the sol-gel method to obtain an alternative compound with similar properties to 45S5. It was named 58S BG (FERRARIS *et al.,* 2000; HENCH, 2015; MOEZZIZADEH; NOJEDEHIAN; HAGHI, 2017; ZHONG; GREENSPAN, 2000). Sepulveda et al. (2002) showed that melt-derived 45S5 glass powders exhibit lower dissolution rates for apatite formation than 58S gel-glass powders (SEPULVEDA; JONES; HENCH, 2002).

To combine BG bioactivity with the mechanical properties of zirconia, Zang *et al.* (2009) proposed the infiltration of BG into zirconia, creating a functionally graded material (FGM) that improves aesthetics, bioactivity, and suppress flexural damage. The FGM has BG incrusted at the top and the bottom, like a sandwich structure: glass/zirconia/glass (G/Z/G). G/Z/G presents strength and contact damage resistance while retaining surface, physical and optical properties similar to porcelain (ZHANG, 2012; ZHANG; REGEROS; KIM, 2009c). The invention applied a powder of BG composition on surfaces of dense pre-sintered zirconia using a solution-precipitation method and covering the ceramic substrate surfaces with a layer of the BG. This process was performed under temperatures ranging from 750 °C up to 1450 °C (ZHANG; REGEROS; KIM, 2009). Despite the aforementioned advantages of this system, there is only a few studies on CPG/Y-TZP, contrasting to a vast literature on glass infiltrated zirconia structures (ZHANG, 2012; ZHANG; SUN; ZHANG, 2012b).

Furthermore, another surface modification has been applied for improving soft tissue integration around zirconia is dopamine (DOP), the precursor of 3,4-dihydroxy-L-phenylalanine (LEE *et al.*, 2007). DOP is a critical component that can self-polymerize and adhere firmly to a wide range of organic and inorganic materials. DOP coatings can enhance antimicrobial properties and facilitate protein adsorption and cell adhesion of inert surfaces (LEE *et al.*, 2007). Liu et al. (2015) explored the influence of DOP coating on zirconia disks regarding soft-tissue integration and antibacterial effect. The coating decreased bacterial activity and enhanced fibroblasts adherence, which has a vital role in the peri-implant soft-tissue integration. Therefore, this surface modification approach holds great potential for improving soft-tissue integration around zirconia abutments, which is another important clinical application of zirconia in implant dentistry (LIU *et al.*, 2015).

Zirconia surface modifications should be further studied, considering chemical bonding and deterioration. Even though zirconia implants offer aesthetic benefits over titanium implants, titanium-based materials still possess higher mechanical strength than zirconia and are currently the first-choice material for dental implants. Implant technology has devoted significant efforts to modify zirconia regarding the morphological and bioactive aspects desirable for an appropriate cell attachment, proliferation, and differentiation during bone healing (PARDUN *et al.*, 2015; YIN *et al.*, 2017). Considering the necessity to enhance the behavior of zirconia-based implants

in dentistry, this thesis was divided in three parts: a literature review, a biological and a mechanical in vitro study of zirconia surface treatment.

1.2. Research objectives

This work aims to develop, through in vitro preliminary studies, bioactive zirconia surface for biomedical applications.

The specific objectives are:

- Produce zirconia surfaces with the sandblasted and acid etched treatment;
- Produce BG-infiltrated zirconia;
- Produce dopamine coated zirconia surfaces;
- To analyze the surfaces produced in terms of roughness, wettability (contact angle) and bioactivity;
- Analyze the static and dynamic mechanical properties of zirconia components embedding the new surfaces;
- Analyze the biocompatibility morphology, cell adhesion and bioactivity;
- Analyze the surface microstructure and chemical composition in scanning electron microscopy (SEM) with Energy-dispersive X-ray spectrometer (EDX).

1.3. Thesis structure

This thesis is structured in five chapters. Chapter 1 comprise the introduction of relevant topics related to this work. Chapter 2 is a literature review that explore the state of art of zirconia surface treatment to enhance the biological and osseointegration behavior of zirconia in implant dentistry. Research chapters are presented on Chapter 3 and Chapter 4. Each one is divided into sections: introduction, materials and methods, results and discussion, and conclusions. References are merged at the end of the document.

On chapter 3 bioactive zirconia surfaces was developed using bioactive glass and dopamine. Therefore, physical and mechanical analyses of the materials, biocompatibility, and cell proliferation, adhesion, and morphology were evaluated. Chapter 4 evaluate the static and dynamic mechanical properties of zirconia structures with bioactive surfaces produced through the infiltration of bioactive glasses. Finally, in Chapter 5 the general conclusions and an outlook for future works are presented.

Chapter 2 – Literature review – Zirconia surface modifications for implant dentistry[1]

2.1. Introduction

In the last decade, yttria-stabilized tetragonal zirconia polycrystal (Y-TZP) has emerged in dentistry as a promising material for various applications such as multi-unit, crowns, onlays, inlays, and implant structures, due to aesthetic outcomes such as color and opacity that mimic a natural teeth appearance (STADLINGER *et al.*, 2010). Zirconia-based materials have been claimed as a biomaterial with a high chemical stability that avoid the release of toxic products to the surrounding tissues (PICONI; MACCAURO, 1999; YIN *et al.*, 2017). Y-TZP provides stimulation of osteogenic cells during osseointegration in combination with unique mechanical characteristics such as high fracture toughness, fatigue resistance, high bending strength, high corrosion resistance, and radiopacity (BONA; PECHO; ALESSANDRETTI, 2015; ZHANG, 2012a). Additionally, some studies have shown that zirconia decrease bacteria adhesion and biofilm accumulation leading to low risk of inflammatory reactions in adjacent peri-implant tissues (KOHAL *et al.*, 2016; SCARANO *et al.*, 2003). Moreover, recent in vitro and in vivo studies have demonstrated that zirconia implants have similar results regarding osseointegration indexes when compared to titanium-based implants (ALBREKTSSON; HANSSON, 1985; DEPPRICH *et al.*, 2008; DUBRUILLE *et al.*, 1999; GAHLERT *et al.*, 2012; KOHAL *et al.*, 2004; KUBASIEWICZ-ROSS; HADZIK; DOMINIAK, 2018). Nevertheless, corrosion and the greyish colour of titanium are both considered as disadvantage since that can affect the health state and appearance of the peri-implant tissues, causing aesthetic drawbacks (KAROUSSIS *et al.*, 2003; MARECI *et al.*, 2016).

In implant dentistry, osseointegration is a biological dynamic process leading to the direct contact of bone tissue to the implant surface that depends on factors related to the implant, surgical site, bone type, and patient conditions (ALBREKTSSON; WENNERBERG, 2004; DEPPRICH *et al.*, 2008; HAN *et al.*, 2016, 2014). The bone to

[1] Published at Materials Science & Engineering C (Impact Factor: 7.328) in January 2019.

implant contact (BIC) can be measured by histomorphometric analyses at different time points over the period of osseointegration (ALBREKTSSON; WENNERBERG, 2004; BOSSHARDT; CHAPPUIS; BUSER, 2017; BRÅNEMARK *et al.*, 1969; GAHLERT *et al.*, 2012; HAN *et al.*, 2014). Previous studies have reported similar results for bone healing surrounding zirconia or titanium implants (DUBRUILLE *et al.*, 1999; KOHAL *et al.*, 2004; SCARANO *et al.*, 2003). However, zirconia-based surfaces have revealed a lower number of bacteria when compared to titanium implant surfaces regarding microbiological assays (ROEHLING *et al.*, 2017; SCARANO *et al.*, 2004). Despite the favorable findings recorded for zirconia-based surfaces, clinical long term results are still lacking and some controversies towards zirconia osseointegration are still being debated. Some previous studies have reported high failure rates and zirconia peri-implant crestal bone loss in human studies (KOHAL *et al.*, 2016). Also, zirconia has been claimed as an inert biomaterial (PICONI; MACCAURO, 1999; YIN *et al.*, 2017) although the adsorption of blood protein, platelets and migration of osteogenic cells suggest a biological interaction with zirconia-based surfaces. That should be further studied considering chemical bonding and the deterioration of zirconia. Even though zirconia implants offer aesthetic benefits over titanium implants, titanium-based materials still possess higher mechanical strength over zirconia and it is currently the first-choice material for dental implants. Nevertheless, implant technology has devoted significant efforts to modify zirconia regarding morphological and bioactive aspects that is desirable for an appropriate cell attachment, proliferation, and differentiation during the surrounding bone healing (PARDUN *et al.*, 2015; YIN *et al.*, 2017). On improving zirconia surfaces, several physicochemical methods have been used such as: grit blasting (BACCHELLI *et al.*, 2009), laser treatment (MOURA *et al.*, 2017), micro-machining, CVD, and PVD. The development of coatings composed of silica, magnesium, graphene, dopamine, and bioactive molecules has been assessed although the development of a functionally graded material for implants has shown an enhancement in mechanical behavior and biological response (MOURA *et al.*, 2017).

Thus, the aim of this study was to perform a literature review on current surface modification techniques to enhance the biological and osseointegration behavior of zirconia-based implants in dentistry.

2.2. Search strategy

A literature review was performed on PUBMED database to identify relevant studies regarding zirconia surface treatment to enhance osseointegration. The electronic search was performed using the following combination of key words and MeSH terms: “zirconia surface treatment” OR “zirconia surface modification” OR “zirconia coating” AND “osseointegration” OR “biological properties” OR “bioactivity” AND “mechanical properties” OR “functionally graded properties”. The inclusion criteria used for this review involved clinical trials, meta analyses, in vivo, and in vitro studies written in English language up to May 2018. Three of the authors (BH, MEG, FHS) independently evaluated the titles and abstracts of potentially relevant previous studies. Selected studies were individually read and analyzed concerning the focus of the present review, which was to discuss and summarize important key publications regarding zirconia surface modifications for dental implants. Author names, journal, publication year, objectives, methods, and main outcomes were retrieved from the selected relevant articles.

2.3. Results and discussion

Previous studies have reported that zirconia surface modification influences the adhesion, proliferation, morphology, and differentiation of fibroblasts and osteoblasts leading to the osseointegration of implant surfaces (ALTMANN *et al.*, 2017; SANON *et al.*, 2015). The understanding of surface physicochemical modifications on the biocompatibility and osseointegration measured by histomorphometric analyses have been evaluated to predict the clinical outcome and peri-implant tissue stability over time (COELHO *et al.*, 2015; LIU *et al.*, 2015). Accordingly, a large number of methods have been developed to change dental implants physicochemical properties to speed up the early and late bone-to-implant response (ALBREKTSSON; WENNERBERG, 2004) as shown in Figure 1 and Table 1.

Figure 1 - Schematics and SEM images on different zirconia surface modifications: machined (LIU *et al.*, 2015), acid etched (QUENTINFLAMANTA *et al.*, 2016), grit blasted (LIU *et al.*, 2015), ZLA (ROEHLING *et al.*, 2017), and multi-layered coatings (KAROLINE PARDUN *et al.*, 2015; LARANJEIRA *et al.*, 2014; LIU *et al.*, 2015).

Table 1 - BIC percentage and roughness values among machined surface, grit blasted surface, acid etched surface, laser, and UV light modified zirconia surface after different time points.

Authores	*In vivo* study	Surface treatment	Roughness (µm)	BIC (%)	Weeks
(SCARANO *et al.*, 2003)	Rabbit	Machined	–	68.4 ± 6 2.4	4
(KIM *et al.*, 2017)	Rabbit	Machined	–	32.15 ± 10.8	4
(ABOUSHELIB; SALEM; MONEIM, 2013)	Rabbit	Machined	–	62.14 ± 2.8	6
(HAN *et al.*, 2016)	Rabbit	Machined	0.788	78.9	8
(HOFFMANN *et al.*, 2012)	Rabbit	Machined	–	33.74 ± 14.5	12
(KOCH *et al.*, 2010)	Dog	Machined	–	59.11 ± 7.5	4
(MONTERO *et al.*, 2015)	Dog	Machined	0.85 ± 0.04	57 ± 15.2	20
(THOMA *et al.*, 2015)	Dog	Machined	–	87.7 ± 25.1	24
(HOFFMANN *et al.*, 2012)	Rabbit	Grit blasted	–	41.350 ± 15.8	12
(SCHLIEPHAKE *et al.*, 2010)	Minipig	Grit blasted	0.98	54.6 ± 17.6	13
(SCHLIEPHAKE *et al.*, 2010)	Minipig	Grit blasted and acid etched	1.162	57.6 ± 23.7	13
(KOHAL, Ralf J. *et al.*, 2004)	Monkey	Grit blasted	–	67.4 ± 17	36
(BACCHELLI *et al.*, 2009)	Sheep	Grit blasted	1.67 ± 0.08	75.1 ± 4.2	12

(GAHLERT *et al.*, 2012)	Pig	Acid etched	0.63 ± 0.05	63 ± 21.5	12
(DEPPRICH *et al.*, 2008)	Minipigs	Acid etched	0.598	71.4 ± 17.8	12
(LINARES *et al.*, 2016)	Minipigs	Grit blasted and acid etched	–	86.24 ± 9.7	8
(JANNER *et al.*, 2018)	Dog	Grit blasted and acid etched	–	71.15 ± 7	16
(KUBASIEWICZ-ROSS; HADZIK; DOMINIAK, 2018)	Minipigs	Grit blasted Acid etched Grit blasted & etched	–	66.75 72.9 68.8	8
(CALVO-GUIRADO *et al.*, 2015)	Dogs	Laser modified	–	47.9	12
(DELGADO-RUIZ *et al.*, 2015)	Dogs	Laser modified (femtosecond laser)	–	60.34 ± 4.3	8
(DELGADO-RUIZ; CALVO-GUIRADO, 2014)	Dogs	Grit blasted Laser modified (femtosecond laser)	2.83 ± 0.2 9.6 ± 0.62	48 ± 3 78 ± 5	8
(CALVO-GUIRADO *et al.*, 2014)	Dogs	Laser modified	–	65 ± 4.4	12
(HOFFMANN *et al.*, 2012)	Rabbit	Laser modified	–	43.87 ± 14.5	12
(BREZAVŠˇCEK *et al.*, 2016)	Rat	UV light (15 min) machined UV light (15 min) rough	0.12 ± 0.02 0.21 ± 0.08	52.7 86.5	4

(–) absent data in the study.

2.3.1. Machined zirconia implants

Implant dentistry chronological records have reported the success and favourable histologic outcomes of titanium machined dental implants over a period of 50 years (YIN *et al.*, 2017). As follows, machined zirconia implant have been studied showing promising results on the enhancement of osseointegration and an additional antibacterial activity. Scarano et al. examined BIC of machined zirconia implants fort 4 weeks and reported a BIC percentage of around 68.4% without the presence of inflammatory or multinucleate cells claiming that machined zirconia implants can be highly biocompatible and osseointegrated (SCARANO *et al.*, 2003). Hafezeqoran et al. compared the BIC percentage of machined zirconia and titanium dental implant from previous studies. Such previous review article reported statistically equivalent BIC values for machined zirconia (33.74 - 84.17%) compared to machined titanium

implants (31.8 - 87.95%). Consequently, the study concluded that machined zirconia implants can be as osseointegrated as machined titanium implants (HAFEZEQORAN; KOODARYAN, 2017). The BIC percentage range of machined zirconia implants analyzed in histological studies can be seen in Table 1. The highest BIC percentage value corresponded to a study (THOMA *et al.*, 2015) which evaluated zirconia implants for 6 months while the lowest BIC values (87%) were related to evaluation for 4 weeks after surgery (KIM *et al.*, 2017). Thoma et al. (2015) showed that non-modified zirconia implants had a statistically similar BIC percentage and peri-implant soft tissue dimensions to acid etched-grit blasted titanium implants although zirconia implants exhibited a considerable fracture rate after 6 months of loading (THOMA *et al.*, 2015).

Considering antibacterial response, Roehling et al. investigated multi-species biofilm adherence on zirconia machined (Y-TZP) surface compared to pure titanium machined surfaces. A statistically significant decrease in the biofilm thickness was noticed on zirconia-based surfaces when compared with titanium machined surfaces (ROEHLING *et al.*, 2017).

2.3.2. Grit blasted and acid etched zirconia surface treatment

Previous studies have reported that airborne particle abrasion known as grit blasted surface treatment followed by acid-etching (SLA treatment) can increase the surface area of zirconia implants for osseointegration (FISCHER; SCHOTT; MÄRTIN, 2016; KOHAL, Ralf J. *et al.*, 2004) (Table 1). The grit blasting process with 50- 110 μm Al_2O_3 particles, has been shown as an alternative to increase the surface area for osteoblasts attachment and then to speed up the osseointegration process. For Gahlert et al., (GAHLERT *et al.*, 2007) and Bacchelli et al., (BACCHELLI *et al.*, 2009), grit blasting zirconia implant surfaces significantly improved the peri-implant osteogenesis and osseointegration when compared to machined titanium surfaces. Gahlert et al. (2007) recorded the removal torque on 64 implants, including zirconia grit blasted with Al_2O_3 particles, machined zirconia, and grit blasted titanium (with 0.2–0.5 μm Al_2O_3) structures. The results showed significantly higher removal torque values for grit blasted zirconia (40.5 N/cm) and titanium (105.2 N/cm) than those recorded on machined zirconia (25.9 N/cm) surfaces (BACCHELLI *et al.*, 2009).

Other studies have shown different results. Kohal et al. (2004) investigated the osseointegration on unloaded zirconia implants compared to titanium implants for five

months after tooth extraction. The titanium implant surfaces were grit blasted with Al_2O_3 and acid etched (H_2O_2/HF) while zirconia implants were only grit blasted with 50-µm Al_2O_3/50 µm. The results showed that the mean height of the soft periimplant tissue cuff was 5 mm around the titanium implants and 4.5 mm around the zirconia implants. The BIC was around 72.9% on titanium implants and 67.4% on zirconia implants. Within these results, the mentioned study concluded that grit blasted zirconia implants revealed similar integration to bone and peri-implant soft tissue dimensions when compared to SLA titanium implants (KOHAL *et al.*, 2004).

Moreover, grit blasting has been performed with additional chemical treatment such as: hypo-phosphorous acid, and the mixture of KOH and NaOH to improve BIC of zirconia. Though, hydrofluoric acid (HF) etching appears to be the first choice to enhance bone apposition resulting in higher implant removal torque values (GAHLERT *et al.*, 2010; QUENTINFLAMANTA; *et al.*, 2016). The incorporation of fluoride at the ceramic surface could enhance osteoblastic differentiation and interfacial bone formation, as found for fluoridated titanium surfaces (COOPER *et al.*, 2006; THOMPSON *et al.*, 2011; VU *et al.*, 2017). A commercially zirconia implant treated with HF etching showed BIC at 81% (OLIVA; OLIVA 2010).

Besides, other studies have reported the effect of acid etching treatment on zirconia surfaces and its impact on biofilm adhesion. Depprich et al. (2008) compared the BIC percentage for 24 Y-TZP acid etched implants (Ra at 0.598 µm) with 24 acid etched titanium implants (Ra at 1.77 µm). The peri-implant tissues were histologically inspected for 1, 2, and 4 weeks. A significant BIC increase was observed on acid etched zirconia implants when compared to titanium implants (DEPPRICH *et al.*, 2008). Also, Roehling et al. (2017) reported a decrease in biofilm growth on grit blasted and acid etched zirconia surface (ZrO_2-ZLA) when compared to titanium grit blasted titanium surface (Ti-SLA) (ROEHLING *et al.*, 2017).

In another study, zirconia disks were acid etched in 5%, 20%, and 40% HF for 30 min, 1 h and 2 h (FLAMANT *et al.,* 2016). A standard and faster roughening was achieved in 40% HF for 60 min, although the mechanical properties of the zirconia was not assessed. In that study, the etching at 40% HF dissolved zirconium and yttrium oxide producing fluoride, and hydroxide complexes. Yttrium oxides have very low solubility in 40% HF leading to the precipitation of yttrium trifluoride octahedral crystals on the surface. Yet, zirconium oxides are partially soluble an bonded to yttrium, zirconium and fluoride precipitates, probably due to the saturation threshold for

zirconium fluoride complexes (FLAMANT; ANGLADA, 2016). Oh et al. (2017) tested HF in two concentrations (10% and 20%) and in different time points (1, 2, 10, and 60 min) on pure zirconia, porcelain, and in bioactive glass that was infiltrated into pre-sintered zirconia. The roughness of zirconia was not affected by the etching time or the acid solution concentration although etched bioactive glass-infiltrated zirconia revealed similar surface topographic aspect when compared to grit blasted/acid-etched titanium (OH *et al.*, 2017).

Hempel et al. (2010) cultured SAOS-2 osteoblasts cells on grit blasted, grit blasted/etched zirconia and compared with grit blasted/ etched titanium. The findings showed an increase in adhesion, spreading, and differentiation of SAOS-2 cells when compared with titanium. However, there was no significant differences between zirconia surface modifications (HEMPEL *et al.*, 2010). Additionally, Bergnmann et al. compared the osteogenic genetic marker for human primary osteoblasts on different zirconia surfaces: machined, grit blasted, acid etched/grit blasted and acid etched/grit blasted/heated with machined titanium implants. The previous study showed that both acid etched surfaces with Ra roughness values of around 1.3 μm had a drastically increase of osteocalcin expression and cell adherence when compared with machined titanium (Ra at 0.54 μm) and machined zirconia (Ra at 0.59 μm). In fact, higher roughness values corresponded to acid etched surfaces with a more favourable area for osteoblasts adhesion (BERGMANN *et al.*, 2015). The roughness values recorded in the previous studies corresponded to the moderate rough titanium implants that has been claimed to promote a high BIC percentage and successful osseointegration in previous in vivo studies (WENNERBERG; ALBREKTSSON, 2009).

An in vivo study reported the BIC percentage around zirconia implants after surface conditioning in different solutions. HF acid etching and immersion in NaOH and KOH was compared regarding the enhancement of osseointegration and therefore the BIC percentage was higher for the etched surfaces in HF. That surface treatment induced the proliferation of multinucleated giant cells around the implant surfaces (SAULACIC *et al.*, 2014). Liñares et al. (2016) compared nine different zirconia or titanium implants considering the following surface treatment to bone integration in minipig mandibles: grit blasting with large grits of 250–500 μm and acid etched with HCl/ H_2SO_4. BIC percentage of the titanium implants was around 84% while zirconia revealed a BIC around 86.2%. Additionally, gingival tissue around zirconia implants showed higher organization of collagen fibres and lower sulcus depth measurements

than that inspected around titanium. That suggested a mature and organized peri-implant soft tissue around zirconia implant surfaces (LINARES *et al.*, 2016).

Even though the described surface treatment has provided surface topographic and biological advantages, the mechanical properties of treated zirconia can change and affect the clinical long-term performance of the implant. The strength and phase transformation of grit blasted zirconia has been questioned by previous studies (AURÉLIO *et al.*, 2016; FISCHER; SCHOTT; MÄRTIN, 2016; ZHANG *et al.*, 2006). Grit blasting can induce stress concentration and consequently a transition from tetragonal to monoclinic phase. Thus, this phase transition can improve zirconia mechanical properties due to the introduction of compressive stress, but can also cause degradation of zirconia affecting density and mechanical stability (FISCHER; SCHOTT; MÄRTIN, 2016). A systematic review reported that the flexural stress of grit blasted yttria-stabilized zirconia increased, regardless abrasion factors and aging effect (AURÉLIO *et al.*, 2016). Studies have also reported that grit blasting decrease the fatigue resistance of zirconia (ZHANG *et al.*, 2006). A study showed that grit blasting zirconia with 105 μm alumina, HF acid etching, and 1 h of heat treatment is a reliable process to increase zirconia Ra roughness to 1.2 μm which is comparable to the standard titanium roughness (Ra at 1.5 μm) that can support a successful osseointegration rate (WENNERBERG; ALBREKTSSON, 2009). That study showed an increase of the zirconia flexural strength after grit blasting, although the fatigue strength was not assessed (FISCHER; SCHOTT; MÄRTIN, 2016; WENNERBERG; ALBREKTSSON, 2009). As a matter of fact, the strength of zirconia might be reduced by particle abrasion, since that can cause deep micro-cracks. Any compression caused by particle abrasion can strengthen and inhibit micro-crack extension due to zirconia phase transformation supporting the results from previous studies on the benefits of grit blasting (AURÉLIO *et al.*, 2016; FISCHER; SCHOTT; MÄRTIN, 2016). Nevertheless, Zhang et al. have shown in their study that the compressive stresses caused by grit blasting are not enough to counteract the strength loss caused by micro-cracks specially under high static load and fatigue tests which resemble real clinical conditions (ZHANG *et al.*, 2006). Clinically, zirconia implants should be grit blasted with soft and round particles, avoiding the use of sharp particles to decrease the formation of micro-cracks. Further studies involving fatigue tests are required to evaluate grit blasting parameters to attain a desired roughness and to decrease micro-crack formation (FISCHER; SCHOTT; MÄRTIN, 2016; ZHANG *et al.*, 2006).

Other studies have also revealed that heat and acid treatment can decrease zirconia flexural strength due to tetragonal to monoclinic phase transformation and low temperature degradation conditions (SATO *et al.*, 2008; SRIAMPORN *et al.*, 2014). In a recent study, Xie et al. evaluated the effects of three types of acid treatment on zirconia. Hydrofluoric (HF), acetic, and citric acid were tested at different concentrations. HF was the most efficient acid to increase roughness, however, 40%HF treatment at room temperature decreased considerably the surface hardness and flexural strength of the samples. As follows that study concluded that the acid concentration should be maximum 5%HF to avoid any potential damage to zirconia mechanical structure (XIE *et al.*, 2015). Fischer et al. showed that zirconia strength decreased after HF etching for 4 h while etching for 1 h was recommended although a short time of etching could not improve the morphological aspects of zirconia implants (XIE *et al.*, 2015). Even though acid etched zirconia has been claimed as a promising material that enhances osseointegration, further studies are suggested to determine etching conditions without affecting the mechanical behavior of zirconia.

2.3.3 Ultraviolet light treated zirconia

Regarding in vitro and in vivo studies, UV light treatment has been claimed to be an effective zirconia surface treatment to enhance the attachment, proliferation, and differentiation of osteoblast without affecting zirconia mechanical properties (BREZAVŠˇCEK *et al.*, 2016; HENNINGSEN, A. *et al.*, 2018). UV light can induce electron excitation, increasing zirconia surface energy. Henningsen et al. reported an increase in wettability of zirconia surfaces treated by UV light to an ultra-hydrophilic state. The water contact angle of grit blasted zirconia surfaces decrease from 51° down to 9.4° after UV light treatment, as seen in Table 2 (HENNINGSEN, Anders *et al.*, 2018). The fact that UV treatment increases zirconia wettability was also supported by another previous study testing UV light for 15 min (BREZAVŠˇCEK *et al.*, 2016). Additionally, histomorphometric analysis revealed that UV treated zirconia specimens had a faster osseointegration process and higher BIC percentage (86.5%) when compared to untreated zirconia for 2 and 4 weeks of implantation. After 4 weeks, untreated samples had still fibrous connective tissue at the implant-bone interface while UV treated samples were almost entirely surrounded by bone (Table 1). Another study showed that UV treated zirconia became super-hydrophilic and increase human

alveolar bone derived osteoblasts attachment and spreading after 21 days when compared to untreated samples concluding that UV treatment can induce faster healing and higher BIC percentage (YANG *et al.*, 2015). Even though, some studies have suggested that UV surface treatment is a promising strategy to promote bone morphogenesis around zirconia implants, additional in vivo studies are required to validate such concept (BREZAVŠˇCEK *et al.*, 2016; TUNA *et al.*, 2015).

Table 2 - Water contact angle and wettability measured in several studies for different types of zirconia surface treatment.

Author	Materials	Treatment	Contact angle (degree)	Wettability	Observations
(AL-RADHA *et al.*, 2012)	Titanium	Polished titanium	74.32 ± 1.34	Hydrophilic	Gritblasting: Zirconia powders with particle size ≤44 µm; 4.5 bar; 3 cm distance
		Titanium blasted with zirconia	87.3 ± 5	Hydrophilic	
		Titanium blasted with zirconia/acid etched	131.51 ± 1.5	Hydrophobic	
(CHO *et al.*, 2015)	ZrO_2-TZP-A-HIP (Y, Nb) - TZP and (Y, Ta) –YZP.	Polished	82.79 ± 2.1	Hydrophilic	Acid etching: 0.2 wt% hydrofluoric acid for 1.5 min
		HA Film by Aerosol Deposition: ~10 µm	6 3.72 ± 2.55	Hydrophilic	Gritblasting: 50 µm Al_2O_3 at 2 bar and 1 bar
		Non-coated zirconia surfaces (sandblasted)	95.0 ± 3.21	Hydrophobic	
(LIU *et al.*, 2015)	Y-ZrO_2 (Zenostar)	Polished + polydopamine coating	64 ± 1	Hydrophilic	HA Film by Aerosol Deposition: ~10 µm Zirconia: Zenostar, Wieland Dental, German dopamine solution: (2 mg/mL in 10 mM Tris-HCl, pH 8.5) and gently shaken for 24 h at room temperature
		Uncoated (Polished)	78 ± 4	Hydrophilic	
(YANG *et al.*, 2015)	Y-ZrO_2 (Zenostar)	Polished + UV light treatment	33.76	Hydrophilic	Zirconia: Zenostar, Wieland Dental, German

		Polished	51.98	Hydrophilic	UV light; 24 h; 10-W bactericidal lamp; 17 mW/cm2 Gritblasting: (Al_2O_3) particles (25 μm) from a distance of about 20 mm at 0.2 MPa
		Sandblasted + UV light treatment	36.15	Hydrophilic	
		Sandblasted	63.87	Hydrophilic	
(MOURA, C *et al*. 2017)	3Y-TZP	As sintered	46.9 ± 5	Hydrophilic	Gritbasting: Al_2O_3; 100 μm particles; 6 bar; 10 mm distance Etching: hydrofluoridine acid (48%) for 30 min; Laser: Nd: YAG laser
		Sandblasting and etching treatment	44.6 ± 3	Hydrophilic	
		Laser irradiation (0.9 W)	38.2 ± 1	Hydrophilic	
		Laser irradiation (1.8 W)	36.4 ± 1	Hydrophilic	
(HENNINGSEN, A. *et al.*, 2018)	Titanium grade IV	Sandblasted + acid etched	111	Hydrophobic	Gritblasting: ZrO_2 particles UV light at λ = 360 nm (0.05mWcm−2) and λ =250 nm (2 mW cm−2) Non-thermal plasma of either Argon and oxygen using a non-thermal plasma reactor
		UV	12.8	Super-Hydrophilic	
		O_2-Plasma	0	Super-Hydrophilic	
		Ar-Plasma	0	Super-Hydrophilic	
	5Y-TZP	Zirconium dioxide blasted	51	Hydrophobic	
		UV	9.4	Super-Hydrophilic	
		O2-Plasma	4.2	Super-Hydrophilic	
		Ar-Plasma	2.9	Super-Hydrophilic	

2.3.4. Zirconia laser modification

Laser treatment is a promising alternative to modify and to enhance zirconia osseointegration (HENNINGSEN *et al.,* 2018; TUNA *et al.,* 2015; LIU *et al.,* 2013; YANG *et al.,* 2015; PARRY *et al.,* 2011). Hoa et al. used a CO_2 laser to modify Y-TZP surfaces and possibly achieve a higher osseointegration index. The defocused CO_2

laser beam was traversed in single time across the Y-TZP surface at different intensities, namely 1.80 and 2.25 kW/cm^2. The CO_2 laser treatment decrease the roughness of the samples from 0.35 μm down to 0.2 μm although that increased the surface energy and consequent wettability of the surface (HAO *et al.,* 2005).

Moura et al. reported the influence of surface texturing on Y-TZP by laser treatment compared to different surface modifications: as sintered sample (AS), grit blasting and acid etching treatment (SE), laser irradiation using two output power of 0.9 W (LI) and 1.8 W (LII). The surface was analyzed by SEM/EDS, water contact angle, friction test by bone plates, and roughness analysis. The water angle contact of laser treated Y-TZP was 36.4° (LI) and 38.2° (LII) while the AS and SE groups showed higher water contact angle values (46.9° ± 5° for AS and 44.6° ± 3° for SE) that showed a lower hydrophilicity. In fact other in vitro studies have shown that CO_2 laser modified zirconia increases osteoblast (hFOB) adherence when compared to untreated samples (HAO *et al.,* 2005). It is important to take in consideration that material water contact angles lower than 90° are considered hydrophilic, and < 20° are super hydrophilic. As follows, lower water contact angle mean values the material has a higher wettability, which is biologically a more attractive surface for osteoblast proliferation, protein adsorption, and osseointegration (HOTCHKISS *et al.,* 2016). The water contact angle and wettability measured in several studies for different types of zirconia surface modifications are shown in Table 1.

Furthermore, laser treatment has been applied to promote microgroove surfaces on zirconia implants. The micro texture could change the collagen fiber organization, peri-implant bone architecture, and human cell metabolism. Studies have shown that surfaces with a regular geometry in the micro-range can increase osteoblast proliferation, adhesion, spreading, and synthesis of matrix protein (CALVO-GIRADO *et al., 2015).* Delgado Ruiz et al. 2015 treated zirconia through femtosecond laser to produce a micro-grooved surface with symmetric microstructures. An animal study showed that laser treated micro-grooved zirconia implants had a high number of transverse collagen fibers and an increased bone remodelling when compared to grit blasted zirconia implants which had parallel collagen fibers and acid-etched titanium implants but low bone remodelling rates. The difference among bone remodelling rates after 4 months of loading could be explained by the presence of blood vessels and bone cells that penetrated in micro-groved zirconia surfaces, which accelerated the osseointegration rate. Also, the presence of transverse collagen fibers results in a

favorable stress distribution environment on loaded implants (DELGADO-RUIZ *et al.,*2015*)*. Laser treated micro-grooved zirconia implants show promising results, however further studies involving humans are required for clinical validation.

2.3.5. Coatings on zirconia

Implant dentistry innovations face the primordial challenge of enhancing biological and mechanical properties of implants by approaches like implant coating. Different coatings on zirconia surfaces have been developed to enhance biocompatibility, antibacterial potential, and bioactivity. Bioactive coatings on zirconia have demonstrated advantages for bioactivity, since they have the ability to induce hydroxyapatite formation in a biological environment, that is essential for subsequent bone proliferation. In literature, different coating materials with favourable biologic properties have been described, such as: silica, magnesium, nitrogen, carbon, calcium phosphate, hydroxyapatite, dopamine, and graphene (PARDUN *et al., 2017;* LI *et al.,* 2014; OH *et al., 2017;* WANG *et al.,* 2010; CHEN *et al.,* 2008; SCHIENLE *et al*., 2015; PARDUN *et al*., 2015; LIU *et al.,* 2013).

Laranjeira et al. compared the in vitro behavior of fibroblast adherence and antibacterial effect on different types of silica-coated micropatterned zirconia surfaces. The study results showed that silica coated zirconia samples with different surface morphological aspects reduced bacterial adhesion. Microstructured bioactive coating can also be an efficient strategy for fibrin network formation, cell growth, and improved soft tissue adherence since it enhances the adsorption of proteins and cell migration (LARANJEIRA *et al.,* 2014*)*. Additionally, Kirsten et al. analysed a novel glass composition (PC-XG3) zirconia coating and its in vitro bioactivity using the simulated body fluid (SBF) immersion test. Smooth and microstructured glass coatings were applied on zirconia implants, which showed a strong adhesion to the zirconia substrate and a significant increased in vitro bioactive behavior after SBF immersion (KIRSTEN *et al.,* 2015). Consequently, silica coatings can increase the zirconia bioactivity promoting hydroxyapatite formation when in contact with body fluids which would stimulate osteoblast proliferation on the implant surface (CATAURO *et al.,* 2015).

*2.3.*6. Magnesium, nitrogen, and carbon coatings

Studies have reported that magnesium (Mg) coatings favor osteoblast proliferation, increasing the zirconia bioactivity (MUSHAHARY *et al.,* 2014). Pardun et al. 2017 reported the influence of Mg addition to zirconia-calcium phosphate and found that Mg-containing coatings promoted a higher cell proliferation and differentiation in comparison to zirconia-calcium phosphate coatings. Microstructural analysis confirmed a porous and a stable coating adhesion not hampered by its composition. Other studies have shown that magnesium-calcium coatings increased the bioactive potential of zirconia. That showed a multi-layered hydroxyapatite (HA) precipitate revealing a “cauliflower” morphology after 7 days of SBF immersion (PARDUM *et al.,* 2015; EWAIS *et al.,* 2017). Moreover, the addition of other elements like nitrogen and carbon have improved the biological and mechanical properties of zirconia (GARMENDIA *et al.,* 2008). Another study showed a high hydrophilicity, bioactivity, and antibacterial potential for zirconia containing a nitrogen-doped hydrogenated amorphous carbon (a-C:H:N) layer. Schienle et al. tested the bacterial adherence to 3Y-TZP with a carbon (a- C:H:N) coating and quantified the adherent microorganisms by estimating the colony-forming unit (CFU) analysis. The a-C:H:N coated Y-TZP surfaces revealed a low adhesion of bacteria on the surface compared to uncoated surfaces (SCHIENLE et al., 2015). Other studies have also coated zirconia with functionalized carbon nano-tubes increasing the roughness, wettability, and cell adhesion of the material favouring zirconia's osseointegration properties (GARMENDIA *et al.,* 2008; KOU *et al.,* 2013).

2.3.7. Hydroxyapatite and calcium phosphate based coatings

Hydroxyapatite (HA) has a similar mineral composition to that of bone, and thus shows bioactive properties favouring tissue response that enhances osseointegration. HA has been used to coat zirconia in order to convert highly stable implant surface into a bioactive one, thus enhancing osseointegration features. Porous zirconia scaffolds coated with HA have been used as a drug delivery system to enhance bone response and assure proper osseointegration (CHO *et al.,* 2015; NALEWEY *et al.,* 2016; LAVOS-VALERETOI *et al.,* 2001). Aboushelib and Shawky evaluated the

osteogenesis ability of CAD/CAM porous zirconia scaffolds enriched with HA. Results revealed a significantly higher volume of new bone formation (33 ± 14%) on HA enriched zirconia scaffolds compared to those of scaffolds free of HA (21 ± 11%), therefore, demonstrating the HA coating enhanced osteogenesis ability of porous zirconia scaffolds (ABOUSHELIB and SHAWKY 2017). Pardun et al., obtained coatings by mixing Y-TZP and HA on various ratios. An increasing content of calcium phosphate resulted in a decrease of the mechanical and chemical stability of the material, while the bioactivity increased after immersion in simulated body fluid. As follows, the author demonstrated excellent interfacial bonding, mechanical strength, and the bioactivity potential of coatings with higher tetragonal zirconia contents (PARDUM *et al*., 2015).

Calcium phosphate is also considered bioactive and thus stimulate bone repair due to their chemical composition close to that of the mineral phase of bone commonly named biological apatite. However, calcium phosphate coatings exhibit a poor stability and provide a weak bonding strength to the substrate. To overcome those drawbacks of calcium phosphate coatings, studies used tricalcium phosphate reinforced hydroxyapatite (HA/TCP) coatings over zirconia surfaces, with open pores larger than 100 μm, a bonding strength of 24 MPa showing a high interfacial bonding between coating and substrate. Additionally, those coatings exhibited absorbable and osteoconductive properties (LE RAY *et al.,* 2010; YANG *et al.,* 2013).

2.3.8. Dopamine

Dopamine, precursor of 3,4-dihydroxy-L-phenylalanine (L-DOPA), was found to be an important component in the adhesive structure of mussels as it can self-cure and adhere strongly to a wide range of organic and inorganic materials (LEE *et al.,* 2008*)*. Polydopamine (PDA) coatings can enhance antimicrobial properties and facilitate the protein adsorption and cell adhesion, accelerating biological processes such as osseointegration (XU *et al.,* 2016). The influence of novel PDA coating on zirconia disks regarding soft-tissue integration and antibacterial effect was explored by a previous study (LIU *et al.,* 2015). Such study evaluated modified surface zirconia with PDA. The surface topography of zirconia coated with PDA can be seen by atomic force microscopy (AFM) and SEM inspection as shown in Figure 1 and Figure 2. The polydopamine coating decreased significantly the bacterial activity and enhanced

fibroblasts adherence, that has an important role in peri-implant soft-tissue integration. Therefore, such surface modification approach holds great potential for improving softtissue integration around zirconia abutments. Additionally, another study reported the coating of zirconia with L-DOPA which was a dopamine-derived residue secreted by marine mussels to enhance the biocompatibility and osteogenic response of zirconia. The preliminary results of this study showed that L-DOPA coated specimens had a higher osteoblast proliferation and spreading when compared to uncoated specimens (LIU *et al.,* 2013).

2.3.9. Graphene coatings

Graphene has been the precursor of a novel multifunctional material that can act as a biocompatible surface coating to improve implant tribological properties and reduce wear (PRIYADARSINI *et al.,* 2018; XIE *et al.,* 2015; CHO *et al.,* 2013). Li et al. 2014 prepared zirconia/graphene (ZrO_2/GNs) composite coatings with a thickness of 5–20 nm using an atmospheric plasma spray system. It was noticed that the wear behavior rate of ZrO_2/GNs reduced down to 1.17 × 10−6 mm3 /N m on 100 N normal loading, which resembled to a 50% decrease compared with the control group (ZrO_2 specimens). Moreover, the results indicated that the ZrO_2/GNs composite coating exhibited excellent wear resistance and low coefficient of friction with the addition of GNs. A GNs-rich transfer layer protected the ZrO_2/GNs composite coatings from severe wear by brittle microfracture, which significantly improved its tribological behavior (LI *et al.,* 2014). Further studies should consider graphene to improve zirconia mechanical performance mainly regarding wear resistance in implant dentistry.

2.3.10. Bioactive graded zirconia-based structures

Zirconia-based materials have a high elastic modulus, high chemical stability in human body, and desirable optical properties for aesthetic outcomes. Nevertheless, the high elastic modulus results in stress shielding of the hard tissue, leading to local bone resorption. Bioactive ceramics (e.g. calcium phosphate ceramics, bioactive glasses) are reactive to the surrounding medium and stablish chemical bonds with adjacent tissues (FERRARIS *et al.,* 2012). Also, those bioactive materials exhibit comparable modulus to hard tissues (bone, enamel, or dentin), which mitigates the stress shielding problems. Unfortunately, bioactive ceramics are relatively weak and thus structurally unstable, which hinders their use in load bearing applications (e.g. dental and orthopedic implants) (ZHANG *et al.,* 2010).

Attempts have been conducted to produce bioactive glass coatings on zirconia substrates but with limited success. These coatings often undergo delamination and fracture caused by the coating/substrate bonding issue, mismatch in coefficient of thermal expansion (CTE), and the abrupt changes in physical properties at the coating/substrate interface. To overcome such issues, Zhang et al 2014 proposed a

bio-inspired strategy regarding transition in chemical composition and properties, as seen in Figure 3 (FABRIS *et al.,* 2016; HENRIQUES *et al.,* 2017). That strategy relies on a functionally graded calcium phosphate-based glass/zirconia (CPG/Y-TZP) system with a low elastic modulus and a flexural strength similar to, or even higher than that recorded for Y-TZP (ZHANG *et al.,* 2010; ZHANG *et al.,* 2012)

The osteoconductive CPG coating can speed up the osteointegration process and prevents micromotion at the implant/tissue interface (ZHANG *et al.,* 2012a; [4,104,111]. In addition, the residual outer surface CPG layer acts as an encapsulation layer, preventing hydrothermal degradation of the Y-TZP interior. Also, CPG can be further transformed to a carbonate apatite (CHA) layer by immersing in mineral precipitate solution or simulated body fluid (SBF) since the newly formed bone is directly attached to a CHA layer. Despite the aforementioned advantages of this system, there is only a few studies on CPG/Y-TZP, contrasting to a vast literature on glass infiltrated zirconia structures (ZHANG *et al.,* 2014a; ZHANG *et al.,* 2009; FABRIS *et al.*, 2017; FABRIS *et al.,* 2016; HENRIQUES *et al*., 2017; ZHANG *et al.,* 2010b; ZHANG *et al*., 2012b; KIM *et al.,* 2010; ZHANG *et al.,* 2009a; ZHANG *et al*., 2009b).

Figure 2 - Zirconia coatings showing biological advantages in terms of bioactivity, osseointegration, and antibacterial effects.

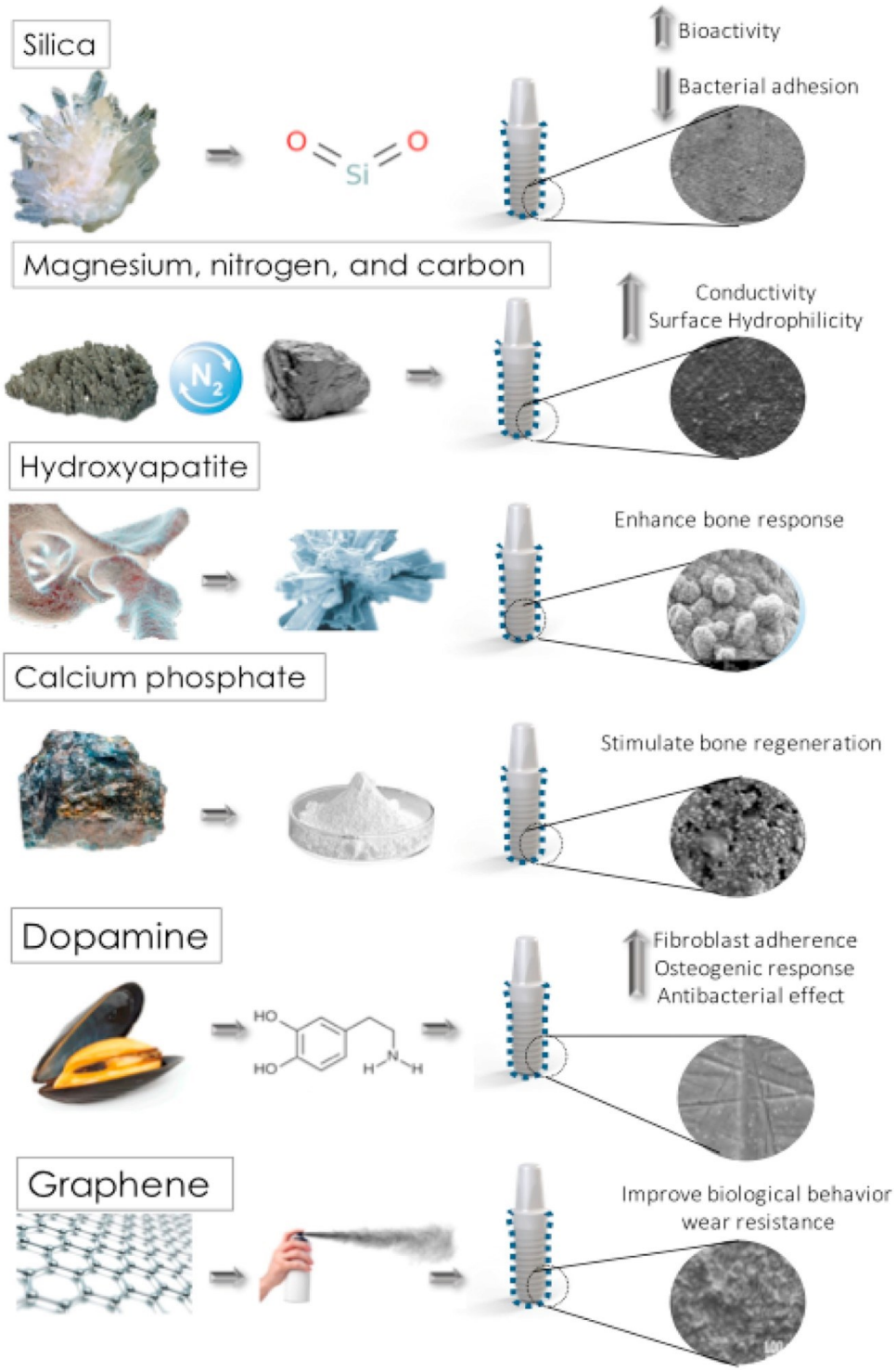

Figure 3 - Optical micrographs of graded CPG/Y-TZP (a) rod (2 mm in radius) and (b) plate (1.2 mm thick) sections consisting of (c) CPG infiltrated Y-TZP (SEM image); (d) Energy dispersive X-ray line mapping from surface to interior, revealing a gradual transition in Ca and Zr contents. Higher magnification SEM images, insets of (c), showing: gradual transition from the surface residual CPG layer (left) to the graded CPG/Y-TZP structure (center) and to dense Y-TZP interior (right), modified from Zhang et al. (2014).

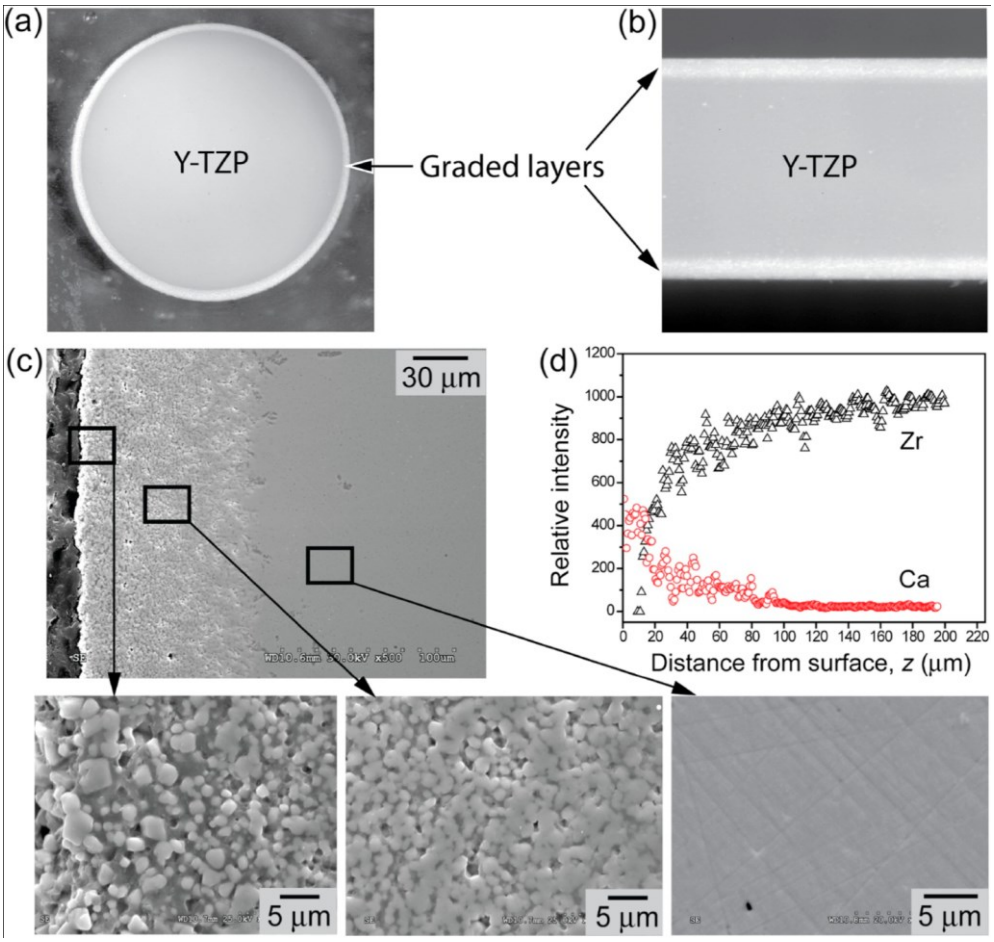

2.4. Conclusions

The present review analysed and explored the techniques currently reported for zirconia surface treatment and concludes important key points depicting desirable osseointegration, mechanical, and antibacterial properties as follow:

- Osseointegration findings depends on time and bone quality, heterogeneous in vivo studies involving different animal models, healing and loading periods, and different surgical sites. Standard guidelines in methods, materials and surfaces are recommended to compare results among scientific studies;
- Machined zirconia implants have shown an adequate osseointegration when compared to machined titanium implants, however, treated zirconia implants have shown higher bone to implant contact percentage. An increase in roughness and improvement of surface morphological aspects can speed up the osseointegration process for both zirconia or titanium implants;
- No surface treatment has been claimed as first choice to increase zirconia osseointegration potential although surface modifications that increase roughness, wettability, and surface energy are recommended to enhance the adhesion, proliferation, and differentiation of osteoblasts. Bioactive based graded structures and coatings are recommended to increase zirconia's bioactivity and osseointegration.
- Grit blasting, acid etching, and heat treatment should not decrease the mechanical properties of zirconia such as flexural strength and fracture toughness. Smooth and round particles for grit blasting are recommended to avoid micro-crack formation. Studies have shown that high HF concentrations, over etching time and thermal treatment are not recommended since they can increase zirconia degradation.
- Functionally bioactive graded zirconia can improve the mechanical strength (e.g., flexural strength and fracture toughness) and biological properties of zirconia. Bioactive materials added on the surface can improve osseointegration and decrease biofilm accumulation;
- In vitro and in vivo studies have shown that machined and acid etched zirconia decrease the adhesion of bacteria when compared to titanium. The low affinity of zirconia to biofilm and a favorable soft tissue adaptation is an

essential aspect since it could reduce peri-implantitis risks which is the major current issue of failures in implant dentistry;

- Modified zirconia-based surfaces should be evaluated in clinical studies to provide realistic point view of how oral biofilms, loading, and other patient conditions may affect the properties of zirconia. A range of mechanical properties values for titanium and zirconia parts (and their application) and the role of these treatments on them would help to show which road we show follow.

Chapter 3 - Dopamine- and graded bioactive glass-zirconia modified surfaces for implant dentistry: an in vitro study[2]

3.1. Introduction

Zirconium dioxide (ZrO_2), commonly known as zirconia, is a biomaterial usually applied in dentistry. This biomaterial presents relevant aesthetic properties, including colour and opacity, that mimic the crown and root of natural teeth. For this reason, dental crowns, onlays, inlays, veneers, and implant structures have been produced based on zirconia (STADLINGER *et al.,* 2010; SCHÜNEMANN *et al.,* 2019; BONA; PECHO; ALESSANDRETTI., 2015). Furthermore, zirconia displays unique biomechanical characteristics such as high fracture toughness, fatigue resistance, bending strength, corrosion resistance, radiopacity, and higher bone affinity than most alternative ceramics (BONA; PECHO; ALESSANDRETTI, 2015; ZHANG, 2012; SIVARAMAN *et al*., 2018). Nevertheless, zirconia has minimal interaction with the surrounding tissue and is considered a bioinert material. Therefore, modifications on zirconia surface could improve cell adhesion, proliferation, and differentiation. Additionally, these modifications could induce an antimicrobial effect, directly influencing peri-implant tissue attachment and maintenance on dental implant surfaces (SCHÜNEMANN *et al.,* 2019; SANON *et al.,* 2015; LIU *et al.,* 2015; PABST *et al*., 2015; MOEZZIZADEH *et al.,* 2017; FREITAS *et al.,* 2018; CHO *et al.,* 2015).

Bioactive glass (BG) 45S5 was the first commercial form of glass-derived biomaterials for bone regeneration, and it is still largely studied due to its bone-bonding properties (HENCH *et al*., 2009; JONES *et al.,* 2013; GALARRAGA-VINUEZA *et al.,* 2018; HENCH *et al.,* 1977). Later, new compositions of BG were developed, including 58S, produced via sol-gel method (MOEZZIZADEH *et al*., 2017; FERRARIS *et al*., 2000; HENCH *et al*., 2015; ZHONG *et al*., 2000). Moreover, melt-derived 45S5 glass powders exhibit lower dissolution rates for apatite formation than 58S gel-glass powders (SEPULVEDA et al., 2002). In order to combine the bioactivity of glass-derived materials with the outstanding mechanical properties of zirconia (Y-TZP), the

[2] Submitted for publication in the Acta biomaterialia (Impact Factor: 7.242).

infiltration of BG on zirconia surfaces was proposed (Zhang, Regeros, Kim 2009). Therefore, functionally graded materials (FGM) were created to improve the bioactivity, flexural strength, and damage resistance (ZHANG *et al.,* 2012; FABRIS *et al.,* 2016; FABRIS *et al.,* 2017; HENRIQUES *et al.,* 2017; ZHANG *et al.,* 2010; ZHANG *et al*., 2012).

In this regard, BG has been proposed for treating zirconia surface since these biomaterials are bioactive and biocompatible and also demonstrate angiogenic and antimicrobial effects (HENCH *et al*., 2009; JONES *et al.,* 2013). Additionally, in the presence of biological fluids, BG binds to the bone by forming a carbonated hydroxyapatite layer, miming the mineral phase of the bone (JONES *et al.,* 2013; GALARRAGA-VINUEZA *et al.,* 2018; RAHAMAN *et al.,* 2011). This layer promotes a stable bond to the living bone and stimulate mesenchymal cells to differentiate into osteoblast-like cells (MOEZZIZADEH *et al.,* 2017; GALARRAGA-VINUEZA *et al.,* 2018; HENCH *et al.,* 1977). Also, bone cells are stimulated towards a path of regeneration and self-repair, accelerating bone tissue healing kinetics (SCHÜNEMANN *et al.,* 2019). Hence, BG coatings on zirconia substrates have been proposed to provide bioactive properties to biomedical components. However, this approach has failed due to the typical delamination and fracture occurrences. These problems occur because of the coating/substrate bonding issue, mismatch in coefficient of thermal expansion (CTE), and the abrupt changes in physical properties at the coating/substrate interface.

In order to overcome this limitation, Zhang et al., 2014 projected a functionally graded calcium phosphate-based glass/zirconia (CPG/Y-TZP) system (Figure 4). This system is based on the surface infiltration of a pre-sintered zirconia substrate, resulting in a gradated compositional and mechanical transition from the surface (CPG) to the bulk (Y-TZP) of the component. The graded BG-zirconia materials have improved mechanical properties over pure Y-TZP, namely lower elastic mismatch to the bone (E_{Bone} ~20GPa; E_{glass} ~50GPa; E_{ZrO2} ~200GPa) and higher flexural strength and damage resistance (SCHÜNEMANN et al., 2019). However, the biological properties of these materials are far less reported. Therefore, it remains to be demonstrated to which extent the mechanical properties are accompanied by relevant improvements at the biological level.

Figure 4 - Micrographs of graded CPG/Y-TZP (A) rod (2 mm radius) and (B) plate (1.2 mm thick) sections consisting of (C) CPG infiltrated Y-TZP (SEM images). Higher magnification SEM images, insets of (C) showing the gradual transition from the surface residual CPG layer (1, left) to the graded CPG/Y-TZP structure (2, centre) and to the dense Y-TZP interior (3, right). Adapted from Zhang et al. 2014. CPG: gradated compositional and mechanical transition from the surface. Y-TZP: bulk of the component.

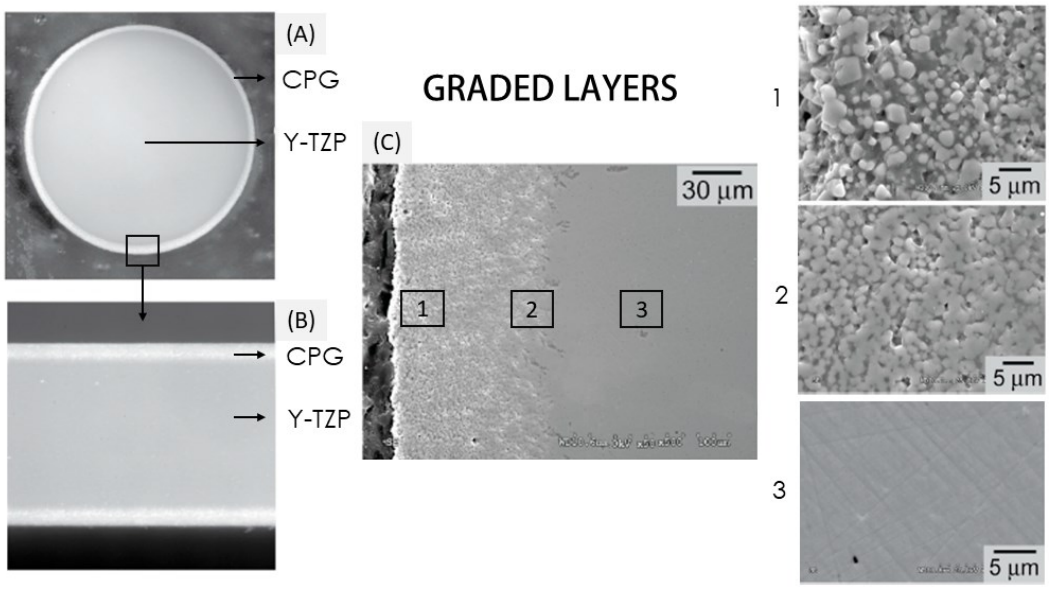

Polydopamine coatings can increase antimicrobial properties, protein adsorption, and cell adhesion (LIU *et al.,* 2015; LEE *et al.,* 2007). Clinically speaking, polydopamine coatings on zirconia can improve soft-tissue integration and antimicrobial effect in the peri-implant tissues (SCHÜNEMANN *et al*., 2019; LIU *et al.,* 2015). In turn, dopamine (DOP), the precursor of 3,4-dihydroxy-L-phenylalanine (L-DOPA), has the ability to self-polymerize and strongly adhere to a wide range of organic and inorganic materials (LEE *et al.,* 2007). Additionally, studies have demonstrated that DOP and its precursors coatings can increase the antimicrobial effect, collagen deposition, fibroblasts adhesion (LEE *et al.,* 2007), and human osteoblasts (MG63) adhesion and spreading (LIU *et al.,* 2013). Previous studies have tried different material compositions and methodologies of zirconia-modified surfaces by bioactive glass or dopamine derivatives (Table 3).

Table 3 - Previous studies on zirconia-modified surfaces by bioactive glasses or dopamine derivatives.

AIM	OUTCOMES	*IN VITRO* METHODS	REF
To evaluate MC3T3-E1 adhesion on laser-sintered coatings of hydroxyapatite or 45S5 bioactive glass on zirconia-textured surfaces. Application: dental implants	Laser-sintered zirconia with a texture pattern of 100 µm width grooves functionalized with hydroxyapatite or 45S5 bioactive glass coatings was biocompatible for MC3T3-E1.	Cell viability assay (Live/dead protocol) and scanning electron microscopy	MESQUITA-GUIMARÃES et al., 2020.
To evaluate cell behavior on a bioactive glass (23.75%Na_2O, 23.75%CaO, 48.5% SiO_2, and 4%P_2O_5) zirconia coating using L929 mouse fibroblasts. Application: prosthetic abutments	The bioactive glass zirconia coating surfaces increased cell migration, proliferation, and spreading, as well as collagen expression compared to pure zirconia surfaces.	Cell proliferation (Alamar Blue staining), morphology (SEM), migration (wound healing), and collagen synthesis (Sirius Red staining) (7 days)	BARROS *et al.,* 2019.
To analyze the behavior of mouse bone marrow-derived mesenchymal stem cells (mBMSC) on zirconia surface modified by infiltration of the precursor sol of 58S bioactive glass followed by gelling and sintering processes. Application: dental implants	The bioactive glass infiltrated zirconia surfaces improved cell adhesion and alkaline phosphatase activity of mBMSC compared to pure zirconia surfaces.	Cell viability assays (Live/dead protocol; 1 and 3 days, and CCK-8; 1, 3, and 7 days), confocal laser scanning microscopy (CLSM; 2 days) and alkaline phosphatase activity (7, 10, and 14 days)	KE *et al.,* 2017
To develop and analyze the cytocompatibility of a novel glass composition of 45S5 (substitution of CaO by MgO and of Na_2O by K_2O) applied as zirconia coating using L929 mouse fibroblasts. Application: dental implants	Proliferation rates were similar for microstructured glass coatings (PC-XG3) and control groups. The material was biocompatible.	Cell proliferation (CellTiter-Blue Cell Viability Assay; 1, 2, 3, and 4 days) and cytotoxicity (Cytotox-ONE Assay; 1 and 4 days)	KIRSTEN *et al.,* 2015
To evaluate the influence of polydopamine-coated zirconia on human gingival fibroblasts (HGF) behavior. Application: prosthetic abutments	Polydopamine coating on zirconia increased cell adhesion and proliferation compared to pure zirconia. HGF exhibited a high degree of spreading and secreted a high level of collagen type I on	Cell adhesion and proliferation (CCK-8; 3 h, 1, 3, 5, and 7 days) cell spreading and morphology (SEM and CLSM; 3 and 24 h), and collagen type I synthesis	LIU *et* al., 2015

	polydopamine-modified zirconia.	(enzyme-linked immunosorbent assay; 3 and 7 days)	
To study the biocompatibility of L-DOPA (3,4-dihydroxy-l-phenylalanine) coating zirconia using human osteoblastic cells (MG63). Application: dental implants	L-DOPA coated zirconia demonstrated higher biocompatibility and cell adhesion and spreading, but similar alkaline phosphatase activity than uncoated zirconia samples.	Cell viability assay (MTT; 1, 3, and 7 days), immunofluorescence, SEM and alkaline phosphatase activity (1, 14, and 21 days)	LIU *et al.,* 2013

SEM: scanning electron microscopy. CLSM: confocal laser scanning microscopy. L-DOPA: 3,4-dihydroxy-L-phenylalanine.

Therefore, this study aimed to develop bioactive zirconia surfaces using bioactive glass and dopamine to improve hard and soft tissue integration around zirconia implants and prosthetic abutments (Figure 5). To meet this goal, physical analyses of the materials, biocompatibility, cell proliferation, adhesion, and morphology were evaluated.

Figure 5 - Clinical application of bioactive glass (BG) coating on zirconia surface of dental implant and prosthetic abutment. DOP: dopamine.

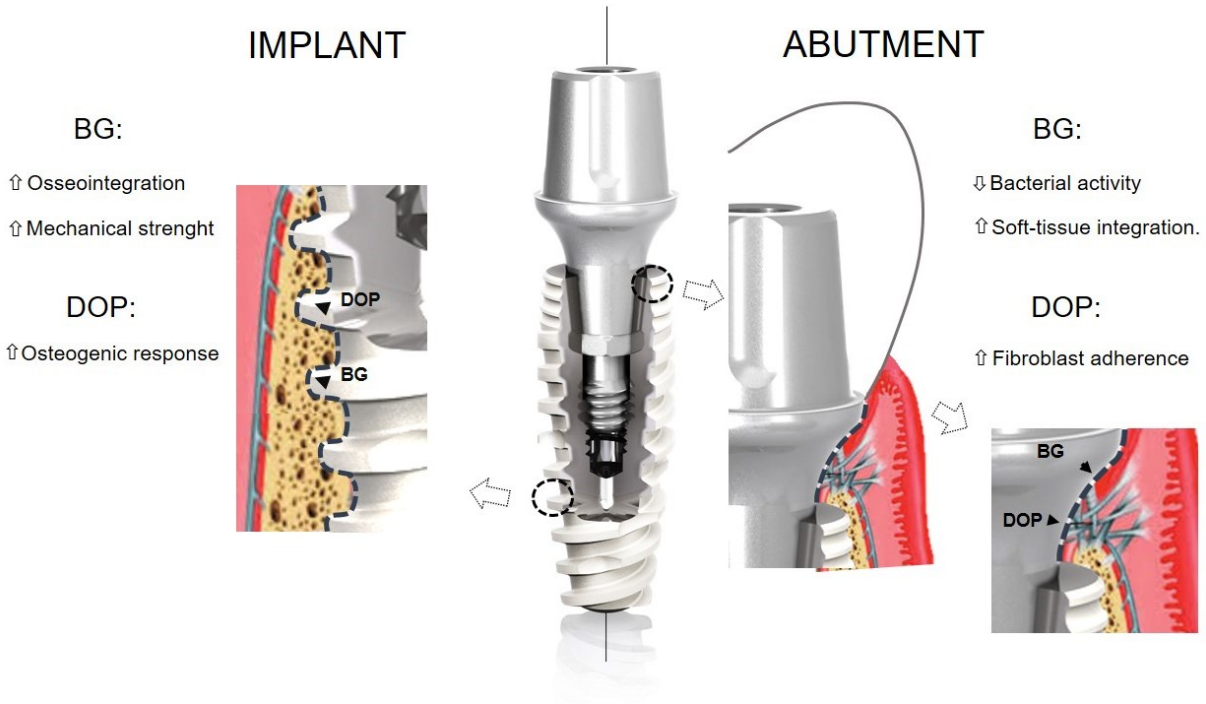

3.2. Material and methods

3.2.1. Zirconia disks preparation

Zirconia disks (n = 280) of 10 mm diameter were prepared using 1 g zirconia powder (Tosoh, Zirconia TZ-3YSB-E, Japan) compacted in a circular stainless-steel die under 100 MPa of pressure for 60 sec. Stearic acid was used as a lubricant, while the good outflow of zirconia powder facilitated the homogeneous distribution of the material. Densified monolithic zirconia disks (n = 40) with a diameter of 8.20 ± 0.01 mm and a thickness of 2.60 ± 0.02 mm were obtained after air sintering for 2 h at 1500 °C and 5 °C/min (10PS, EDG, Brazil). The remaining zirconia compacts (n = 200) were used to produce the BG-infiltrated specimens, as described in Section 2.4.

3.2.2. Sol-gel production of bioactive glass

58S BG, triethyl phosphate (Sigma-Aldrich, St. Louis, USA), and nitric acid (HNO_3, 68%, Vetec, Brazil) was used to dissolve $Ca(N\text{-}O_3)2.4H_2O$ (Sigma-Aldrich, St. Louis, USA). The molar ratios of SiO_2, P_2O_5, and CaO were calculated according to the 58S BG composition. Tetraethyl orthosilicate (TEOS, Sigma-Aldrich, St. Louis, USA) and TEP were placed in a glass recipient containing EtOH (Sigma) under magnetic stirring. $Ca(N\text{-}O_3)2.4H_2O$ was dissolved in 2M HNO_3 and then added to water at a molar ratio TEOS:H_2O of 1:4. The solution was stirred for 1 h and dried in an incubator at 70 ºC for 24 h. Subsequently, the material was thermally treated at 600 ºC for 24 h and milled in a planetary ball mill at 400 rpm for 1 h to obtain the BG powder.

3.2.3. Melting route of bioactive glass 45S5

Bioactive glass 45S5 (45%wt SiO2, 24.5%wt Na2O, 24.5%wt CaO, 6%wt P2O5) powder was processed by the melt quenching technique. To produce 100g of BG was used 45g of silica (SiO2 - Sigma Aldrich, 99.9%, CAS 0676-86-0), 41.98g of sodium carbonate (Na2CO3 - Lafan, 99%, CRQ 10.232-F), 43.58g of calcium carbonate (Ca2CO3), and 6g of phosphorus pentoxide (P2O5 – Scientific Exodus,

99.5%, CAS 1314-56-3). The precursor powders were dry homogenized for 30 min at 150 rpm (Mill CT 242 Servitech). Melting was performed at 10 °C/min in the Jung melting furnace (Blumenau, Brazil) using a platinum crucible. The first burning stage was at 900°C, 30 min for the homogeneous decomposition of carbonates and release of CO2; the fusion at 1450 °C for 2 h resulting in a homogeneous vitreous. After melting, the platinum crucible was immersed in water. The grinding to obtain the powder was carried out in a planetary mill (Retsch PM 100), with a jar and agate spheres, for 80 min at 400 rpm.

3.2.4. Zirconia surface modifications

Zirconia specimens were divided into 7 groups (Figure 6), according to the surface treatment (n = 40 per group).

Figure 6 - Scheme of zirconia (Y-TZP) specimens according to the surface treatment. BG: bioactive glass. DOP: dopamine.

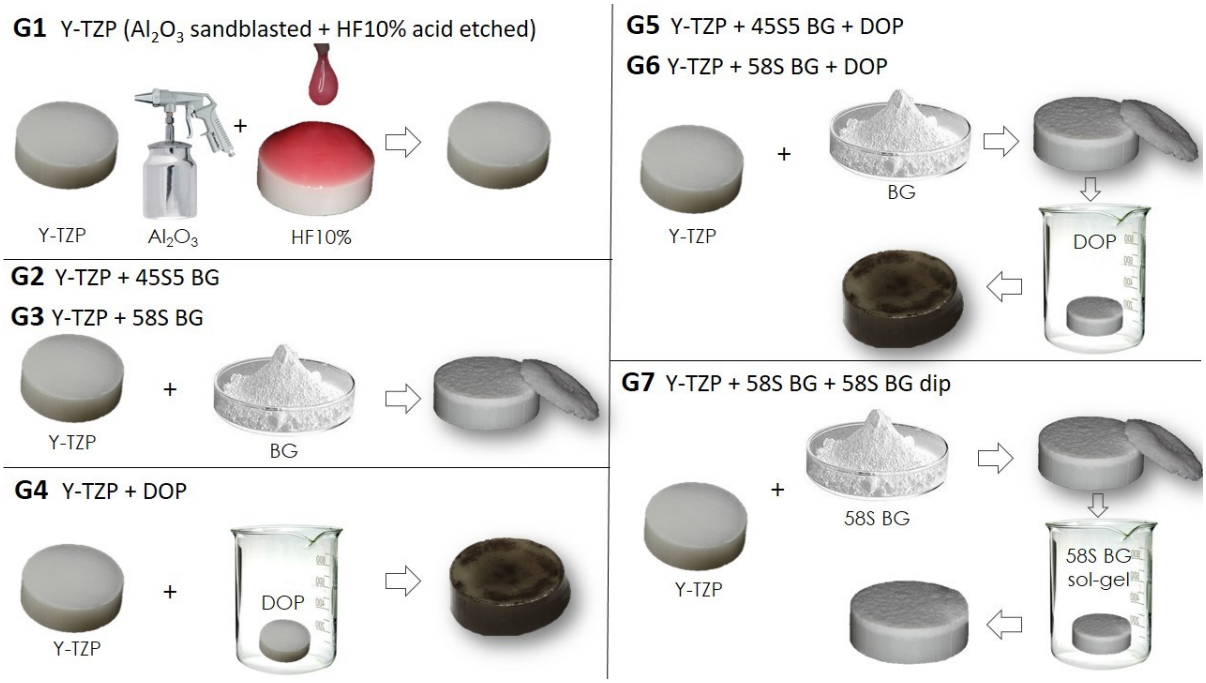

3.2.4.1. Sandblasted and acid-etched zirconia specimens

The sintered disks were sandblasted (Renfert Basic Eco, USA) with Al_2O_3 particles grits of 110 μm and 4 bar to obtain a macro-rough surface and acid-etched with 10% hydrofluoric acid (Condac porcelana, FGM, Brazil) for 1 h at room temperature, washed 1 min in tap water, and cleaned ultrasonically. Group with this treatment: G1.

3.2.4.2. Graded BG-zirconia specimens

Zirconia compacts (disks) were covered on their top surface by a paste formed by BG powder (58S or 45S5) and distilled water (powder/water proportion: 1 g BG powder / 0.3 mL water). Afterwards, disks were sintered at 1500°C for 2 h at 5 °C/min, allowing the BG to infiltrate the surface while zirconia densification occurred simultaneously. The infiltrated specimens were washed for 1 min with distilled water. Groups with this treatment: G2, G3, G5, G6, and G7.

3.2.4.3. Dopamine (DOP) coated specimens

Zirconia compacts were immersed in a solution of DOP (2 mg/mL) dissolved in 10 μM Tris-HCl (pH 8.5) by stirring at room temperature for 24 h. The colour of the solution gradually changed from clear to dark brown due to pH-induced oxidative polymerization. Samples were removed from the DOP solution, gently rinsed with distilled water for 10 min and dried with N2 gas flow. Groups with this treatment: G4, G5, and G6.

3.2.4.4. BG-coated graded BG-zirconia specimens

G3 samples, produced as described in Section *2.4.2,* were dipped for 10 sec in 58S BGs sol-gel to obtain an additional BG layer. Disks were sintered at 600 °C for 2 h at 5 °C/min. Group with this treatment: G7.

3.2.5. Surface characterization

3.2.5.1. Surface roughness measurements

The average surface roughness (Ra in mm) of all specimens was determined with a profilometer (Bruker, DektakXT Stylus, Billerica, USA). The resolution was 0.01 mm; the transverse length (length of the surface examined by the instrument) was 4.0 mm; and the speed of the diamond stylus with a 5-mm tip radius was 0.5 mm/s. Three equidistant parallel measurements were made with a perpendicular stylus on different areas of the specimen. All measurements were performed perpendicular to the direction of the airborne-particle abrasion. The average reading was designated as the Ra value of each specimen. One calibrated operator recorded all measurements.

3.2.5.2. Contact angle measurements

The contact angle is defined as the angle at the intercept of a plane tangent to a drop and the plane containing the substrate-liquid interface. The wettability of the zirconia surface with different surface treatments was characterized by means of the contact angle formed between the surface and the deionized water (4 μL). For the measurements, an automated goniometer with a charge-coupled device camera was used to record the image of a liquid drop placed onto the surface by a microsyringe while image-processing software determined the contact angle. One calibrated operator obtained 2 measurements for each specimen, and the average was determined.

3.2.5.3. X-ray Diffraction (XRD) for phase transformation analysis

X-ray Diffraction (XRD) with a Cu-Kα source (D 8 Advance X-ray diffractometer, Bruker AXS, Karlsruhe, Germany) was used to determine the crystalline phases of the 3Y-TZP surfaces. XRD spectra were collected before and after fatigue test on five random samples over a 2θ range between 3◦ and 90◦ at a step size of 0.05◦ and

0,02°/s. The monoclinic phase fraction was calculated by the Garvie-Nicholson method.

3.2.6. Cell cultures

Mesenchymal cells from human exfoliated deciduous teeth (SHED; Curitiba Biotech®, Brazil) were cultivated in Dulbecco's Modified Eagles' Medium (DMEM; Gibco, Thermo Fisher Scientific, USA) with 10% fetal bovine serum (FBS; Gibco, Thermo Fisher Scientific, USA). Murine pre-osteoblasts MC3T3-E1 subclone 4 (American Type Culture Collection, USA) were cultivated in modified α-Minimum Eagles' Medium (modified α-MEM; Gibco, Thermo Fisher Scientific, USA) with 10% FBS. Both cell lines were expanded in culture flasks until 80% confluence and then enzymatically disaggregated to apply over zirconia samples. Zirconia disks (G1 to G7) were carefully placed in triplicate into wells of 48-well plates. After, 2.0×10^4 cells were seeded over each disk and the cellular control was set by plating the cells directly onto the wells. To avoid cells in the plate bottom, cell suspensions were cautiously placed over the samples and incubated at 37 °C and 5% CO_2 for 8 h to allow cell adhesion. Then, the respective culture medium for each cell line was added over the samples and the culture plates were incubated again. Culture medium was changed every 2 to 3 days. Tests were performed after 3 and 7 days in cell culture.

3.2.7. Cell viability assays

To evaluate the cytotoxicity of the samples, cell viability was assessed through MTS [3-(4,5-dimethylthiazol-2-yl)-5-(3-carboxymethoxyphenyl)-2-(4-sulfophenyl)-2H-tetrazolium, inner salt, CellTiter 96®, Promega, Madison, WI, USA]. This test is based on reducing the MTS tetrazolium compound by viable cells to generate a coloured formazan dye that is soluble in cell culture media. This conversion is performed by NAD(P)H-dependent dehydrogenase enzymes in metabolically active cells. Analyzes were performed according to the manufacturer's recommendations, and the formazan dye was quantified by measuring the absorbance at 540 nm (SpectraMax M2e, Molecular Devices, USA).

3.2.8. Cell proliferation assays

To determine the effect of samples on cell proliferation, Quant-iT TM PicoGreen® dsDNA Reagent (P7589, Invitrogen, Thermo Fisher Scientific, CA, USA) was employed. This test acts by quantifying double-stranded DNA (dsDNA), even in small amounts in the solution, minimizing RNA and single-stranded DNA (ssDNA) fluorescence detection. Analyzes were performed according to the manufacturer's recommendations. Readings were performed on a fluorescence spectrophotometer (SpectraMax M2e, Molecular Devices, USA) at 360/440 nm (Ex/Em).

3.2.9. Cell morphology and adhesion analyses

Cell morphology and adhesion over the sample surfaces were evaluated through scanning electron microscopy (SEM; TM3030, Hitachi, Japan) at 15 kV. After 3 or 7 days in cell culture, samples were washed twice with PBS, fixed with 4% glutaraldehyde for 30 min, and dried with serial washes of ethanol (50%, 60%, 70%, 80%, 90%, 100%, and 100%) and with one drop of hexamethyldisilazane (HDMS, Sigma-Aldrich, USA). Samples were coated with Gold-Palladium before SEM analyses.

3.2.10. Statistical analyses

Statistical analyses of the quantitative results were performed using GraphPad Prism 8 (GraphPad Software Inc., USA). Repeated measures one-way analysis of variance (ANOVA) followed by Tukey’s multiple comparison test were applied. Statistical analyses were performed for each experimental time separately, comparing all groups. The level of significance was set at $p < 0.05$.

3.3. Results

3.3.1. Surface analysis

Considering the surface wettability is one of the important factors in the process of osseointegration and, consequently, in the implant's short and long-term stability, the surface samples' contact angles were measured. The surface treatment performed by dopamine and bioactive glass techniques generated changes in the surface roughness parameters, producing textures at meso, micro, and nanoscale leading to an enhanced surface wettability. Surface roughness values of the zirconia dicks for all different surfaces are presented in Table 4. An increase in roughness was observed in G3, G4, G5, G6, and G7 compared to G1 and G2. The contact angle measurements are presented in Table 4 and Figure 7. Results shows hydrophobic surface on G1 and G7 ($90^0 < \theta < 120^0$), a hydrophilic surface on G2, G3, G5, and G6 ($10^0 < \theta < 90^0$). G4 showed super-hydrophilic surface ($0 < 10^0$).

Table 4 - Mean of Roughness (Ra/mm) and contact angle (CA/degrees) values of each group.

Group	***Ra***		***CA***
	Sa(nm)	*Sq(nm)*	
G1 (Y-TZP)	0.352 ± 0.03	0.497 ± 0.07	95.95 ±5.17
G2 (Y-TZP + 45S5 BG)	0.653±0.11	0.842±0.16	40.3±3.98
G3 (Y-TZP + 58S BG)	6.81±0.60	9.06±1.11	46.1±0.98
G4 (Y-TZP + DOP)	4.87±1.31	6.06±1.75	X*
G5 (Y-TZP + 45S5 BG + DOP)	4.73±0.66	6.37±1.07	46.3±5.86
G6 (Y-TZP + 58S BG + DOP)	5.14±0.55	7.22±0.83	61.4±4.82
G7 (Y-TZP + 58S BG + 58S BG dip)	5.33±1.07	7.26±1.27	110.7±5.09

* It was not possible to measure due to the high wettability of the droplet.

Figure 7 - Representative image of cross-sectional views of water droplet in specimens.

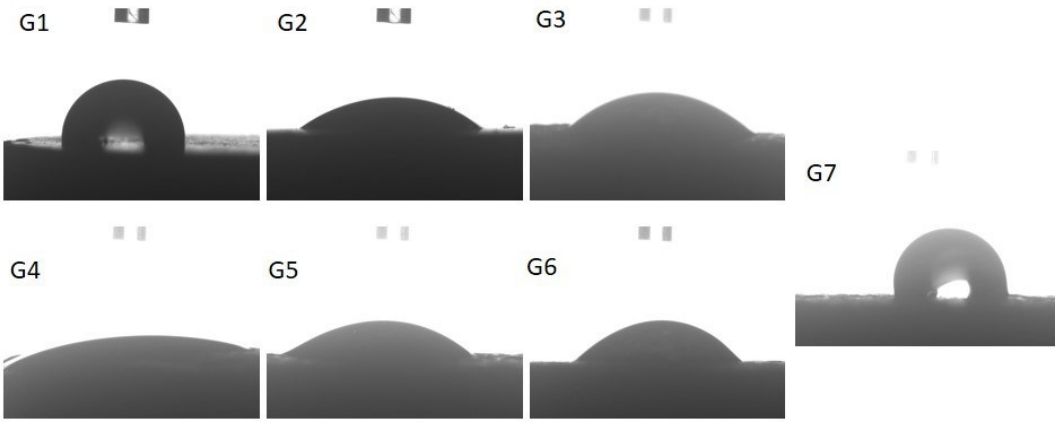

3.3.2. Cell viability assays

Considering the cellular control (CC) as 100% cell viability, we showed that G1, G2, and G5 led to less than 70% of viability for MSC on day 3 (Figure 8A, p = 0.0039), while, on day 7, all groups showed more than 80% cell viability for MSC (Figure 8B, p = 0.1861). Regarding osteoblasts, G5 exhibited less than 50% cell viability on day 3 (Figure 8C, p = 0.0013), while all other groups promoted similar cell viabilities. On day 7, all groups promoted osteoblast viabilities higher than 95% and G3 presented cell viability higher than cellular control (Figure 8D, p = 0.0074).

Figure 8 - Cell viability assays. Viabilities percentages were calculated in relation to cellular control (100%). A-B) Mesenchymal stem cells (MSCs) from human exfoliated deciduous teeth (SHED) or C-D) Osteoblasts (MC3T3-E1) on A-C) day 3 and B-D) day 7 of cell culture. Equal letters mean no significant differences among groups (ANOVA/Tukey's post-hoc, p <0.005).

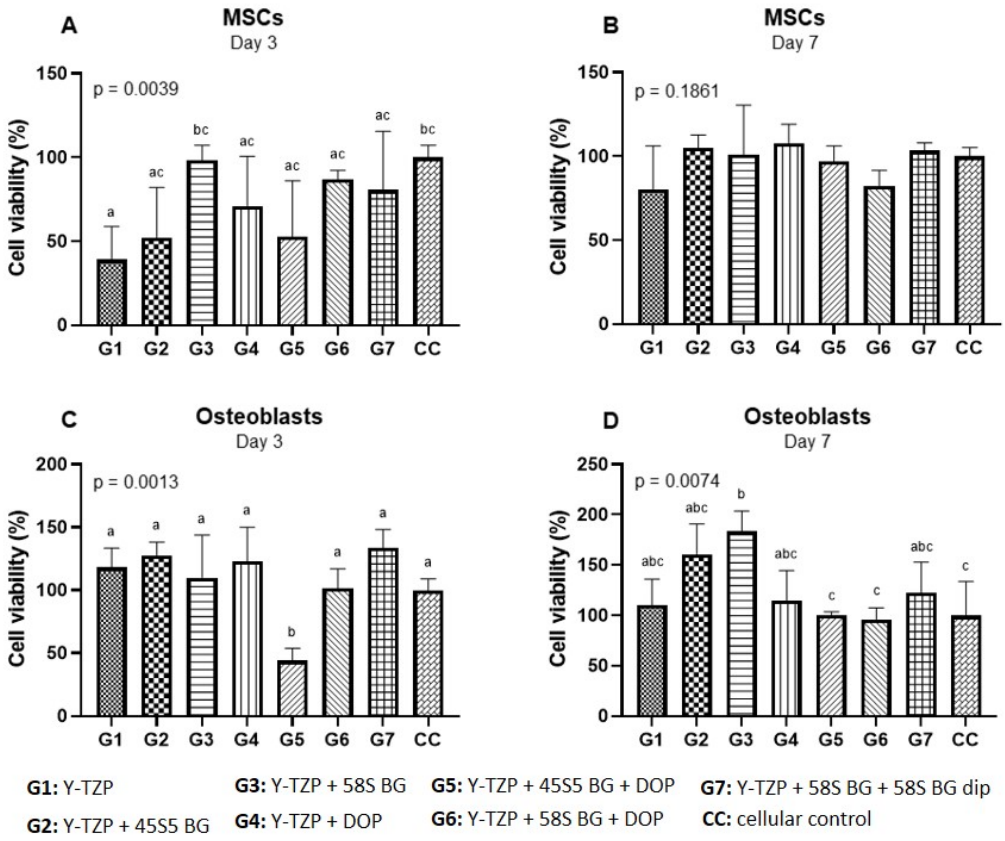

3.3.3. Cell proliferation assays

To determine the cell proliferation, we analyzed the DNA content on the samples. In this case, CC was used to compare the results as it represents cell behavior in standard conditions. Regarding MSCs, G5 showed a reduced cell proliferation rate in comparison to G1, G2, G3, and G4, but similar to G6, G7, and CC on day 3 (Figure 9A, p = 0.0007). On day 7, G7 demonstrated a reduced MSCs proliferation rate, but similar to G2, G3, G5, G6 (Figure 9B, p = 0.0025). For osteoblasts, all experimental groups (G1 to G7) showed similar proliferation rates on day 3, but lower than CC (Figure 9C, p <0.0001). On day 7, CC exhibited the highest osteoblast proliferation rate, similar to G2, G3, and G4 (Figure 9D, p = 0.0088). Cell

proliferation was reduced to half of the values considering all groups from day 3 to day 7 of the experiment for both MSCs and osteoblasts.

Figure 9 - Cell proliferation assays. Proliferation rates were calculated in relation to the standard curve to quantify the dsDNA of the cells. A-B) Mesenchymal stem cells (MSCs) from human exfoliated deciduous teeth (SHED) or C-D) Osteoblasts (MC3T3-E1) on A-C) day 3 and B-D) day 7 of cell culture. Equal letters mean no significant differences among groups (ANOVA/Tukey's post-test, $p < 0.005$).

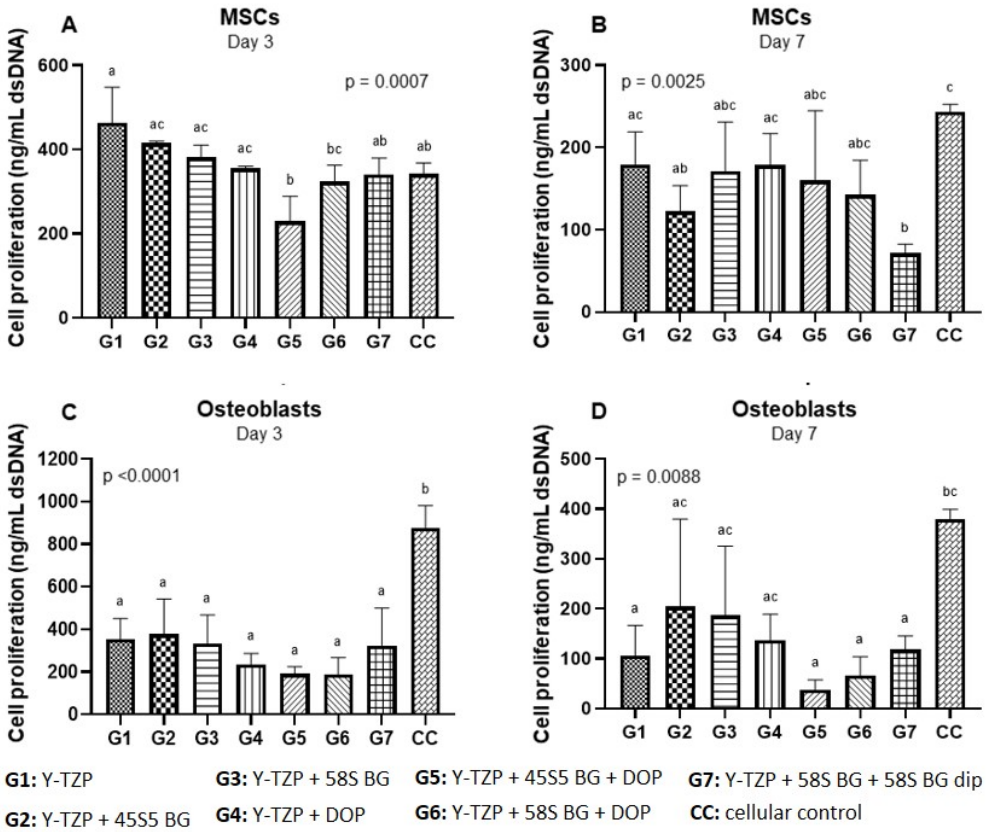

3.3.4. Cell morphology and adhesion analyses

We further performed scanning electron microscopy of the samples to observe the cell coverage and adhesion to the different surfaces (Figure 10). For MSCs, G1 showed reduced cell coverage, while the other groups (G2-G7) demonstrated full cell coverage on their surfaces on day 7 of the experiments. For osteoblasts, full coverage of cells was obtained for all groups. The high magnification figures embedded at the top left corner of the main figures show details of cells adhered to samples´ surfaces.

Figure 10 - Cell micrographs on day 7 of cell culture of experimental groups (G1 to G7). The first image (cc) shows zirconia surface with no cells for comparison. Images with red borders represent greater magnified fields (x2.5k) for detailed analyses. A) Mesenchymal stem cells (MSCs) from human exfoliated deciduous teeth (SHED) and B) Osteoblasts (MC3T3-E1).

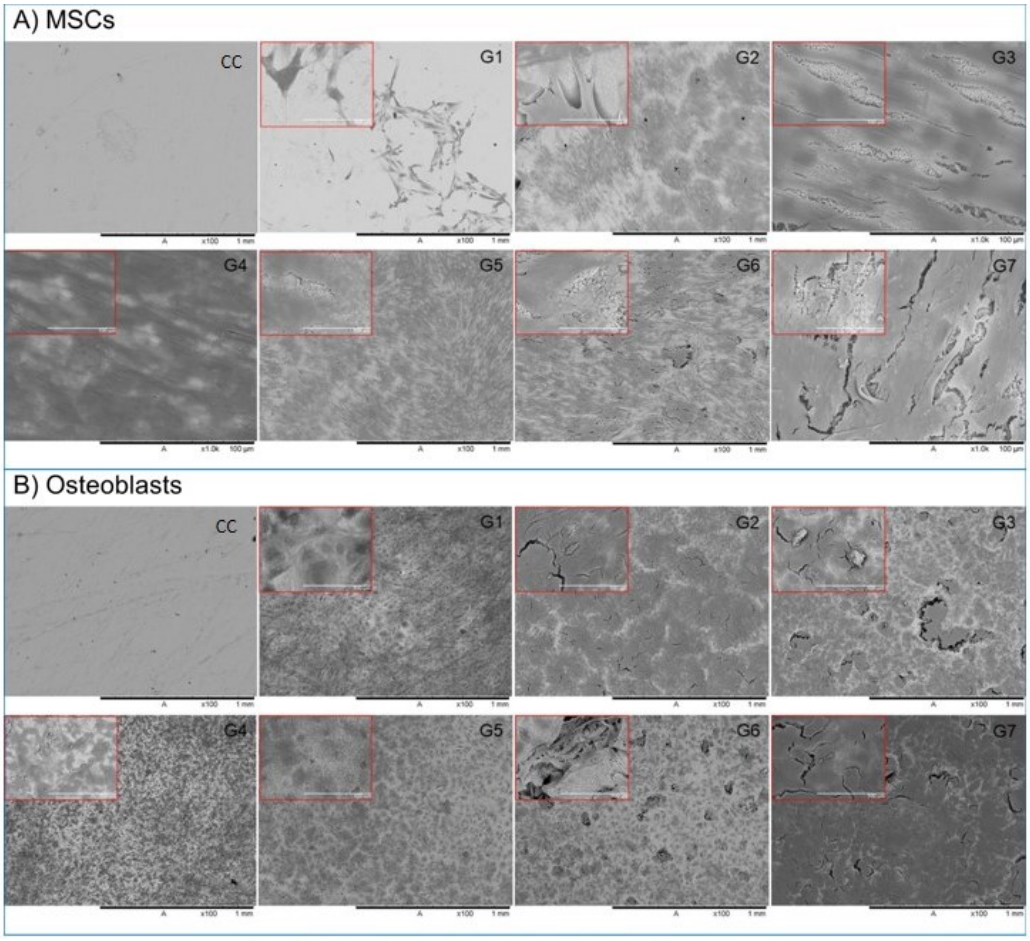

G1: Y-TZP
G2: Y-TZP + 45S5 BG
G3: Y-TZP + 58S BG
G4: Y-TZP + DOP
G5: Y-TZP + 45S5 BG + DOP
G6: Y-TZP + 58S BG + DOP
G7: Y-TZP + 58S BG + 58S BG dip
CC: cellular control

3.4. Discussion

Zirconia is a biomaterial widely used in the dental field due to its aesthetic properties (STADLINGER *et al.,* 2010; SCHÜNEMANN *et al.,* 2019; BONA *et al.,* 2015), unique biomechanical characteristics, and higher affinity to the bone than most alternative biocompatible ceramics (BONA *et al.,* 2015; ZHANG *et al.,* 2012). However, since zirconia is considered bioinert and unable to establish biological interactions with oral tissues, several surface modification strategies have been implemented to overcome this disadvantage. In this study, dopamine- and graded bioactive glass-zirconia surfaces were developed and assessed regarding their biocompatibility, cell proliferation, and adhesion of osteoblasts and human mesenchymal cells. We observed that all proposed modifications promoted biocompatible zirconia surfaces on day 7. However, on day 3, ZrO_2 (G1), ZrO_2 treated with 45S5 BG (G2), and ZrO_2 treated with 45S5 and DOP (G5) promoted MSCs viabilities rates under 70% for MSCs. Also, such reduced osteoblast viability was induced only by ZrO_2 treated with 45S5 and DOP (G5) on day 3. Regarding cell proliferation, there was a remarkable reduction in cell proliferation rates from day 3 to day 7 of all groups, which is an important indication of cell commitment to the differentiation path. Concerning cell adhesion to the sample surfaces, all groups presented a full coverage of the surfaces by osteoblasts and MSCs, except for G1 with MSCs, meaning that the surface modifications allowed cell sitting, which is essential to allow osseointegration to the surrounding tissues.

When a new material is proposed for clinical applications, important biological in vitro assays are needed to respond to some questions. First, the material should be biocompatible, i.e., it should not lead to damage to cells and surrounding tissues due to inflammatory reactions. Then, the material should give biological information to allow cells to adhere and spread over the surface, allowing the cells to exert their functions. Finally, a bioactive material should improve cell proliferation until a sufficient number to support the healing of the surrounding tissues and the differentiation process to allow osseointegration (SORDI *et al.,* 2021; FABRIS *et al.,* 2021; JONES *et al.,* 2003; JONES *et al.,* 2004; GOUGH *et al.,* 2004; ZHANG *et al.,* 2020). Herein, the zirconia-modified surfaces by infiltration of bioactive glass and/ or coating with dopamine proved to be biocompatible with human mesenchymal stem cells and murine osteoblasts. The tested surfaces also allowed cell adhesion and spreading after 3 and 7 days of cell

culture. More interestingly, the zirconia-treated samples led to a sharp reduction in cell proliferation of both mesenchymal stem cells and osteoblasts, which might indicate cell commitment to the osteogenic differentiation (PLEWINSKI *et al.,* 2013). Nevertheless, further osteogenic analyses should be performed to show the osteoblastic differentiation of cells, such as alkaline phosphatase activity, detection of bone proteins, and evaluation of extracellular matrix mineralization. Montazerian *et al.* 2015 also observed higher cell proliferation rates in the first experimental times (1 and 3 days) with a sharp reduction thereafter. These authors analyzed the proliferation of human osteoblastic cells (MG63) for 1, 3, 6, 12, and 18 days under the application of glass or polycrystalline glass-ceramic powders containing zirconia. Therefore, this preliminary in vitro study is a screening of novel biomaterials that should be further tested for their potential for osteogenic differentiation.

The manufacturing of graded bioactive glass-zirconia surfaces includes high sintering temperatures (1500ºC), which are necessary for the densification of zirconia but can be detrimental to bioactive glass bioactivity. In that sense, Kaur et al. (2014) reported a delay in apatite formation on bioactive glass-infiltrated zirconia surfaces compared to pure bioactive glass. This foreseen shortcoming was addressed in this study with the inclusion of G7, where a fresh bioactive glass layer (sintered at low temperature, 600ºC) was applied over a graded bioactive glass-zirconia surface. Interestingly, no significant improvement was seen regarding cell viability and cell proliferation relative to G3 (bioactive glass-infiltrated zirconia). In a similar study led by Ke *et al.,* 2017, zirconia-modified surfaces by infiltration of the precursor sol of 58S bioactive glass followed by gelling and sintering processes (but not a graded system as used in this study) showed improved cell adhesion and alkaline phosphatase activity of mouse bone marrow-derived mesenchymal cells (mBMSCs) compared to pure zirconia surfaces. Herein, G7 presented no cytotoxicity to the cells tested, and showed great cell adhesion and reduction in cell proliferation rates from day 3 to day 7, which might be an indication of the cell commitment to a differentiation process. However, these results were not significantly different from what was demonstrated by the other groups. This shows that zirconia may not require an additional BG layer, as previously recommended by Gouveia *et al.,* 2021 which is rather beneficial since it reduces the preparation time and materials used to synthesize the biomaterial.

Laser-sintered zirconia functionalized with 45S5 bioactive glass coatings revealed 90% of osteoblast viability (MESQUITA-GUIMARÃES *et al.,* 2020). A novel

glass composition of 45S5 given by the substitution of CaO by MgO and of Na_2O by K_2O (PC-XG3) led to similar L929 mouse fibroblasts proliferation rates to pure zirconia surfaces and low cytotoxicity (KIRSTEN *et al.,* 2014). Similarly, a bioactive glass (23.75%Na_2O, 23.75%CaO, 48.5% SiO_2, and 4%P_2O_5) infiltrated on zirconia surface increased mouse fibroblasts L929 proliferation, collagen expression, and cell migration and spreading capability compared to pure zirconia surfaces (BARROS *et al.,* 2019). Thus, literature has demonstrated that modifications to the zirconia surface by coating or infiltration of bioactive glass increase bioactivity and offer cells biological information to allow cell adhesion, proliferation, and differentiation, with no cytotoxic effects and no interference on the mechanical properties of zirconia (ZHANG *et al.,* 2014; MESQUITA-GUIMARÃES *et al.,* 2020; BARROS *et al.,* 2019; KE *et al.,* 2017; KIRSTEN *et al.,* 2014), which was confirmed in this study. However, we used novel approaches for bioactive glass infiltration.

The dopamine coating of different substrates such as pure zirconia (G4), 45S5 bioactive glass infiltrated zirconia (G5), and 58S bioactive glass infiltrated zirconia (G6) was intended to assess whether the underlying surface that received this coating would influence the cellular response. Incorporating dopamine in the bioactive glass increased cell viability, adhesion, and proliferation. Conversely, dopamine alone reduced cell adhesion and was not bioactive compared to the other groups. We then infer that dopamine did not add beneficial biological effects over those offered by the infiltration of bioactive glasses. It is important to highlight, however, that this was the first study that applied bioactive glass and dopamine derivatives together for zirconia surface biofunctionalization.

Despite the limitations of this in vitro study (experimental materials, dark colour of dopamine, bioactive glass infiltration control), all the proposed zirconia-modified surfaces tested in the present study revealed promising results on the preliminary biological analyses. Nevertheless, further studies are proposed to evaluate cell differentiation to the osteogenic path, including multiple mRNAs and secreted proteins analyses, followed by in vivo analyses.

3.5. Conclusion

Based on the present findings, the following conclusions could be drawn:

- Y-TZP specimens infiltrated with 45S5 BG, 58S BG, and covered with dopamine were successfully produced.

- Despite the high processing temperature, all groups present full coverage of osteoblasts. Also, the higher osteoblast proliferation was promoted by Y-TZP samples with bioactive glass infiltrated (Y-TZP + 45S5 BG and Y-TZP + 58S BG).

- Y-TZP + 58S BG + 58S dip (day 7) promoted the lowest mesenchymal cell proliferation and the highest roughness, indicating that there is no necessity for an extra deposition of 58S.

- Regardless of the treatment carried out on the surface of Y-TZP, the biological results were more promising compared to the Y-TZP control group.

- Finally, the authors believe the infiltration and coating technique can be applied to implants manufacturing process, promoting excellent biological performance in vitro.

Chapter 4 - Static and dynamic mechanical behaviour of Y-TZP structures with bioactive surfaces obtained by the infiltration of 45S5 and 58S bioactive glasses[3]

4.1 Introduction

Zirconium dioxide (ZrO_2), also known as zirconia, has emerged in dentistry field as a promising material for various applications such as dental bridges, crowns, onlays, inlays, and implant structures, due to its aesthetic properties such as colour and opacity that mimic natural teeth appearance (STADLINGER et al., 2010). Zirconia displays unique biomechanical characteristics such as high fracture toughness, fatigue resistance, bending strength, corrosion resistance, radiopacity, as well as higher affinity to bone tissue than most alternative biocompatible ceramics (BONA; PECHO; ALESSANDRETTI, 2015; ZHANG, 2012). Despite zirconia implants offer aesthetic benefits over titanium implants, titanium still reports superior mechanical and osseointegration potential over zirconia. With reports of more than 30 years of follow-up, titanium is still considered the gold standard material for dental implant applications (BRÅNEMARK et al., 1969). Nevertheless, titanium corrosion and greyish color are considered disadvantages since it affects peri-implant tissues and appear through the peri-implant mucosa, influencing negatively on oral aesthetic (KAROUSSIS et al., 2003; MARECI et al., 2016). To overcome the aesthetic disadvantage of titanium, zirconia has been extensively studied for dental implants and has shown favorable results in terms of aesthetic and biological outcomes (ALBREKTSSON; HANSSON, 1985; DEPPRICH *et al.*, 2008; DUBRUILLE *et al.*, 1999; KOHAL, Ralf J. *et al.*, 2004).

Despite the favorable findings recorded for zirconia-based surfaces, some previous studies have reported high failure rates and zirconia peri-implant crestal bone loss in human clinical studies (KOHAL et al., 2016). Also, zirconia has been considered a bioinert material, meaning it does not form chemical bonds or has biologic interactions with the surrounding tissues meaning it does not form chemical bonds or has biologic interactions with the surrounding tissues (PICONI; MACCAURO, 1999; YIN *et al.*, 2017). With intention to improve zirconia surface, enhancement in mechanical behavior and biological response, some physical and chemical coating methods have been investigated. Typical approaches have been using bioactive

[3] Will be submitted soon to Journal of the Mechanical Behavior of Biomedical Materials.

materials (e.g., calcium phosphates or bioactive glasses) as surface coatings on zirconia, despite delamination problems often impair this solution (FABRIS et al., 2016). Another strategy, suited for avoiding delamination issues, was proposed by Zang et al., 2009b, which relies on a functionally graded calcium phosphate-based glass/zirconia (CPG/Y-TZP) system with a low elastic modulus and a flexural strength similar to, or even higher than that recorded for Y-TZP through the infiltration of glass into zirconia, creating a FGM (ZHANG, 2012; ZHANG; REGEROS; KIM, 2009c).

The use of bioactive glasses (BG) on zirconia surface is proposed aiming to combine the outstanding mechanical properties of a zirconia bulk with the peculiar properties of the bioactive glasses at the surface of an implant. It is known that the essential condition for glasses to form an interfacial bond with living bone is the establishment of a hydroxyapatite layer at their surface. BG are able to stimulate bone cells towards a path of regeneration and self-repair, thus significantly accelerating tissue healing kinetics. Regeneration is due to calcium and phosphate ions release, which are present at BG composition and perform an important role at bone metabolism (angiogenesis, grow and tissue mineralization).

45S5 bioactive glass was the first commercial bioactive glass and it is still largely studied due to its outstanding bone bonding properties. In the 90s, a new bioactive glass was developed via sol–gel, named 58S bioactive glass, in order to obtain an alternative compound with similar properties to those of 45S5 (FERRARIS et al., 2000; HENCH, 2015; MOEZZIZADEH; NOJEDEHIAN; HAGHI, 2017; ZHONG; GREENSPAN, 2000). Sepulveda et al. (2002) showed that melt-derived 45S5 glass powders exhibit lower dissolution rates for apatite formation in comparison to 58S gel-glass powders (SEPULVEDA; JONES; HENCH, 2002)

In addition to the osteointegration benefits, the surface modification approach holds also great potential for improving soft-tissue integration around zirconia implants, which is another important clinical application in implant dentistry (LIU et al., 2015). In this sense, this work aims to produce zirconia structures with bioactive surfaces through infiltration of two types of bioactive glasses, namely the 45S5 BG and the 58S BG, and to assess the static and dynamic mechanical behavior of zirconia-BG structures. Complementary analysis on the surface- and subsurface- microstructure are also conducted.

4.2. Materials and methods

4.2.1. Bioglass 45S5 Synthesis

Bioactive glass 45S5 (45%wt SiO_2, 24.5%wt Na_2O, 24.5%wt CaO, 6%wt P_2O_5) powder was processed by the melt quenching technique. To produce 100 g of bioglass it was used 45 g of silica (SiO_2 - Sigma Aldrich, 99.9%, CAS 0676-86-0), 41.98 g of sodium carbonate (Na_2CO_3 - Lafan, 99%, CRQ 10.232-F), 43.58 g of calcium carbonate (Ca_2CO_3) and 6.00 g of phosphorus pentoxide (P_2O_5 – Scientific Exodus, 99.5%, CAS 1314-56-3). The precursor powders were dry homogenized for 30 min at 150 rpm (Mill CT 242 Servitech). Melting was carried out at 10 °C/min in Jung melting furnace (Blumenau, Brazil) using a platinum crucible. The first burning stage was at 900°C, 30 min for the homogeneous decomposition of carbonates and release of CO_2; the fusion at 1450 °C for 2 h resulting in a homogeneous vitreous. After melting, the platinum crucible was immersed in water. The grinding to obtain the powder was carried out in a planetary mill (Retsch PM 100), with a jar and agate spheres, for 80 min at 400 rpm (PLEWINSKI *et al.*, 2013).

4.2.2. Bioglass 58S synthesis

Bioactive glass 58S (58%wt SiO2, 33%wt CaO, 9%wt P_2O_5) powder was processed by the sol-gel technique. First, tetraethyl orthosilicate (TEOS) (98%, Sigma Aldrich, USA), triethyl phosphate (TEP) (99.8%, Sigma Aldrich, USA) and calcium nitrate tetrahydrate ($Ca(NO_3)_2.4H_2O$) (Vetec, Brazil) were used as precursors of silicon, phosphorous and calcium oxide. Ethyl alcohol (EtOH, P.A., Synth, Brazil) was used as solvent of TEOS and TEP, and nitric acid (HNO_3, 68%, Vetec, Brazil) was used to dissolve $Ca(N\text{-}O_3)_2.4H_2O$.

The molar ratios of SiO_2, P_2O_5, and CaO were calculated according to the 58S BG composition. TEOS and TEP were placed in a glass recipient containing EtOH under magnetic stirring. $Ca(N\text{-}O_3)_2.4H_2O$ was dissolved in 2*M* HNO_3 and then added to water at a molar ratio TEOS:H_2O of 1:4. Then, the solution was stirred for 1 h and placed for drying in a chamber at 70ºC over a period of 24 h. Subsequently, the material was thermally treated at 600ºC for 24 h and milled in a planetarium ball mill at 400 rpm

for 1 h to obtain the bioactive glass powder (GALARRAGA-VINUEZA *et al.*, 2018; MESQUITA-GUIMARÃES *et al.*, 2017).

4.2.3. Zirconia surface modification

Zirconia disks (N=60) were prepared using 2.2 g yttria-stabilized Tetragonal Zirconia Polycrystal powder (Tosoh, Zirconia TZ-3YSB-E, Japan), compacted in a cylindrical stainless steel die, using a applied pressure of 2.5 tons during 30 s. Stearic acid was used as a lubricant to ensure the good flowability of the zirconia powder and facilitated the homogeneous distribution of the material. The zirconia green compacts had a diameter of 16.00 ± 0.02 mm and a thickness of 2.10 ± 0.02 mm (Figure 11) (FABRIS *et al.*, 2021).

Figure 11 – Schematic representation of the press, sintering and BG infiltration technique used for the production of substrates. 1º Step: pouring the Y-TZP powder inside the stainless-steel die cavity; applying pressure; green compact extraction, and sintering. 2º Step: disk covered with 1g of BG powder + 0.06 ml of distillate water and sintering.

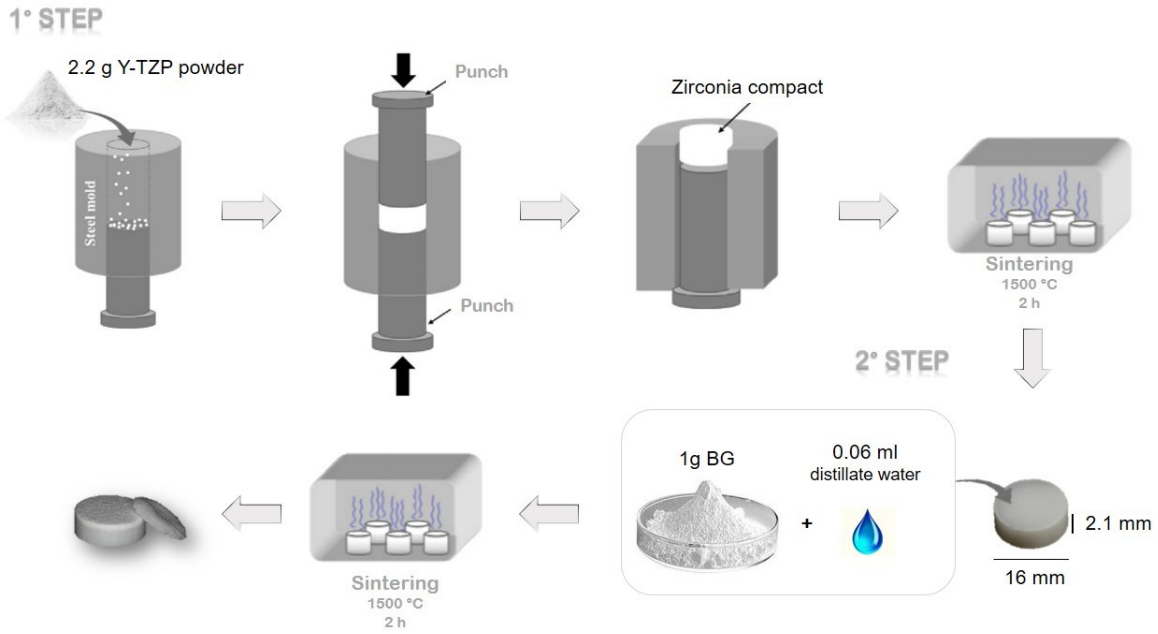

The disks were divided in three groups (n=20) according to the surface treatment: (1) Y-TZP group: control group, the disks were sintered 1500 °C for 2 h, 5

°C/min. In the sequence, the disks were sandblasted (Renfert Basic Eco, USA) with Al_2O_3 particles grits of 110 μm and 4 bar to obtain a macro-rough surface and acid etched with 10% hydrofluoric acid for 1 h at room temperature, washed 1 min in tap water and cleaned in an ultrasonic water bath (LIU et al., 2017). (2) 58S BG and (3) 45S5 BG group: Y-TZP disks were sintered 1500 °C for 2 h, 5 °C/min. In the sequence, the disks were covered with a paste formed by 58S powder and distilled water (proportion: 1 g of BG powder with 0.06 ml distillate water for 45S5 and 0.03 ml distillate water for 58S) and infiltrated at the same time and temperature to make the glass infiltration. Bioglass excess was removed ultrasonically and sandblasted with Al_2O_3 particles grits of 110 μm and 4 bar.

4.2.4. Microstructure analysis

The specimens' surfaces (non-infiltrated and infiltrated groups) were analysed by Scanning Electron Microscopy (SEM). Three specimens were cross-sectioned and Scanning Electron Microscope images were obtained to analyse the BG infiltration depth and subsurface microstructure. Energy Dispersive Spectroscopy (EDS) was used to assess the chemical composition of specimens at specific locations.

An X-Ray diffractometer with a Cu-Kα source (D 8 Advance X-ray diffractometer, Bruker AXS, Karlsruhe, Germany) was used to determine the crystalline phases of the Y-TZP surfaces. X-Ray Diffraction (XRD) spectra were collected before and after fatigue tests on five random Y-TZP samples over a 2θ range between 3º and 90º at a step size of 0.05º and 0,02º/s. The monoclinic phase fraction was obtained by the Rietveld refinement method (YOUNG, 1989).

4.2.5. Bulk density and roughness analysis

The maximum density (M_d) was determined using the Archimedes principle with water displacement method. The density was calculated using Equation 1:

$$Md = \frac{m1 \times d}{m3 - m1} \quad (1)$$

m1: mass of sintered body at room temperature (g).

m2: sintered body was kept in boiling water for one hour. After cooling down to room temperature, the mass of the soaked body (m2) was measured in the water at room temperature (g).

m3: after removing water from the surface, mass (m3) of the sintered body is measured (g).

d: water density (1.0 g/cm^3).

Five specimens from each group were submitted to a roughness analysis on a white light interferometer (Zygo, NewView 7300, Montgomery, USA) considering the parameters recommended by ISO:4287-1997 (Ra and Rz). Three readings were performed on 0.25mm^2 of analysing area and using the Mountains Maps 7.1 software to obtain images and values for each specimen.

4.2.6. Mechanical characterization

Biaxial flexural strength was tested using a piston on three balls device, according to ISO 6872:2013 for testing dental ceramic materials, and an universal testing machine (Instron-EMIC, 23-5S, MA, USA) The samples were loaded at the center of the upper surface and supported by three hardened steel balls with 1.5 mm diameter, positioned 120 degrees apart, forming a 10 mm support circle. The modified surfaces were oriented to the tensile side (downside) and 10 samples of each group were analysed.

This test was applied to non-fatigued samples of all groups (n=10) and also to the surviving samples of the fatigue tests to assess for their residual strength. The maximum applied load was recorded and the biaxial flexural strength was calculated according to the ISO 6872. Additionally, the data was analysed using the Weibull statistics according to the following equation:

$$P_{F(\sigma c)} = 1 - \exp\left[-\left(\frac{\sigma_c}{\sigma_0}\right)^m\right] \quad (3)$$

Where PF (σc) is the probability of failure, σc the fracture strength, σ0 the characteristic strength (PF(σc) = 63.2%) and m is the Weibull modulus. Accordingly,

plotting ln [ln 1/(1−Pf)] against ln σ will provide a slope with the value of the Weibull modulus. Fracture surfaces of tested specimens were analysed using SEM.

The fatigue test was performed on a pneumatic mechanical cycling machine (Biocycle V2, Biopdi) following the ISO: 6872-2015 guidelines. Samples were placed on a ball on three ball device and loaded for 500.000 cycles at 2 Hz and 50 N, to represent approximately 5 clinical years (SPYROPOULOU et al., 2016).

4.2.7. Statistical analysis

Weibull analysis were used to estimate the flexural strength of specimens under static loading conditions. For the dynamics test, statistical analyses were performed using statistical software (OriginPro, OriginLab, version 8.5, Northeamton, MA, USA). The results were analyzed using one-way ANOVA followed by the Tukey Test.

4.3 Results

4.3.1. Surface microstructure

Figure 12 shows the top view of the surfaces of the different groups of specimens. The Y-TZP sample (Figure 12A) is characterized by a rough surface due to the sandblasting and etching treatments. The infiltrated samples (Figure 12B and 12C) presented a microstructure characterized by the presence of BG glass at the grain boundaries of the zirconia particles.

Figure 12 - SEM images of different surfaces: A) monolithic zirconia B) zirconia infiltrated with bioglass 45S5 and C) zirconia infiltrated with bioglass 58S. Images B and C are characterized by the presence of BG at the grain boundaries of the zirconia particles.

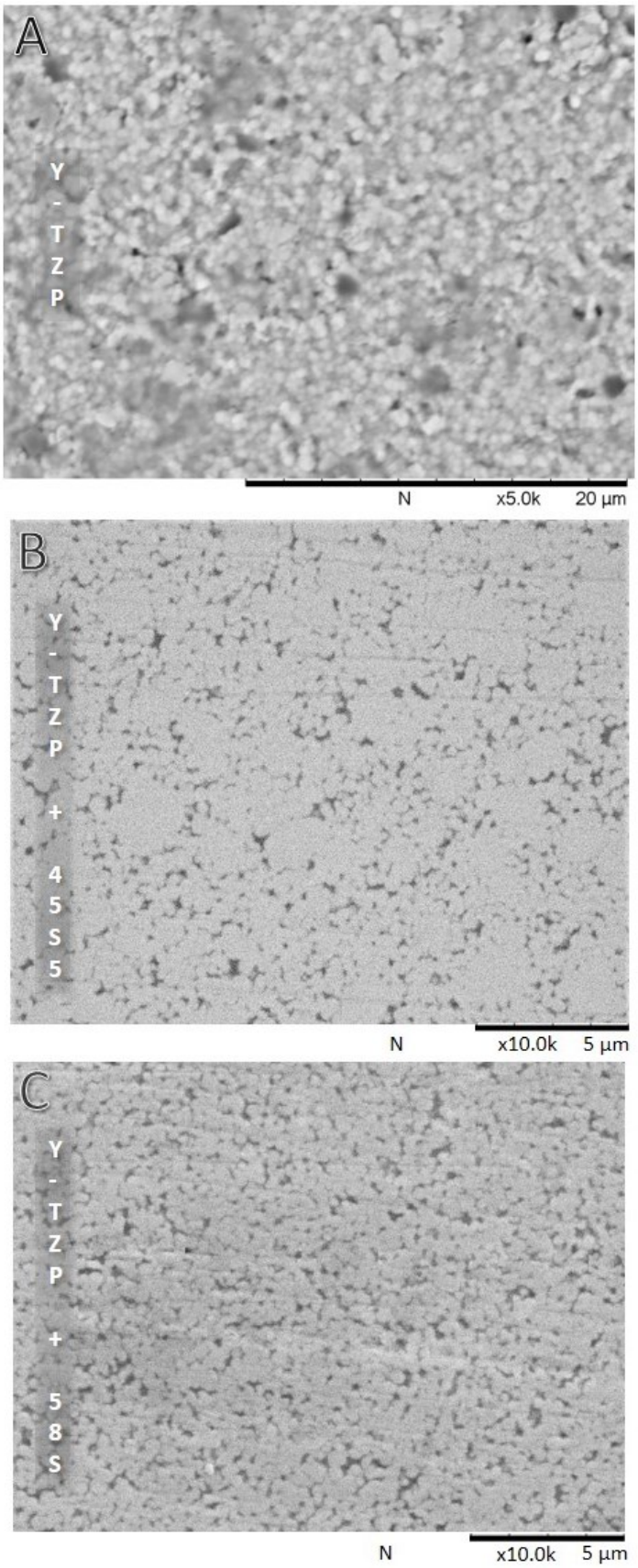

45S5 BG and 58S BG were successfully infiltrated in the zirconia substrate, producing a BG-infiltrated zirconia specimen as can be seen in Figure 13 and Figure 17. The infiltration was measure using ImageJ analysis software. The total thickness of the samples was 2.1 mm, presenting an average bioglass infiltration depth of around 0,92±0,11 mm for Y-TZP + 45S5 BG group and 0,887±0,10 mm for Y-TZP + 58S BG group. It is possible to observe a few porosity, detected along the different regions of the specimen (Figure 14), which can be considered detrimental to the mechanical performance. The microscopic observations could be correlated with the chemical analyses of the samples (figure 13), which confirms the presence of chemical BG elements.

Figure 13 – SEM cross section images of BG-infiltrated groups before fatigue tests and the EDX analysis performed on infiltrated zone.

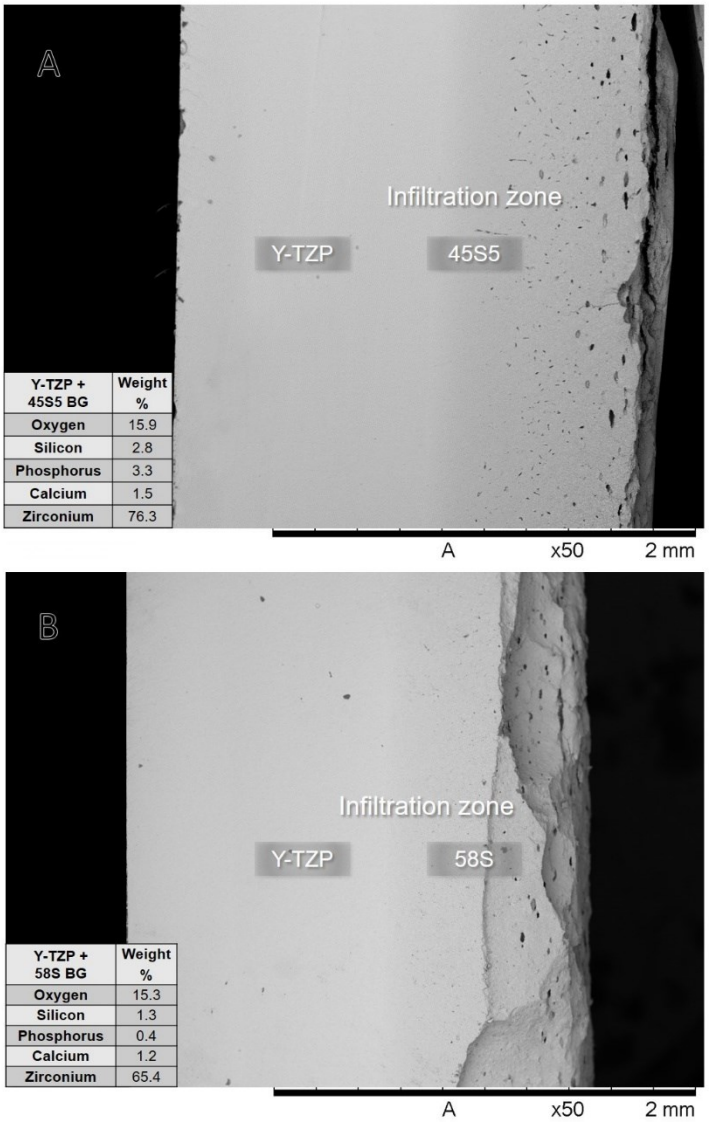

Y-TZP + 45S5 BG	Weight %
Oxygen	15.9
Silicon	2.8
Phosphorus	3.3
Calcium	1.5
Zirconium	76.3

Y-TZP + 58S BG	Weight %
Oxygen	15.3
Silicon	1.3
Phosphorus	0.4
Calcium	1.2
Zirconium	65.4

.

Figure 14 – Micrograph of a porous found on Y-TZP + 45S5 BG.

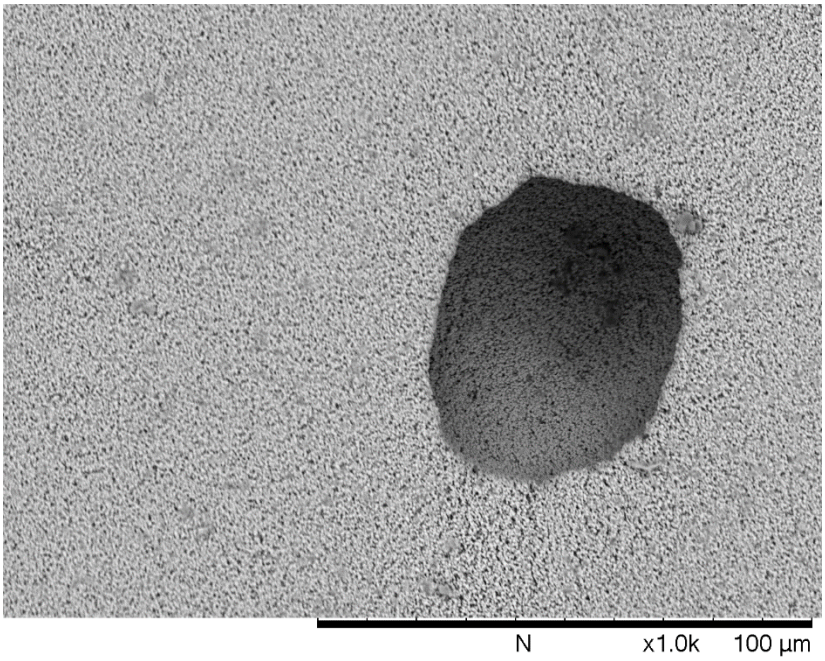

4.3.2. Density and roughness analysis

The density (g/cm$_3$) and the porosity (%) calculated by the Archimedes method for all groups are shown in Table 5. It can be seen the bulk density was maintained between 94 and 98% for all types of the groups. Table 5 also shows the roughness values, where the surface morphology is described using 3D-roughness parameters (Sa and Sq). Y-TZP group presented lowest roughness (Sa: 0.92µm and Sq: 1.07µm) when compared to Y+TZP 45S5 (Sa: 4.31µm and Sq: 5.7µm) and Y-TZP + 58S BG (Sa: 4.08 and Sq: 5.21), which means that the BG infiltration resulted on zirconia surfaces with increased roughness.

Table 5 - Roughness and density results of different surface treatments

Groups	**Roughness**		**Density**	
	Sa (µm)	*Sq (µm)*	*Density (g/cm3)*	*Density (%)*
Y-TZP	0.92 ± 0.67	1.07 ± 1.06	5.99 ± 0.06	98
Y-TZP + 45S5 BG	4.31 ± 2.16	5.70 ± 1.67	5.70 ± 0.10	94
Y-TZP + 58S BG	4.08 ± 0.69	5.21 ± 0.87	5.75 ± 0.03	95

4.3.3. Mechanical results

Figure 15 and Table 6 shows the biaxial flexural strength results obtained for the non-infiltrated and BG-infiltrated zirconia groups. It can be seen that, regardless of the type of bioactive glass used (45S5 BG or 58S BG), the flexural strength of infiltrated specimens were below the results obtained for the monolithic zirconia specimens. Although the non-fatigued groups exhibited higher strength values than those registered for fatigued groups, statistical testes showed no significant difference on the biaxial strength after the fatigue test. Statistical tests (Two-way ANOVA with Tukey test, level of significance = 0.05) show statistically significant difference in biaxial strength only between the different groups of materials.

The characteristic strength (σc) of non-fatigued Y-TZP exhibited the highest value (651MPa) whereas the lowest value was registered for Y-TZP + 58S BG with fatigue had the 56MPa.

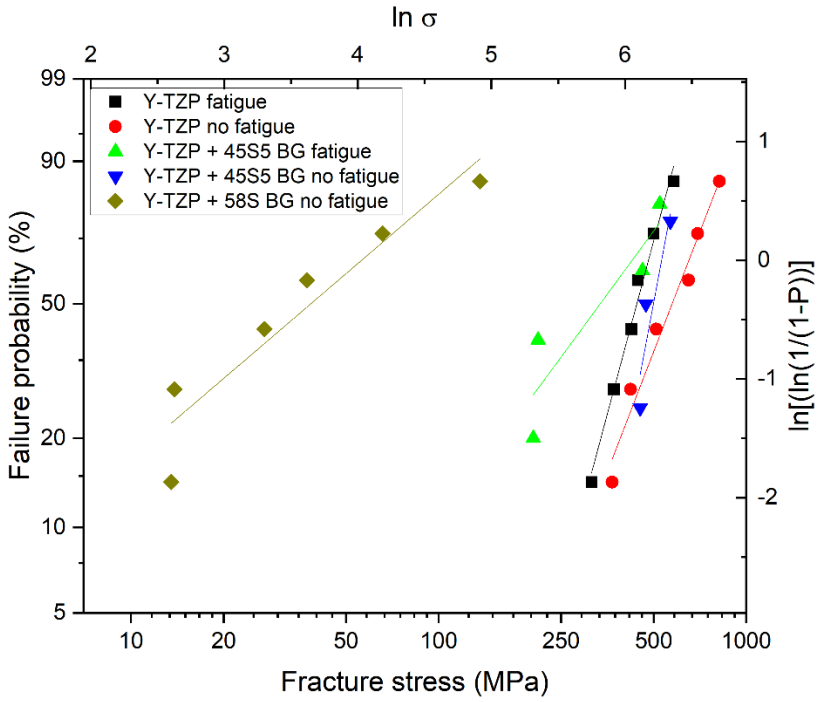

Figure 15 - Weibull plots of surface porous zirconia specimens fractured in biaxial flexural strength tests.

Table 6 - Biaxial flexural strength results of BG-infiltrated zirconia and pure zirconia groups, for non-fatigued and fatigued conditions.

Group	Mean Strength ± std. dev.	Weibull char. Strength, (σ_0)	Weibull modulus, (*m*)
Y-TZP fatigue	433 ± 94	481	4.2
Y-TZP no fatigue	579 ± 144	651	2.9
Y-TZP + 45S5 BG fatigue	349 ± 144	427	1.5
Y-TZP + 45S5 BG no fatigue	496 ± 50	531	6.0
Y-TZP + 58S BG no fatigue	101 ± 244	56	0.9

* Tukey test showed that all groups are significantly different between themselves.

Figure 16 shows the typical fracture patterns of specimens obtained after biaxial flexural strength tests. Specimens fractured in two or three parts and no correlation was observed between the number of broken pieces and the respective flexural strength.

It was noted that Y-TZP and Y-TZP + 58S BG groups presented more fractures in 2 pieces, while Y-TZP + 45S5 BG group obtained fractures in two and three parts equally.

Figure 16 – Typical fracture patterns observed for the specimens after biaxial flexural test. The red circle indicate the central location of the loading piston.

3 broken pieces	2 broken pieces
Y-TZP = 3 sample	Y-TZP = 7 sample
Y-TZP + 45S5 BG = 5 sample	Y-TZP + 45S5 BG = 4 sample
Y-TZP + 58S BG = 2 sample	Y-TZP + 58S BG = 6 sample

Table 7 shows the data obtained from the mechanical cyclic tests, where the number of failed specimens and the average number of cycles at failure are presented for each group. Y-TZP group revealed a greater resistance to fatigue, where only one specimen fractured after 482127 cycles. The BG infiltered groups, on the other hand, revealed high susceptibility to cyclic loading, with the majority of the specimens failing during the fatigue test. Y-TZP + 45S BG group had 7 fractured samples and the maximum value registered varied between 1 and 2122 cycles (one sample fractured at 490000 cycles). A similar behaviour was observed for Y-TZP + 58S BG, where eight samples fractured during fatigue testing, withstanding between 1 and 4965 cycles.

Table 7 – Data on mechanical cycling tests for zirconia and BG-infiltrated zirconia: number of failed specimens and number of cycles at fracture.

Groups	Reported failure	Number of cycles at failure (Average± Standard Deviation)
Y-TZP	1	482127 cycles*
Y-TZP + 45S5 BG	6	56,5 $\pm$ 841,37
Y-TZP + 58S BG	8	155 $\pm$ 1715

* only one sample fractured

Figure 17 shows the infiltration zone of the different groups (BG-infiltration arrows indicate the bioglass transition to monolithic zirconia zone) and it can be seen that, in both specimens, failure started on the infiltrated part of the discs, which corresponds to the tensile surface in the flexural test. The fracture surfaces revealed typical fracture patterns of zirconia materials, namely the presence of a compression curl (CC). The compression curl is a feature often seen is specimens subjected to flexural tests, as the stress gradient formed makes the crack to slow down and to change direction, thus creating a curve. The fracture origin is at the opposite direction to the compression curl.

Figure 17 - SEM micrographs of cross section on different groups: A) Y-TZP + 45S5 and B) Y-TZP + 58S, after mechanical tests. The presence of typical brittle marks such as compression curl (CC) can be observed.

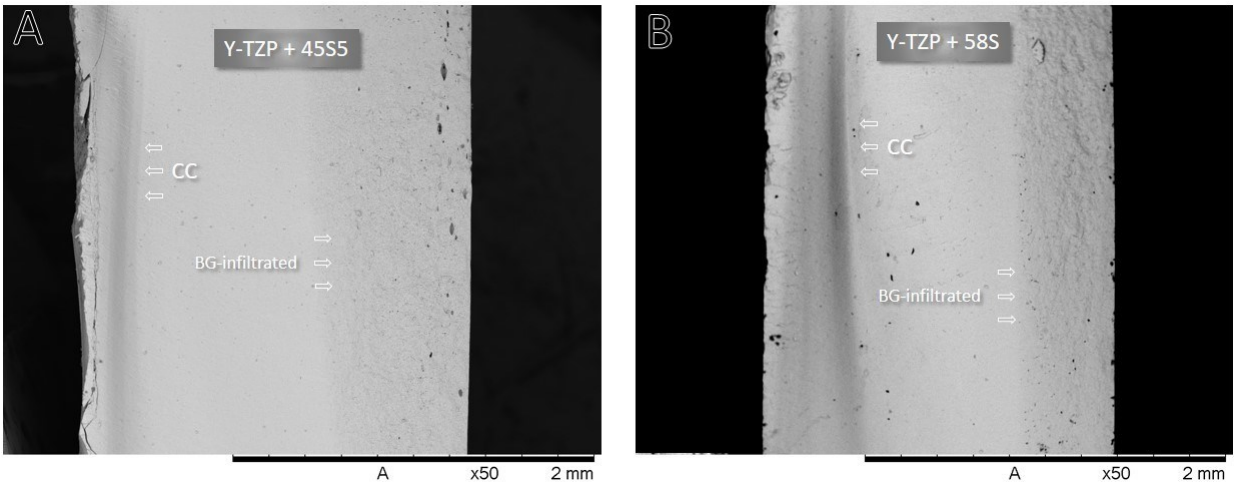

4.3.4. XRD analysis

The X-ray diffractograms taken for zirconia groups (Y-TZP samples), before and after mechanical cyclic loading tests, are presented in Figure 18. It is possible to observe that the monoclinic and tetragonal phases of the Y-TZP samples were found before and after fatigue, but in different percentages: non-fatigued specimens exhibited 92,4% and 7,6% of tetragonal and monoclinic phase, respectively. After fatigue tests, the phase content changed to 80,1% of tetragonal phase and 19,9% of monoclinic. All samples revealed the tetragonal zirconia characteristic peak at 2θ 30.2° and a high-intensity diffraction peak at 2θ 50.2°

Figure 18 - XRD for Y-TZP samples before and after fatigue tests. M) Monoclinic zirconia and T) tetragonal zirconia.

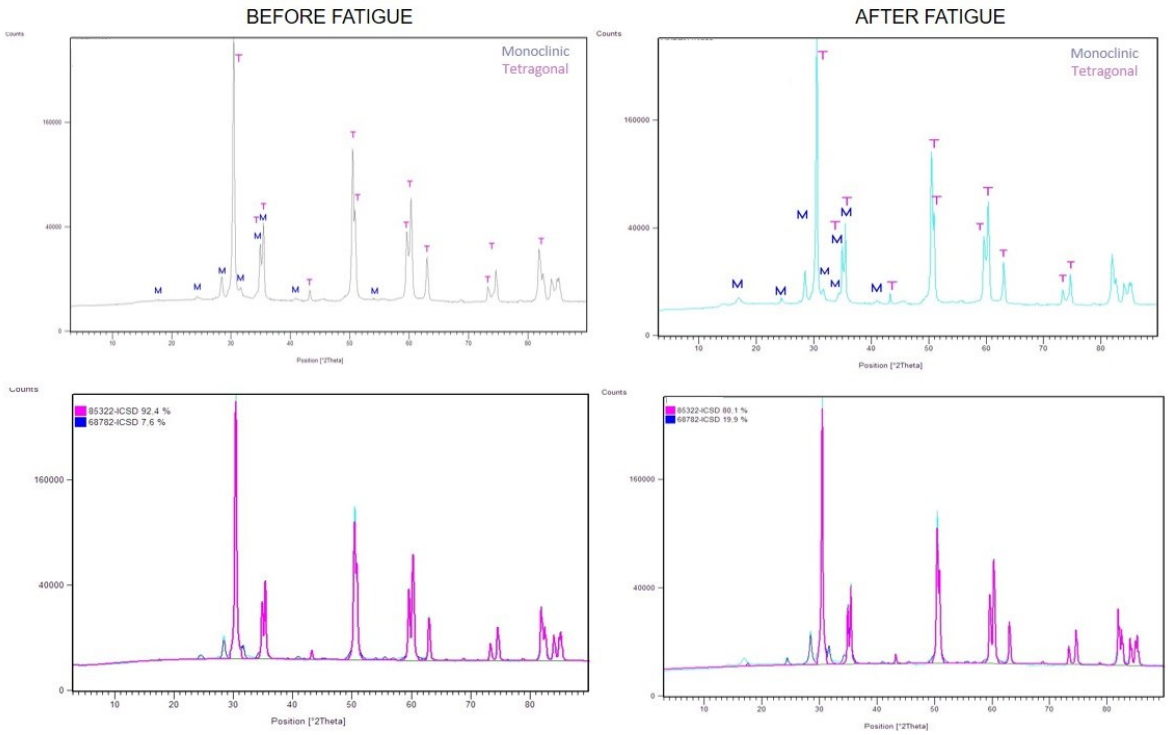

4.4 Discussion

The use of zirconia as a viable alternative to titanium can be recognised if provides good long-term prognosis in patients. For that, mechanical tests are important to evaluate the survival success of zirconia implants. This study aimed at assessing the mechanical behaviour of zirconia (Y-TZP) specimens infiltrated with different bioactive glasses (45S5 BG and 58S BG) as compared to pure zirconia (Y-TZP) ones.

This work combined the densification of Y-TZP and the BG infiltration in two steps: pre-sintering of Y-TZP at 1500 °C for 2 hours and posteriorly sintered with BG in the same time and temperature. SEM images and EDS analyses showed that all zirconia discs were successfully infiltrated with both types of bioactive glasses (45S5 and 58S). The infiltration layer depth was measured to be roughly 1 mm in both groups, more precisely 0,92 mm and 0,89 mm in 45S5 BG and 58S BG groups, respectively. This results was higher than expected when compared to other studies (FABRIS et al., 2021) and a few factors on the infiltration method can influenced this result, such as the sintering time (DURKAN et al., 2022), the compaction pressure of the Y-TZP (TRUSOVA et al., 2022), or the bioactive glasses used in this study.

The SEM images show that BG infiltration modified the zirconia surface at the chemical and morphologic levels, creating a microstructure characterized by sub-micrometric zirconia particles embedded in a glass matrix and also some porosity in the infiltrated region. These values demonstrate the challenge in producing BG-zirconia parts with proper mechanical strength for use in biomedical applications, as porosity negatively influence the strength of ceramics, as revealed by the strength data in this study, thus making the infiltration treatment an disadvantage, with regard to the strength, when using the processing conditions here reported.

Previous studies have reported that roughness surfaces influence drastically on osseointegration of zirconia implants (SCHÜNEMANN *et al.*, 2019) and the flexural strength (DENG et al., 2022; KHAYAT et al., 2018). Considering this, the Y-TZP surface was treated with intention to increasing the roughness of the material. The results showed similar value of those reported in literature to monolithic zirconia (Y-TZP Ra at 0.92μm) (KHAYAT et al., 2018). Concerning to BG-infiltrated zirconia, both groups presented higher roughness (Y-TZP + 45S5 BG: 4,31 μm Sa and Y-TZP + 58S BG Sa at 4.08 μm). No others studies were found to comparing BG roughness results, however, it is known that higher roughness are more favourable area for osteoblasts adhesion, consequently, presents better cell adherence and osseointegration. On the other hand, the disadvantage of extremely rough surfaces are the lower strength imparted by the higher number of surface cracks and defects (SCHÜNEMANN *et al.*, 2019; PICONI, C.; MACCAURO, 1999).

This fact is confirmed in this work when we analyse the performance of the materials concerning to flexural strength results. The 58S BG provided lower fracture resistance than 45S5 BG, in agreement with the higher porosity found on SEM images of the specimens' cross-section (Figure 3). Meanwhile, it is important to emphasize that the present study showed general lower flexural strength values for pure zirconia (579 + 144 MPa) when compared to previous studies [approximately 900 to 1400 MPa (DURKAN et al., 2022; KHAYAT et al., 2018)], probably due to sandblasted procedure. Flexural strength results decrease further with the BG infiltration (496±50MPa on Y-TZP + 45S5 BG and 101± 244MPa on Y-TZP + 58BG). A possible explanation for such behaviour may be the excessive sintering time. Durkan et al, 2022 (DURKAN et al., 2022) affirm that the flexural strength of zirconia significantly decreased when sintered during 3 hours compared with 2 hour, therefore, zirconia sintering time affect negatively the zirconia biaxial flexural strength. In this research, the Y-TZP was sintered for 2h

and then sintered again for the same time, totalling 4h, which probably justifies the significantly reduction of flexural strength. In addition, and regarding the BG-infiltrated specimens, the high infiltration depth together with the porosity formation in the infiltration layer should have accounted for the majority of the strength reduction. The flexural strength research of Y-TZP infiltrated with BG is very scarce, no previous study was found, proving the need for further studies about zirconia infiltrated with bioactive glass. An important point that must be discussed here is the high sintering temperature (1500ºC) used in our study to produce the BG-infiltrated zirconia specimens, which may impact the bioactive properties of the BG. Ma et al. 2010 (MA et al., 2010) showed that the bioactivity of 58S BG decrease when subjected to a temperature as high as 1200ºC, due to its crystallization. On the other hand, Gouveia et al, 2021 (GOUVEIA *et al.*, 2021) showed similar results to the abovementioned report, even if 58S BG exposed to 1500º C did reveal certain bioactivity.

Is important to consider the difference in coefficient of thermal expansion (CTE) between substrate Y-TZP (around 10×10^{-6} K^{-1}) typically higher than the bioglass (around 12–15 $\times10^{-6}$ K^{-1}). The CTE of the glasses needs to be as equal as possible to value of zirconia (or a little lower on surface) to prevent the development of the long-range thermal stress in graded structure, which can influence on internal stress, delamination and fracture (FABRIS et al., 2021).

The biaxial flexural strength data, prior and after fatigue tests, are presented in Figure 15 and Table 6. The results are presented using the Weibull analysis, which is commonly used by engineers as statistical method to study the strength reliability and variability analysis for describing failure of brittle materials (PITTAYACHAWAN et al., 2007). The two Weibull parameters presented in Table 2 are the Weibull modulus (m) and the characteristic strength, or Weibull scale parameter (σ0). The Weibull modulus (m) expresses the variability and predictability of results while the characteristic strength (σ0) is the strength value σ. A high Weibull modulus indicates smaller defects and greater structural reliability. The m values obtained for the different types of specimens oscillated between 0,4 and 4,2 which is lower than the values reported in literature for dental ceramics (between 5 to 15) (OZER et al., 2018; ROEDEL et al., 2019). These results can also explain the variability of results, possibly due to the vast presence of pores at the infiltrated layers. The low number of samples for the mechanical tests is an important limitation on this work. Usually, at least 10 samples are necessary to properly evaluate their mechanical resistance using the Weibull

method. However, low number of samples survived the fatigue test, generating groups with just a few samples. Thus, direct conclusions can not be drawn from the calculated Weibull parameters. On the other hand, the analysis allows the comparison between the different groups and provides insights on the behavior of the samples under mechanical loading.

Regarding the fracture of the samples on the biaxial flexural test, it was noted that samples fractured mostly into two parts, which contrasts to Börger et al. (BÖRGER; SUPANCIC; DANZER, 2004) findings. According to this author, the fracture normally occur in three extensions and the reason for fail is the thickness of the sample, if the specimen is too thin and its elastic modulus is too low buckling may occur. Yanaba and Hayasi (YANABA; HAYASHI, 1996) indicated that samples with fracture in two parts have greater toughness than samples fractured in three parts. Still, it was noticed that the irregular fracture occurred most frequently in the samples with zirconia infiltrated with bioactive glass 45S5 BG and 58S BG, which was probably due to the presence of pores and further evidenced by their lower density. In addition, some BG samples fracture distant from the piston loading site, also indicating the possible presence of large defects (pores) in the sample.

More structured studies that assess the mechanical capacities of different types of zirconia with their exact composition, sintering process and manufacturing process are also needed to set standardized guidelines according to the ASTM (American Society for Testing and Materials) and ISO (International Organization for Standardization) in the manufacturing of zirconia implants. Although in this study the infiltration of bioactive glass showed low mechanical strength, the gradation of properties between dissimilar materials through the infiltration technique remains an excellent constructive approach, as already shown in in previous works. Several studies applied this type of solution to the issue of coupling materials with different CTEs, because promote an incorporation of transition layers with intermediate properties between the coating and the implant (FABRIS et al., 2017, 2021; HENRIQUES et al., 2012; MIRANDA et al., 2016). In this sense, new iterations should be explored in order to produce bioactive glass-infiltrated zirconia parts with both bioactive behaviour and high mechanical strength, such as: scanning different pre-sintering temperatures; drastically reduce the infiltration depth; test alternative bioactive glasses with higher thermal-compatibility to zirconia, among others.

4.5 Conclusion

This study aimed at producing zirconia structures with bioactive surfaces through infiltration of two types of bioactive glasses, 45S5 BG and 58S BG, and to assess the static and dynamic mechanical behavior of zirconia-BG structures. Based on the findings of this in vitro study, the following conclusions can be drawn:

- 45S5 BG-zirconia and 58S BG-zirconia specimens were successfully produced by an infiltration technique.
- BG-infiltrated zirconia disks underperformed relative to zirconia monolithic discs, both in static and fatigue conditions. Considering mechanical outcomes, such findings suggest that BG-infiltrated zirconia implants needs more studies for use as an alternative solution to monolithic zirconia implants for implant dentistry.

Chapter 5 - Final remarks

Advances in engineering have improved the zirconia surfaces to accelerate bone-healing response and clinically decrease the patient's edentulous period. Moreover, zirconia has been coated with bioactive compounds and multifunctional molecules, which can induce an osteogenic stimulus, cell adherence, and an additional antibacterial effect. In this way, zirconia can change from a “criticized bioinert” surface to a “bioactive” and multifunctional one pursuing the most favorable biologic and mechanical peri-implant tissue responses. Current studies show that zirconia can be converted into a bioactive system embedding diverse biomolecules that can mimic bone tissue structure at macro-, micro-, and nano-scale. Still, future in vitro, in vivo, and long term clinical studies are required to evaluate success rates of treated zirconia implants. Further studies should evaluate zirconia implants over time in terms of peri-implant bone stability, absence of inflammation, infection, mobility, and mechanical complications that will give a clearer panorama on guidelines for surface modification of zirconia implants.

For the continuation of this work, we suggest the following:

- Study and develop a bioactive glass with thermal properties that are more compatible with zirconia.
- Optimize the infiltration process of bioactive glasses to produce an infiltrated layer of small thickness (<50 μm) without defects.
- Investigate the mechanical and biological behaviour of the developed solutions.
- Conduct clinical studies on modified zirconia-based surfaces to provide a realistic perspective of how oral biofilms, loading, and other patient conditions may affect the properties of zirconia.

REFERENCES

ABOUSHELIB, M. N.; SALEM, N. A.; MONEIM, N. M. A. El. Influence of Surface Nano-Roughness on Osseointegration of Zirconia Implants in Rabbit Femur Heads Using Selective Infiltration Etching Technique. **Journal of Oral Implantology**, v. 39, n. 5, p. 583–590, 2013.

ABOUSHELIB M N, SHAWKY R. Osteogenesis ability of CAD/CAM porous zirconia scaffolds enriched with nano-hydroxyapatite particles. **International Journal of Implant Dentistry**. v. 21, 2017.

AL-RADHA, A. S. D. *et al.* Surface properties of titanium and zirconia dental implant materials and their effect on bacterial adhesion. **Journal of Dentistry**, v. 40, n. 2, p. 146–153, 2012.

ALBREKTSSON, T.; HANSSON, H. Interface analysis of titanium and zirconium bone implants. **Biomaterials**, v. 6, n. 2, p. 97–101, 1985.

ALBREKTSSON, Tomas; JOHANSSON, C. Osteoinduction, osteoconduction and osseointegration. **European Spine Journal**, v. 10, p. 96-101, oct. 2001.

ALBREKTSSON, T.; WENNERBERG, A. Oral implant surfaces: Part 1--review focusing on topographic and chemical properties of different surfaces and in vivo responses to them. **The International journal of prosthodontics**, v. 17, n. 5, p. 536–543, 2004.

ALTMANN, B. *et al.* Cellular transcriptional response to zirconia-based implant materials. **Dental Materials**, v. 33, n. 2, p. 241–255, 2017.

AURÉLIO, I. L. *et al.* Does air particle abrasion affect the flexural strength and phase transformation of Y-TZP? A systematic review and meta-analysis. **Dental Materials**, v. 32, n. 6, p. 827–845, 2016.

BACCHELLI, B. *et al.* Influence of a zirconia sandblasting treated surface on peri-implant bone healing: An experimental study in sheep. **Acta Biomaterialia**, v. 5, n. 6, p. 2246–2257, 2009.

BARROS, Suelen Aline de Lima *et al*. Influence of Zirconia-Coated Bioactive Glass on Gingival Fibroblast Behavior. **Brazilian Dental Journal**, v. 30, n. 4, p. 333-341, jul. 2019.

BERGMANN, C. *et al.* Microstructured zirconia surfaces modulate osteogenic marker

genes in human primary osteoblasts. **Journal of Materials Science: Materials in Medicine**, v. 26, n. 1, p. 1–11, 2015.

BONA, A. Della; PECHO, O. E.; ALESSANDRETTI, R. Zirconia as a Dental Biomaterial. **Materials**, v. 8, p. 4978–4991, 2015.

BÖRGER, A.; SUPANCIC, P.; DANZER, R. The ball on three balls test for strength testing of brittle discs: Part II: Analysis of possible errors in the strength determination. **Journal of the European Ceramic Society**, v. 24, n. 10–11, p. 2917–2928, 2004.

BOSSHARDT, D. D.; CHAPPUIS, V.; BUSER, D. Osseointegration of titanium, titanium alloy and zirconia dental implants: current knowledge and open questions. **Periodontology 2000**, v. 73, n. 1, p. 22–40, 2017.

BRÅNEMARK, P. I. *et al.* Intra-osseous anchorage of dental prostheses. I. Experimental studies. **Scandinavian journal of plastic and reconstructive surgery**, v. 3, n. 2, p. 81–100, 1969.

BREZAVŠˇCEK, M. *et al.* The Effect of UV Treatment on the Osteoconductive Capacity of Zirconia-Based Materials. **material**, v. 9, n. 958, p. 1–19, 2016.

CALVO-GUIRADO, J. L. *et al.* Histological, radiological and histomorphometric evaluation of immediate vs. non-immediate loading of a zirconia implant with surface treatment in a dog model. **Clinical Oral Implants Research**, v. 25, n. 7, p. 826–830, 2014.

CALVO-GUIRADO, J. L. *et al.* Zirconia with laser-modified microgrooved surface vs. titanium implants covered with melatonin stimulates bone formation. Experimental study in tibia rabbits. **Clinical Oral Implants Research**, v. 26, n. 12, p. 1421–1429, 2015.

CATAURO M, *et al.,* Investigation on bioactivity, biocompatibility, thermal behavior and antibacterial properties of calcium silicate glass coatings containing Ag. **Journal of Non-Crystalline Solids.** 422 p. 16–22, 2015.

CHANG J and ZHOU Y L. Surface modification of bioactive glasses, **Materials, properties and applications.** v. 24, p. 392–405, 2012

CHEN Y, et al. Anti-bacterial and cytotoxic properties of plasma sprayed silver-containing HA coatings. **Journal of Materials Science: Materials in Medicine** v.

3603–3609, 2008.

CHO, Y. *et al.* Osteogenic responses to zirconia with hydroxyapatite coating by aerosol deposition. **Journal of Dental Research**, v. 94, n. 3, p. 491–499, 2015.

CHO BH and KO W.B. Preparation of graphene-ZrO_2 nanocomposites by heat treatment and photocatalytic degradation of organic dyes. **Journal of Nanoscience and Nanotechnology**. v.13, p. 7625–7630, 2013.

COELHO, P. G. *et al.* Osseointegration: Hierarchical designing encompassing the macrometer, micrometer, and nanometer length scales. **Dental Materials**, v. 31, n. 1, p. 37–52, 2015.

COOPER, L. F. *et al.* Fluoride modification effects on osteoblast behavior and bone formation at TiO2 grit-blasted c.p. titanium endosseous implants. **Biomaterials**, v. 27, n. 6, p. 926–936, 2006.

DAVIES, John E. *et al*. Understanding Peri-Implant Endosseous Healing. **Journal of Education**, v. 67, n. 8, p. 932-949, aug. 2003.

DELGADO-RUIZ, R. A. *et al.* Peri-implant bone organization surrounding zirconia-microgrooved surfaces circularly polarized light and confocal laser scanning microscopy study. **Clinical Oral Implants Research**, v. 26, n. 11, p. 1328–1337, 2015.

DELGADO-RUIZ, R. A.; CALVO-GUIRADO, J. L. Histologic and Histomorphometric Behavior of Microgrooved Zirconia Dental Implants with. **Clinical Implant Dentistry and Related Research**, v. 16, n. 6, p. 856–872, 2014.

DENG, X. shan *et al.* Effect of grinding parameters on surface integrity and flexural strength of 3Y-TZP ceramic. **Journal of the European Ceramic Society**, v. 42, n. 4, p. 1635–1644, 2022.

DEPPRICH, R. *et al.* Osseointegration of zirconia implants compared with titanium: an in vivo study. **Head & Face Medicine**, v. 4, n. 4, p. 1–8, 2008.

DORKHAN, M *et al*. Adherence of human oral keratinocytes and gingival fibroblasts to nano-structured titanium surfaces. **Bmc Oral Health**, v. 14, n. 75, p. 1-9, jun. 2014.

DUBRUILLE, J. H. *et al.* Evaluation of combinations of titanium, zirconia, and alumina implants with 2 bone fillers in the dog. **The International journal of oral &**

maxillofacial implants, v. 14, n. 2, p. 271–277, 1999.

DURKAN, R. *et al.* Biaxial flexural strength and phase transformation characteristics of dental monolithic zirconia ceramics with different sintering durations: An in vitro study. **Journal of Prosthetic Dentistry**, v. 128, n. 3, p. 498–504, 2022.

ENCARNAÇÃO, Isis Carvalho *et al*. Analysis of Bone Repair and Inflammatory Process Caused by Simvastatin Combined With PLGA+HA+βTCP Scaffold. **Implant Dentistry**, v. 25, n. 1, p. 140-148, feb. 2016.

EWAIS EMM, *et al*., Combined effect of magnesia and zirconia on the bioactivity of calcium silicate ceramics at C\S ratio less than unity, **Material Science and Engineering C** v. 70, p. 155–160, 2017.

FABRIS, D. *et al.* Biomechanical behavior of functionally graded S53P4 bioglass-zirconia dental implants: Experimental and finite element analyses. **Journal of the Mechanical Behavior of Biomedical Materials**, v. 120 , p. 104565-104576, 2021.

FABRIS, D. *et al.* The bending stress distribution in bilayered and graded zirconia-based dental ceramics. **Ceramics International**, v. 42, n. 9, p. 11025–11031, 2016.

FABRIS, D. *et al.* Thermal residual stresses in bilayered, trilayered and graded dental ceramics. **Ceramics International**, v. 43, n. 4, 2017.

FERRARIS, M. *et al.* Coatings on zirconia for medical applications. **Biomaterials**, v. 21, n.8, p. 765–773, 2000.

FISCHER, J.; SCHOTT, A.; MÄRTIN, S. Surface micro-structuring of zirconia dental implants. **Clinical Oral Implants Research**, v. 27, n. 2, p. 162–166, 2016.

FLAMANT, Q. *et al.* Selective etching of injection molded zirconia-toughened alumina: Towards osseointegrated and antibacterial ceramic implants. **Acta Biomaterialia**, v. 46, p. 308–322, 2016.

FLAMANT, Q.; ANGLADA, M. Hydrofluoric acid etching of dental zirconia. Part 2: Effect on flexural strength and ageing behavior. **Journal of the European Ceramic Society**, v. 36, n. 1, p. 135–145, 2016.

FREITAS, Alice Ramos de et al. Oral bacterial colonization on dental implants restored with titanium or zirconia abutments: 6-month follow-up. **Clinical Oral Investigations**, v. 22, n. 6, p. 2335-2343, jan. 2018.

GAHLERT, M. *et al.* A Comparison Study of the Osseointegration of Zirconia and

Titanium Dental Implants. A Biomechanical Evaluation in the Maxilla of Pigs. **Clinical Implant Dentistry and Related Research**, v. 12, n. 4, p. 297–305, 2010.

GAHLERT, M. *et al.* Biomechanical and histomorphometric comparison between zirconia implants with varying surface textures and a titanium implant in the maxilla of miniature pigs. **Clinical Oral Implants Research**, v. 18, n. 5, p. 662–668, 2007.

GAHLERT, M. *et al.* In vivo performance of zirconia and titanium implants : a histomorphometric study in mini pig maxillae. **Clinical Oral Implants Research**, v. 23, p. 281–286, 2012.

GALARRAGA-VINUEZA, M. E. *et al.* Mesoporous bioactive glass embedding propolis and cranberry antibiofilm compounds. **Journal of Biomedical Materials Research - Part A**, v. 106A, n. 6, p. 1614–1625, 2018.

GARMENDIA N, *et al.* Zirconia coating of carbon nanotubes by a hydrothermal method, **Journal of Nanoscience and Nanotechnology**. v.8, p.5678–5683, 2008

GOUGH, J. E. *et al*. Nodule formation and mineralization of human primary osteoblasts cultured on a porous bioactive glass scaffold. **Biomaterials**, v. 25, n. 11, p. 2039-2046, may 2004.

GOUVEIA, P. F. *et al.* In-vitro mechanical and biological evaluation of novel zirconia reinforced bioglass scaffolds for bone repair. **Journal of the Mechanical Behavior of Biomedical Materials**, v. 114, n. October 2020, 2021.

HAFEZEQORAN, A.; KOODARYAN, R. Effect of Zirconia Dental Implant Surfaces on Bone Integration: A Systematic Review and Meta-Analysis. **BioMed Research International**, v. 2017, 2017.

HAN, J. *et al.* Biomechanical and histological evaluation of the osseointegration capacity of two types of zirconia implant. **International Journal of Nanomedicine**, v. 11, p. 6507–6516, 2016.

HAN, J. M. *et al.* The surface characterization and bioactivity of NANOZR in vitro. **Dental Materials Journal**, v. 33, n. 2, p. 210–219, 2014.

HAO L, LAWRENCE J, CHIAN KS. Osteoblast cell adhesion on a laser-modified zirconia based bioceramic, **Journal of Materials Science: Materials in Medicine**. v.16, p. 719–726, 2005.

HEMPEL, U. *et al.* Response of osteoblast-like SAOS-2 cells to zirconia ceramics

with different surface topographies. **Clinical Oral Implants Research**, v. 21, n. 2, p. 174–181, 2010.

HENCH, L. L. *et al.* Analysis of bioglass fixation of hip prostheses. **Journal of Biomedical Materials Research**, v. 11, n. 2, p. 267–282, 1977.

HENCH, L. L. Opening paper 2015- Some comments on Bioglass: Four Eras of Discovery and Development. **Biomedical glasses**, v. 1, n. 1, p. 1–11, 2015.

HENCH, L. L. *et al*. Genetic design of bioactive glass. **Journal of the European Ceramic Society**, v. 29, n. 7, p. 1257-1265, apr. 2009.

HENNINGSEN, A. *et al.* Changes in surface characteristics of titanium and zirconia after surface treatment with ultraviolet light or non-thermal plasma. **European Journal of Oral Sciences**, n. 10, 2018.

HENRIQUES, B. *et al.* Experimental evaluation of the bond strength between a CoCrMo dental alloy and porcelain through a composite metal-ceramic graded transition interlayer. **Journal of the Mechanical Behavior of Biomedical Materials**, v. 13, p. 206–214, 2012.

HENRIQUES, Bruno et al. Influence of interlayer design on residual thermal stresses in trilayered and graded all-ceramic restorations. **Materials Science And Engineering: C**, v. 71, p. 1037-1045, feb. 2017.

HOFFMANN, O. *et al.* Osseointegration of zirconia implants with different surface characteristics: an evaluation in rabbits. **The International journal of oral & maxillofacial implants**, v. 27, n. 2, p. 352–358, 2012.

HOTCHKISS KM, G.B *et al.* Titanium surface characteristics, including topography and wettability, alter macrophage activation, **Acta Biomaterialia.** v. 31, p. 425–434, 2016.

JANNER, S. F. M. *et al.* Bone response to functionally loaded, two-piece zirconia implants: A preclinical histometric study. **Clinical Oral Implants Research**, v. 29, n. 3, p. 277–289, 2018.

JONES, J. R. *et al*. Effect of surfactant concentration and composition on the structure and properties of sol-gel-derived bioactive glass foam scaffolds for tissue engineering. **Journal of Materials Science**, v. 38, n. 18, p. 3783-3790, sep. 2003.

JONES, Julian R. *et al*. Large-Scale Production of 3D Bioactive Glass Macroporous Scaffolds for Tissue Engineering. **Journal of Sol-Gel Science and Technology**, v. 29, n. 3, p. 179-188, mar. 2004

JONES, J. R. *et al*. Review of bioactive glass: from Hench to hybrids. **Acta Biomaterialia**,, v. 9, n. 1, p. 4457-4486, jan. 2013.

KOU W, T. *et al.* An in vitro evaluation of the biological effects of carbon nanotube-coated dental zirconia, **ISRN Dentistry**, p. 1–6, 2013.

LAVOS-VALERETOI C, et al. A study of histological responses from Ti-6Al-7Nb alloy dental implants with and without plasma-sprayed hydroxyapatite coating in dogs**, Journal of Materials Science: Materials in Medicine**. V. 12, p. 273–276, 2001.

NALEWEY, *et al.* Reproducibility of ZrO_2-based freeze casting for biomaterials, **Material Science and Engineering C,** v. 61, p. 105–112, 2016.

PARDUN K. *et al.* Magnesium-containing mixed coatings on zirconia for dental implants: mechanical characterization and in vitro behavior. **Journal of Biomaterial Applied.**, v. 30, n. 1, p. 104–108, 2015.

PARDUN k, et al., Mixed zirconia calcium phosphate coatings for dental implants: tailoring coating stability and bioactivity potential, **Material Science of Engineering C**. v. 48 p. 337–346, 2015.

KAROUSSIS, I. K. *et al.* Long-term implant prognosis in patients with and without a history of chronic periodontitis: a 10-year prospective cohort study of the ITI Dental Implant System. **Clinical oral implants research**, v. 14, n. 3, p. 329–339, 2003.

KAUR, Gurbinder *et al*. A review of bioactive glasses: their structure, properties, fabrication and apatite formation. **Journal of Biomedical Materials Research Part A**, v. 102, n. 1, p. 254-274, may 2014.

KHAYAT, W. *et al.* Effect of grinding and polishing on roughness and strength of zirconia. **Journal of Prosthetic Dentistry**, v. 119, n. 4, p. 626–631, 2018.

KE, Jinhuan *et al*. Enhancing the Bioactivity of Yttria-Stabilized Tetragonal Zirconia Ceramics via Grain-Boundary Activation. **Acs Applied Materials & Interfaces**, v. 9, n. 19, p. 16015-16025, may. 2017

KIRSTEN, A. et al. Bioactive and Thermally Compatible Glass Coating on Zirconia Dental Implants. **Journal of Dental Research**, v. 94, n. 2, p. 297-303, nov. 2015.

KIM J W, LIU L and Zhang Y. Improving the resistance to sliding contact damage of zirconia using elastic gradients, **Journal of Biomedical Materials Research Part B: Applied** v. 94, p. 347–352, 2010.

KIM, H. *et al.* Comparison of peri-implant bone formation around injection- molded and machined surface zirconia implants in rabbit tibiae. **Dental Material Journal**, v. 34, n. 4, p. 508–515, 2017.

KOCH, F. P. *et al.* Osseointegration of one-Piece zirconia implants compared with a titanium implant of identical design: A histomorphometric study in the dog. **Clinical Oral Implants Research**, v. 21, n. 3, p. 350–356, 2010.

KOHAL, Ralf J *et al.* Loaded custom-made zirconia and titanium implants show similar osseointegration: an animal experiment. **Journal of periodontology**, v. 75, n. 9, p. 1262–1268, 2004.

KOHAL, R. J. *et al.* Peri-implant bone response to retrieved human zirconia oral implants after a 4-year loading period: A histologic and histomorphometric evaluation of 22 cases. **Journal of Biomedical Materials Research - Part B Applied Biomaterials**, v. 104, n. 8, p. 1622–1631, 2016.

KUBASIEWICZ-ROSS, P.; HADZIK, J.; DOMINIAK, M. Osseointegration of zirconia implants with 3 varying surface textures and a titanium implant: A histological and micro-CT study. **Advances in clinical and experimental medicine : official organ Wroclaw Medical University**, v. 27, p. 1173–1179, 2018.

LARANJEIRA, M. S. *et al.* Modulation of human dermal microvascular endothelial cell and human gingival fibroblast behavior by micropatterned silica coating surfaces for zirconia dental implant applications. **Science and technology of advanced materials**, v. 15, n. 2, p. 025001, 2014.

LEE, H. *et al.* Mussel-Inspired Surface Chemistry for Multifunctional Coatings. **Science**, v. 318, n. 5849, p. 426–430, 2007.

LE RAY *et al.,* A new Technological Procedure Using Sucrose as Porogen Compound to Manufacture Porous Biphasic Calcium Phosphate Ceramics of Appropriate Micro- and Macrostructure. **Ceramics international.** v. 36, p. 93–101, 2010.

LI, H. *et al.* Microstructure and wear behavior of graphene nanosheets-reinforced zirconia coating. **Ceramics International**, v. 40, n. 8, p. 12821–12829, 2014.

LINARES, A. *et al.* Histological assessment of hard and soft tissues surrounding a novel ceramic implant: A pilot study in the minipig. **Journal of Clinical Periodontology**, v. 43, n. 6, p. 538–546, 2016.

LITTUMA, Gustavo J. S. *et al*. Titanium coated with poly(lactic-co-glycolic) acid incorporating simvastatin: biofunctionalization of dental prosthetic abutments. **Journal Of Periodontal Research**, v. 55, n. 1, p. 116-124, sep. 2019.

LIU, *et al.* A new modified laser pre treatment for porcelain zirconia bonding, **Dental Materia**ls, v. 29 p. 559–565, 2013

LIU, J. *et al.* A novel method of surface modification by electrochemical deoxidation: Effect on surface characteristics and initial bioactivity of zirconia. **Journal of Biomedical Materials Research - Part B Applied Biomaterials**, v. 105, n. 8, p. 2641–2652, 2017.

LIU, M. *et al.* Surface modification of zirconia with polydopamine to enhance fibroblast response and decrease bacterial activity in vitro: A potential technique for soft tissue engineering applications. **Colloids and Surfaces B: Biointerfaces**, v. 136, p. 74–83, 2015.

LIU, Y. T.; LEE, T. M.; LUI, T. S. Enhanced osteoblastic cell response on zirconia by bio-inspired surface modification. **Colloids and Surfaces B: Biointerfaces**, v. 106, p. 37–45, 2013.

MA, J. *et al.* Influence of the sintering temperature on the structural feature and bioactivity of sol-gel derived SiO2-CaO-P2O5 bioglass. **Ceramics International**, v. 36, n. 6, p. 1911–1916, 2010.

MARECI, D. *et al.* Corrosion resistance of ZrTi alloys with hydroxyapatite-zirconia-silver layer in simulated physiological solution containing proteins for biomaterial applications. **Applied Surface Science**, v. 389, p. 1069–1075, 2016.

MESQUITA-GUIMARÃES, J. *et al.* Processing and strengthening of 58S bioactive glass-infiltrated titania scaffolds. **Journal of Biomedical Materials Research - Part A**, v. 105, n. 2, p. 590–600, 2017.

MESQUITA-GUIMARÃES, J. *et al*. Cell adhesion evaluation of laser-sintered HAp and 45S5 bioactive glass coatings on micro-textured zirconia surfaces using MC3T3-E1 osteoblast-like cells. **Materials Science and Engineering**: C, v. 109, p. 110492, apr. 2020.

MIRANDA, G. *et al.* Design of Ti6Al4V-HA composites produced by hot pressing for biomedical applications. **Materials and Design**, v. 108, p. 488–493, 2016.

MOEZZIZADEH, M.; NOJEDEHIAN, H.; HAGHI, H. V. Effect of bioglass and silica coating of zirconia substrate on its bond strength to resin cement. **Dental Materials Journal**, v. 36, n. 1, p. 54–62, 2017.

MONTAZERIAN, Maziar *et al*. Bioactivity and cell proliferation in radiopaque gel-derived CaO–P2O5–SiO2–ZrO2 glass and glass–ceramic powders. **Materials Science and Engineering: C**, v. 55, p. 436-447, oct. 2015.

MONTERO, J. *et al.* Comparison of Clinical and Histologic Outcomes of Zirconia Versus Titanium Implants Placed in Fresh Sockets: A 5-Month Study in Beagles. **The International Journal of Oral & Maxillofacial Implants**, v. 30, n. 4, p. 773–780, 2015.

MOURA, C. G. *et al.* Effect of laser surface texturing on primary stability and surface properties of zirconia implants. **Ceramics International**, v. 43, n. 17, p. 15227–15236, 2017.

MUSHAHARY D *et al*, Collagen type-I leads to in vivo matrix mineralization and secondary stabilization of Mg–Zr–Ca alloy implants. **Colloids and Surfaces B: Biointerfaces** v.122, p. 719–728, 2014.

OH, G. *et al.* Surface Characteristics of Bioactive Glass-Infiltrated Zirconia with Different Hydrofluoric Acid Etching Conditions. **Journal of Nanoscience and nanotechnology**, v. 17, n. 4, p. 2645–2648, 2017.

OLIVA, J.; OLIVA, X. Five-year success rate of 831 consecutively placed Zirconia dental implants in humans: a comparison of three different rough surfaces. **The International journal of oral & maxillofacial implants**, v. 25, n. 2, p. 336–344, 2010.

OZER, F. *et al.* Effect of thickness and surface modifications on flexural strength of monolithic zirconia. **Journal of Prosthetic Dentistry**, v. 119, n. 6, p. 987–993, 2018.

PABST, A. M. et al. Influence of CAD/CAM zirconia for implant-abutment manufacturing on gingival fibroblasts and oral keratinocytes. **Clinical Oral Investigations**, v. 20, n. 5, p. 1101-1108, sept. 2015.

PARRY J.P, *et al,* Laser micromachining of zirconia (Y-TZP) ceramics in the

picosecond regime and the impact on material strength, **International Journal of Applied Ceramic Technology**. v.8, p. 163–171, 2011

PICONI, C.; MACCAURO, G. Zirconia as a ceramic biomaterial. **Biomaterials**, v. 20, n. 1, p. 1–25, 1999.

PITTAYACHAWAN, P. *et al.* The biaxial flexural strength and fatigue property of Lava™ Y-TZP dental ceramic. **Dental Materials**, v. 23, n. 8, p. 1018–1029, 2007.

PLEWINSKI, M. *et al.* The effect of crystallization of bioactive bioglass 45S5 on apatite formation and degradation. **Dental Materials**, v. 29, n. 12, p. 1256–1264, 2013.

PRIYADARSINI, S. Mukherjee, M. Mishra. Nanoparticles used in dentistry: a review. **Journal of Oral Biology and Craniofacial Research.** v. 8, p. 58–67, 2018.

QUENTINFLAMANTA; *et al.* Hydrofluoric acid etching of dental zirconia. Part 1: etching mechanism and surface characterization. **Journal of the European Ceramic Society**, v. 36, n. 1, p. 121–134, 2016.

RAHAMAN, M. N. et al. Bioactive glass in tissue engineering. **Acta Biomaterialia**, v. 7, n. 6, p. 2355-2373, jun. 2011

RAHMAN, M. S; et al. TGF-β/BMP signaling and other molecular events: regulation of osteoblastogenesis and bone formation. **Bone Research**, v. 3, n. 1, p. 1-20, apr. 2015.

ROEDEL, S. *et al.* Production and characterization of zirconia structures with a porous surface. **Materials Science and Engineering C**, v. 101, n. February, p. 264–273, 2019.

ROEHLING, S. *et al.* In Vitro Biofilm Formation on Titanium and Zirconia Implant Surfaces. **Journal of Periodontology**, v. 88, n. 3, p. 298–307, 2017.

SANON, C. *et al.* A new testing protocol for zirconia dental implants. **Dental Materials**, v. 31, n. 1, p. 15–25, 2015.

SATO, H. *et al.* Mechanical properties of dental zirconia ceramics changed with sandblasting and heat treatment. **Dental Materials Journal**, v. 27, n. 3, p. 408–414, 2008.

SAULACIC, N. *et al.* Acid and Alkaline Etching of Sandblasted Zirconia Implants: A Histomorphometric Study in Miniature Pigs. **Clinical Implant Dentistry and Related**

Research, v. 16, n. 3, p. 313–322, 2014.

SCARANO, A. *et al.* Bacterial Adhesion on Commercially Pure Titanium and Zirconium Oxide Disks: An In Vivo Human Study. **Journal of Periodontology**, v. 75, n. 2, p. 292–296, 2004.

SCARANO, A. *et al.* Bone response to zirconia ceramic implants: an experimental study in rabbits. **The Journal of oral implantology**, v. 29, n. 1, p. 8–12, 2003.

SCHIENLE, S. *et al.* Microbial adhesion on novel yttria-stabilized tetragonal zirconia (Y-TZP) implant surfaces with nitrogen-doped hydrogenated amorphous carbon (a-C:H:N) coatings. **Clinical Oral Investigations**, v. 20, n. 7, p. 1719–1732, 2016.

SCHLIEPHAKE, H. *et al.* Mechanical anchorage and peri-implant bone formation of surface-modified zirconia in minipigs. **Journal of Clinical Periodontology**, v. 37, n. 9, p. 818–828, 2010.

SCHÜNEMANN, Fernanda H et al. Zirconia surface modifications for implant dentistry. **Materials Science & Engineering C for Biological Applications**, v.98 p. 1294-1305, 2019.

SEPULVEDA, P.; JONES, J. R.; HENCH, L. L. In vitro dissolution of melt-derived 45S5 and sol-gel derived 58S bioactive glasses. **Journal of Biomedical Materials Research**, v. 61, n. 2, p. 301–311, 2002.

SIVARAMAN, Karthik et al. Is zirconia a viable alternative to titanium for oral implant? A critical review. **Journal Of Prosthodontic Research**, v. 62, n. 2, p. 121-133, apr. 2018.

SORDI, Mariane Beatriz *et al*. Effect of dexamethasone as osteogenic supplementation in in vitro osteogenic differentiation of stem cells from human exfoliated deciduous teeth. **Journal of Materials Science**: Materials in Medicine, v. 32, n. 1, p. 1-9, jan. 2021.

SPYROPOULOU, P. E. *et al.* Composition, phase analysis, biaxial flexural strength, and fatigue of unshaded versus shaded Procera zirconia ceramic. **Journal of Prosthetic Dentistry**, v. 116, n. 2, p. 269–276, 2016.

SRIAMPORN, T. *et al.* Dental zirconia can be etched by hydrofluoric acid. **Dental Material Journal**, v. 33, n. 1, p. 79–85, 2014.

STADLINGER, B. *et al.* Comparison of zirconia and titanium implants after a short

healing period. A pilot study in minipigs. **International Journal of Oral and Maxillofacial Surgery**, v. 39, n. 6, p. 585–592, 2010.

THOMA, D. S. *et al.* Histological analysis of loaded zirconia and titanium dental implants: An experimental study in the dog mandible. **Journal of Clinical Periodontology**, v. 42, n. 10, p. 967–975, 2015.

THOMPSON, J. Y. *et al.* Adhesion/cementation to zirconia and other non-silicate ceramics: Where are we now?. **Dental Materials**, v. 27, n. 1, p. 71–82, 2011.

TRUSOVA, E. A. *et al.* Influence of Graphene Sheets on Compaction and Sintering Properties of Nano-Zirconia Ceramics. **Materials**, v. 15, n. 20, 2022.

TUNA, T. *et al.* Influence of ultraviolet photofunctionalization on the surface characteristics of zirconia-based dental implant materials. **Dental Materials**, v. 31, n. 2, p. e14–e24, 2015.

TUNA, T *et al.* Effect of ultraviolet photofunctionalisation on the cell attractiveness of zirconia implant materials, **European Cells & Materials**. v. 29 p. 82–94, 2015.

VU, V. T. *et al.* Acid etching of glass-infiltrated zirconia and its biological response. **The Journal of Advanced Prosthodontics**, v. 9, n. 2, p. 104–109, 2017.

WANG G *et al.,* Microstructure, bioactivity and osteoblast behavior of monoclinic zirconia coating with nanostructured surface, **Acta Biomaterialia** v. 6, p. 990–1000, 2010.

WEIBULL, W. A statistical distribution function of wide applicability. **J Appl Mech**, v. 18, p. 293–7, 1951.

WENNERBERG, A.; ALBREKTSSON, T. Effects of titanium surface topography on bone integration: A systematic review. **Clinical Oral Implants Research**, v. 20, n. SUPPL. 4, p. 172–184, 2009.

XIE, H. *et al.* Effects of acid treatment on dental zirconia: An in vitro study. **Plos One**, v. 10, n. 8, p. 1–12, 2015.

XU M, et al., Hierarchical bioceramic scaffolds with 3D-plotted macropores and mussel-inspired surface nanolayers. **Nanoscale**. v. 12, p. 13790–13803, 2016.

YANABA, Y.; HAYASHI, K. Relation between fracture surface area of a flexural strength. **Materials Science and Engineering A**, v. 209, p. 169–174, 1996.

YANG, J. *et al.* Micro-porous calcium phosphate coatings on load-bearing zirconia

substrate : Processing , property and application. **Ceramics International**, v. 39, n. 6, p. 6533–6542, 2013.

YANG, Y. *et al.* Ultraviolet light-treated zirconia with different roughness affects function of human gingival fibroblasts in vitro: The potential surface modification developed from implant to abutment. **Journal of Biomedical Materials Research - Part B Applied Biomaterials**, v. 103, n. 1, p. 116–124, 2015.

YIN, L. *et al.* A Review of Engineered Zirconia Surfaces in Biomedical Applications. **Procedia CIRP**, v. 65, p. 284–290, 2017.

YOUNG, R. A. **The Rietveld Method**, 1989.

ZHANG, Y. *et al.* Damage accumulation and fatigue life of particle-abraded ceramics, 2006.

ZHANG Y and KIM J, Graded structures for damage resistant and aesthetic all ceramic restorations, **Dental Materials**. v. 25, p. 781–790, 2009a

ZHANG Y and LA M A. Optimization of ceramic strength using elastic gradients. **Acta Materialia.** v. 57, p. 2721–2729, 2009b.

ZHANG, Y.; REGEROS, R.; KIM, J. US 2009/0118114 A1Patent Application. **United States**, v. 1, n. 19, 2009c.

ZHANG, Y. et al. Graded Structures for All-ceramic Restorations. **Journal Of Dental Research**, v. 89, n. 4, p. 417-421, mar. 2010a.

ZHANG Y, KIM J and THOMPSON V P. US7858192 B2 - Graded Glass/Ceramic/Glass Structures for Damage Resistant Ceramic Dental and Orthopedic Prostheses, 2010b.

ZHANG Y and KIM J W. Graded zirconia glass for resistance to veneer fracture, **Journal of Dentistry Restorative**. v. 89, p. 1057–1062, 2010c.

ZHANG, Y. Overview- Damage resistance of graded ceramic restorative materials. **Journal of the European Ceramic Society**, v. 32, n. 11, p. 2623–2632, 2012a.

ZHANG, Y.; SUN, M.; ZHANG, D. Designing functionally graded materials with superior load-bearing properties. **Acta Biomaterialia**, v. 8, n. 3, p. 1101–1108, 2012b.

ZHANG, Yu et al. **Bioactive graded zirconia-based structures**. US n. US8703294B2. Application: 22 sep. 2008. Patent: 22 apr. 2014.

ZHONG, J.; GREENSPAN, D. C. Processing and properties of sol-gel bioactive glasses. **Journal of biomedical materials research**, v. 53, n. 6, p. 694–701, 2000.

ZHUKOVA, Y *et al*. Cell Guidance on Nanostructured Metal Based Surfaces. **Advanced Healthcare Materials**, v. 6, n. 7, feb. 2017.